MASTER THESIS

Design of Mechanical Systems - 4

Investigation of the Noise and Thermal Response When the Material of a Control Box Is Modified
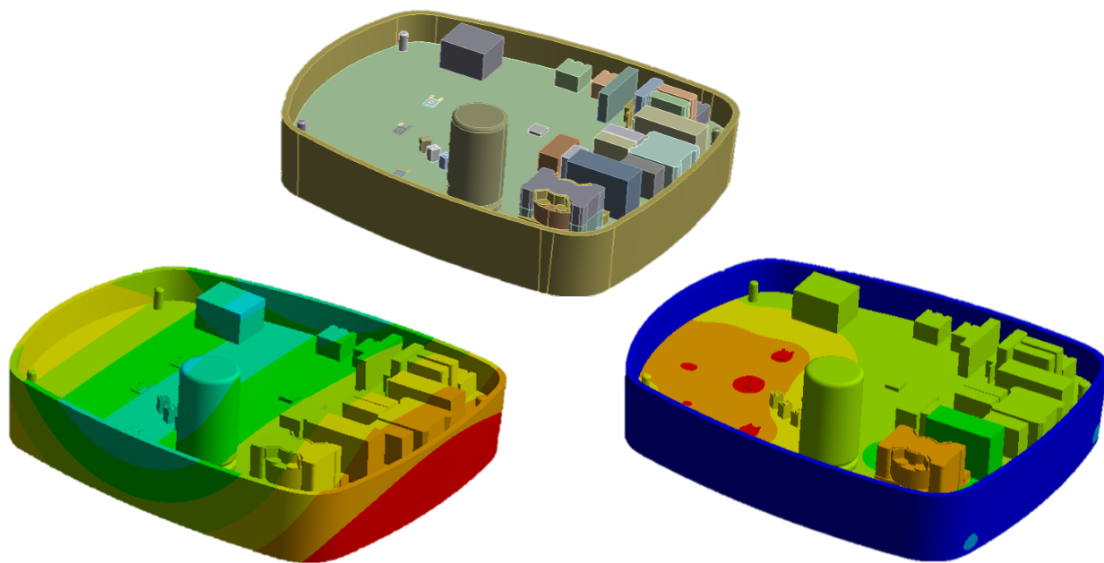
Marta Bermejo Escudero

Aalborg University

02-06-2022

Title:

Investigation of the Noise and Thermal Response When the Material of a Control Box Is Modified

Theme:

Master Thesis

Project period:

Spring semester 2022

Participant:

Marta Bermejo Escudero

University Supervisor:

Sergey Sorokin - Professor of the Department of Mechanical and Manufacturing Engineering

Grundfos Holding A/S Supervisors:

Nielas Winther Laue - Senior Structural Specialist

Lasse Søgaard Ledet - Lead Product Simulation Specialist

Number of Pages: 55

Date of Completion: 02-06-2022

Abstract:

This project is the spin-off of a previous one thus, the bases and motivations are defined first. Then, the numerical scheme of the software used, ANSYS, is included, in terms of vibrations. To decrease computational time, the equivalent radiated power is used to estimate the noise instead.

Afterwards, benchmark, mesh and directivity studies are done. Moreover, a material study of the case is included, considering three cases: full polycarbonate, mixed aluminium and polycarbonate, and full aluminium. This study incorporates modal and harmonic analyses, with the Mode Superposition method. The study revealed that the model with the full polycarbonate case has lower natural frequencies and a greater noise at low frequencies, than when aluminium is present. However, results may be affected by the chosen damping ratio.

Later, the material change is studied in terms of thermal analysis. The temperature decreases with the presence of aluminium on the case. The model can withstand temperatures with no issues regardless of the material.

Finally, a manual parametric study is done. It shows a strong negative correlation between the thickness of the case and the maximum equivalent radiated power. Additionally, the position of one of the screws has a medium positive correlation with the maximum temperature. Therefore, it is possible to minimize both responses with the parameters.

Abstract in Danish

Dette projekt er et udspring fra et tidligere projekt. Derfor er grundelementerne og motivationen for projektet først beskrevet. Efterfølgende er det numeriske system omhandlende vibrationer af det anvendte software, ANSYS, beskrevet. For at reducere beregningstiden, anvendes equivalent radiated power til at estimere støjen.

Efterfølgende udføres benchmark, mesh og retningsvirknings studier. Ydermere, er et materialestudie af emnet inkluderet. Materialestudiet undersøger tre tilfælde af materialekombinationer af emnet: Komplet polycarbonat, blandet aluminium og polycarbonat og komplet aluminium. Dette studie inkluderer modal og harmoniske analyser med Mode Superposition metoden. Studiet afslørede at modellen med komplet polycarbonat emne har den laveste egenfrekvens og en større støj ved en lav frekvens sammenlignet med modellen med komplet aluminium. Det skal dog bemærkes, at resultatet kan være påvirket af den valgte dæmpningsfaktor.

Ydermere er ændringen af materialet undersøgt i forhold til en termisk analyse. Temperaturen falder når emnet er lavet i komplet aluminium. Konklusionen er dog at emnet kan modstå temperaturen uanset om det er lavet i aluminium eller polycarbonat.

Slutligt er der udført et manuelt parametrisk studie. Studiet viser en stærk negative sammenhæng mellem tykkelsen af emnet og den maksimale equivalent radiated power. Yderligere, viser studiet at positionen af det ene af skruetårnene i emnet har en medium positiv sammenhæng med den maksimale temperatur. Hvorfor det er muligt at minimere begge responser med parametrene.

Preface

This project is written by one 4th semester graduate student in the master's program *Mechanical Engineering - Design of Mechanical Systems* at the Faculty of Engineering and Science at Aalborg University. The project is a spin-off of the project written during a project-oriented stay at Grundfos Holding A/S, Denmark, during the 3rd semester.

This project aims to study the influence of the change of material in the case of a control box in terms of noise and temperature. The results should be obtained for full polycarbonate case, mix aluminium and polycarbonate case, and full aluminium case. Moreover, a parametric study should be conducted to find if there is an influence of several parameters on the responses and if they can be minimised.

I would like to thank my university supervisor, Sergey Sorokin, and my Grundfos supervisors, Nielas Winther Laue and Lasse Søgaard Ledet, for allowing me to do my Master's Thesis with you. Thank you for your excellent guidance and support during this process.

I also wish to thank my family and my partner because without all of you it would not have been possible to get to where I am today. Thank you for supporting me and helping me, for making this work more bearable and for having encouraged me to finish it on time and full of illusion.

Finally, to all of you who have dedicated your time to support me, friends and classmates of Design of Mechanical Systems. Thank you for your guidance at the university during these two years of my master's degree and for introducing me to Danish culture. It has been a pleasure to meet you and I hope to see you again soon.

To all of you, thank you for being close to me. I hope you enjoy the reading.

Marta Bermejo Escudero

Reading Guide

Throughout this report, the company known as Grundfos Holding A/S will be referred to as Grundfos. The model from the project-oriented stay at Grundfos, during the 3rd semester, will be referred to as DMS3 model and the new model from this 4th semester as DMS4 model. Figures and pictures in this report are either drawn or captured by the author unless stated otherwise. All contours legends from the colour plots obtained from ANSYS Mechanical are defined in SI-units. The Harvard referencing system is used for referencing sources throughout the report, e.g. (Last name/institution, year of publication). The bibliography contains a list where further information on the implemented sources is elaborated. At the end of the report, several appendices have been inserted with alphabetical numbering.

Contents

Introduction ⟨1⟩

This project is a continuation of *Parametric stability and thermal optimisation analysis of an aluminium part* (Bermejo, 2022), referred to as the DMS3 project in the following sections. Therefore, the DMS3 project is used as a basis and the conclusions found are the starting point.

DMS3 project involved a control box form of two parts, bottom and cover. The bottom part was made out of aluminium whereas the cover was of polycarbonate. The difference in the material was that the cover was not designed to dissipate heat as all heat was to be dissipated from the bottom. Also, several fins were defined to try to dissipate more heat through the bottom.

The goal of the project was to maximise the thermal performance and minimise the cost of the model. For doing so the model was parametrized first and then a feasibility study was done. Once this was stated, the optimisation of the design, concerning the fins of the model, was performed. Different combinations of the fins were done and analysed, considering the mass and the maximum temperature of the model.

As the power loads were applied at the points where most heat was dissipated due to the electronic components, the heat was too concentrated in the areas of the application and it was almost not possible to modify the temperature of the model. Therefore, the conclusion from the optimisation was based on the fact that the temperature could not be decreased and thus, more focus was done on the cost. The cost involves not only the mass of the model but also the tooling as it is directly related to the combination of the fins that is present on the bottom case.

Hence, by removing the fins from the control box, the mass was decreased by 10% and the cost of the tooling by 4%, which means saving of $52.400\,€$ per $100.000\,$pcs. By doing this, the maximum temperature of the model was only increased by 7% and the model had no issues withstanding those temperatures without damaging the components. Thus, it was believed that the best option was to remove the fins from the model since the entire part itself acted as a fin and no additional material was needed.

In any company, the objective is to manufacture parts with good performance at a low cost. With the change of material to polycarbonate in both parts, it is possible. The model has to be redesigned to be able to apply the heat sources and no fins are included in the new model as the polycarbonate is a worst conductor than aluminium and the fins will not affect the results. However, the change of material will affect the noise and temperature of the model.

Therefore, the goal of this project is to study how the change of the case material affects the noise and temperature of the control box and then parameterized the design to try to minimize both responses.

Problem Analysis 2

As mentioned in the introduction, this project is a continuation of the DMS3 project (Bermejo, 2022) with several modifications, to the design and the material. With the material change, the mechanical properties of the control box are modified and therefore there is an influence on the temperature gradient. Moreover, the new design of the model is defined. This new design will be used in the rest of the report unless otherwise indicated.

2.1 Temperature Gradient Influence

In DMS3, the bottom part of the case was made of aluminium whereas the cover of polycarbonate. Nevertheless, now both parts are made of polycarbonate trying to decrease the cost of the model. The material used in DMS3 for the aluminium is a special kind known as silumin. Nevertheless, aluminium 6061 has been used in this project to have all the properties of the material. For the polycarbonate, a plastic or PC - copolymer, with high heat resistance - is used. Now, the different mechanical properties have to be considered, see Table 2.1. Notice that all the values are obtained from Granta Design team at ANSYS (AnsysGranta, 2022) and they are calculated at a room temperature of $23\,°C$.

Properties		Aluminium	Polycarbonate
Isotropic Elasticity	Young's Modulus [GPa]	69,040	2,303
	Poisson's Ratio	0,33	0,4002
	Bulk Modulus [GPa]	67,686	3,846
	Shear Modulus [GPa]	25,955	0,82238
Isotropic Secant Coefficient of Thermal Expansion [1/°C]		$2,278 \cdot 10^{-5}$	$9,786 \cdot 10^{-5}$
Tensile Ultimate Strength [MPa]		313,1	62,82
Tensile Yield Strength [MPa]		259,2	61,93
Isotropic Thermal Conductivity [W/m.°C]		155,3	0,1998
Specific Heat Constant Pressure [J/kg.°C]		915,7	1190
Density [kg/m^3]		2.713	1.160

Table 2.1. *Structural and thermal properties of aluminium and polycarbonate at* $23\,°C$.

As the material is changed, the influence of the mechanical properties in the temperature gradient has to be considered. As shown in the table above, the isotropic thermal conductivity of the aluminium is much higher than the one of the polycarbonate, meaning that aluminium is a much

better conductor than the polycarbonate. This is directly related to how the heat is dissipated and therefore distributed on the part when it is under-functioning conditions. The case will achieve a higher temperature when is made of aluminium as more heat will be dissipated from the outside to the outside.

Polycarbonate is a thermoplastic polymer containing carbonates groups and its high strength makes it resistant to impact and fracture. It is extremely durable and resistant to harsh conditions. Moreover, this material is considered almost unbreakable and can withstand extreme temperatures, around $270\,°C$ for several hours or sudden gusts of heat up to $1.166\,°C$ without distortion, breakage or heat absorption. The melting temperature for polycarbonate is around $288\,°C$ to $316\,°C$. Nevertheless, over $135\,°C$ polycarbonate is not thermally stable and does not offer a good heat resistance. The glass transition temperature is around $147\,°C$ and it softens gradually above this point. When it is over $155\,°C$ then, it flows. To improve the heat resistance, it is possible to add flame retardants without impacting the material properties. In addition, its lifespan is considered long and therefore, the cost of replacement is low (Fleming, 2020). On the other hand, aluminium has a melting temperature of $580\,°C$ to $650\,°C$. However, the properties are considerably affected when it is exposed significant times at temperatures above the $150\,°C$ to $200\,°C$ (Kaufman, 2016).

As shown later in section 4.1, the bases of the vibration analysis rely on the equation of motion, Equation 4.8. One of the terms in this equation is the stiffness matrix, which is calculated as shown in Equation 4.11. From this equation, it is evident that the vibration analysis results are directly related to Young's Modulus, E. The Young's Modulus is a measure of a solid's stiffness or resistance to elastic deformation under load. It relates stress - force per unit area - to strain - proportional deformation - along an axis or line and it depends upon temperature and pressure (Helmenstine, 2019). It is determined with the equation $E = \frac{\sigma}{\varepsilon}$ and therefore, it is directly related to the stress. If the temperature rises then, the molecular bonding strength gets weaker and then Young's Modulus decreases. Therefore, there is a negative correlation between modal frequencies and temperature, meaning that if the temperature of the model increases then the modal frequencies decrease (Liu et al., 2016).

In addition, thermal expansion needs to be considered as it is the phenomenon where an object or body expands in reaction to being heated. The amount that material expands is given by the value of the coefficient of thermal expansion. This is the fractional growth of the material per degree change in temperature. The larger the value, the more it will expand when the temperature is increased (Boucher, 2019). Therefore, concerning the values from Table 2.1, polycarbonate will expand more than aluminium and will cause higher stresses in the parts.

2.2 Model Definition

Even if the project is based on the outcome of the project from DMS3, the model needed to be modified. The changes are corresponding mainly to the change in the material. As this is changed, the way of applying the power sources had to be modified as not all the power could be concentrated in one specific point as in DMS3. Moreover, in this project, all the components are present on the Printed Circuit Board (PCB) and not in the case itself as in the last project.

Therefore, there are now three main parts, bottom, cover and PCB. The different electronic components are defined on the PCB and the screws are defined to join the three main parts, see Figure 2.1.
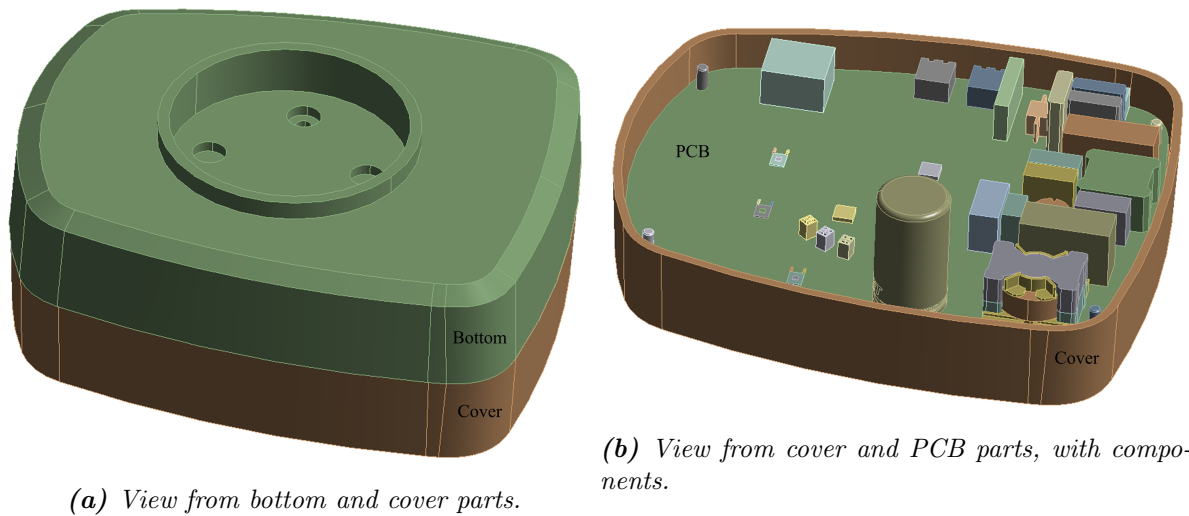
(a) *View from bottom and cover parts.*

(b) *View from cover and PCB parts, with components.*

Figure 2.1. *Model view.*

As mentioned in the introduction, chapter 1, the material of the case is changed from aluminium to polycarbonate. However, the PCB itself, the different components and the screws are made of different materials. The named parts can be seen in Figure 2.2.
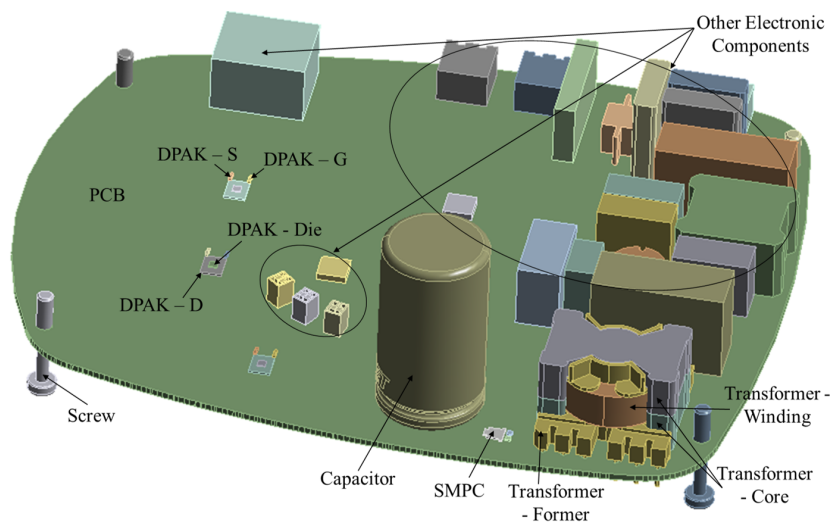
Figure 2.2. *Parts of the model.*

The association of the part and the material can be seen in Table 2.2. As shown in the table, the PCB is made of 90 % of FR4, glass-reinforced epoxy laminate material, and 10 % of copper. This is done by having different layers on the board, FR4 and copper mix. In addition, there are several copper explicit nets which make better the conductivity between the electronic components and the PCB. However, to simplify the model, only one solid has been created for the PCB, defined with FR4 material. This simplification will not have an impact on the vibration analysis as it is believed that the stiffness change will be minor as 90 % of the PCB is made of FR4. However, it

will influence the thermal analysis and therefore, some modifications to the thermal properties will be done in chapter 6.

Part	Material
Bottom	Polycarbonate
Cover	Polycarbonate
Screws	Steel
PCB	FR4 (90 %) + Copper (10 %)
Capacitor	Aluminium
Transformer - Former	Polycarbonate
Transformer - Winding	Copper
Transformer - Core	Ferrite
DPAK - S,D,G	Copper
DPAK - Die	Silicon
SMPC	Copper
Other Electronic Components	Copper

***Table 2.2.*** *Materials used for every part in the model.*

Later on, the connections between the different parts of the model were defined by hand. Here, the components that are welded to each other were set to bonded contact whereas the components that can move and therefore, start being in contact with others, were defined as frictional.

Contact Body	Target Body	Contact Type
PCB	Bottom	Frictional
PCB	Cover	Frictional
Bottom	Capacitor	Frictional
Bottom	Screw	Bonded
Cover	Screw	Bonded
Screw	PCB Hole	Frictional
DPAK	DPAK	Bonded
PCB	DPAK	Bonded
PCB	SMPC	Bonded
Transformer	Transformer	Bonded
PCB	Transformer	Bonded
PCB	Capacitor	Frictional
PCB	Capacitor Screw	Bonded
Capacitor	Capacitor Pin	Bonded
Capacitor Pin	PCB Hole	Bonded
Capacitor Screw	Capacitor Pin	Bonded
PCB	Other Electronic Components	Bonded
Other Electronic Components	Other Electronic Components	Frictional

Table 2.3. *Materials used for every part in the model.*

For simulating the real behaviour, the case should be coupled to the stator house. Nevertheless, for simplicity and time efficiency, it was decided to leave it out and consider only the effect of the boundary conditions that this will imply. These boundary conditions are two fixed support on

the holes from the bottom part where the mounting is done. Refer to Figure 2.3 for visualising the positions of mounting and the similitude to the defined constraints.
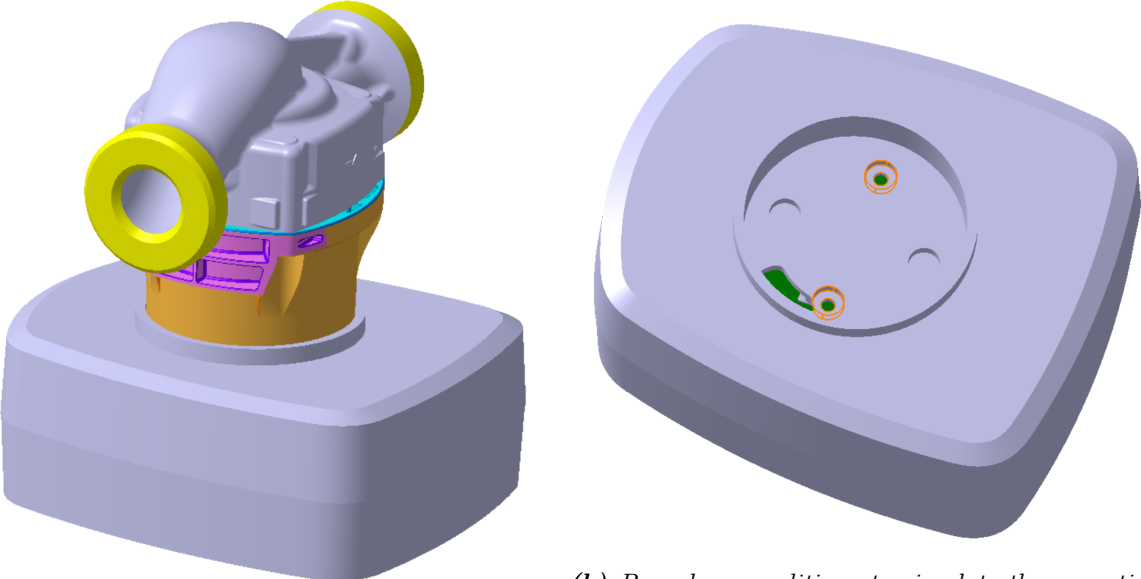
(a) *Real mounting of the stator house.*

(b) *Boundary conditions to simulate the mounting of the stator house.*

Figure 2.3. *Mounting of the model.*

Problem Formulation 3

With offset in the problem analysis of the preceding chapter, the problem is formulated. Since it is desired to change the material of the control box, then a study of the influence on the mechanical properties concerning the gradient of temperature was done. Later on, the new design of the model was defined.

As mentioned in the introduction, the goal of the project is to calculate the vibrations of the system, free and forced vibrations. Then, they should be converted into noise and analysed if it is possible to decrease this magnitude. Moreover, it has to be verified that the new model can withstand the temperatures that the model will reach during the performance. All of these are what lead to the following problem formulation:

> *"What influence does the material change of the case of a control box have on the noise level and temperature? Can both responses be minimized when the case is made of polycarbonate?"*

To answer the problem formulation from above, first, the numerical scheme is defined. It is done for ANSYS Workbench 2021 R2 software as it is the one used for the analysis. Later on, the theory from this chapter is applied and the different studies are performed. Two different studies are conducted, first vibrations analysis and then thermal analysis. Inside the first one, a subdivision is made between the different studies that have been performed such as benchmark, mesh and directivity study. Moreover, a material study is done for three cases: full polycarbonate case, mix aluminium and polycarbonate case, and full aluminium case. Inside this study, a differentiation between free vibrations - Modal Analysis - and force vibrations - Harmonic Analysis has been included. The results from the harmonic analysis have been translated to sound power level to study the noise of the model. The second analysis, thermal analysis, is done to evaluate the temperatures that the model has when it is under-functioning conditions. A material study is done for the same three cases as in vibrations.

Once the results are obtained then, a parametric study is performed when the case is made of polycarbonate to study the influence of some parameters in the noise and temperature results. Finally, a discussion and a conclusion are included to summarise the report and give the keys to the project.

Numerical Scheme in ANSYS 4

Vibration or oscillation is a mechanical phenomenon that includes any motion that repeats itself after some time. Depending on the considered system, there are different types of vibrations. With a focus on dynamic problems, structural dynamic problems and wave propagation problems can be differentiated. Moreover, a subdivision is found inside the first group, free vibrations or eigenfrequency problems and forced vibrations or time-history analysis. Free vibrations analyses are performed when the structure might suffer from the resonance of an unknown dynamic load. It is possible to predict resonance if the lowest eigenfrequencies are found. The method used for this analysis is called eigenfrequency analysis - Modal Analysis. For the second subdivision, forced vibrations - Harmonic Analysis, there is a known load history and the frequency and size are of considerable size. From this analysis, it is convenient to find the displacements, strains and stresses as a function of time (Lund and Lindgaard, 2020).

Vibration analyses are usually performed with a Finite Element Model (FEM) or numerical model, and the method used is known as the Finite Element Analysis (FEA). The software used to solve the model from this project is ANSYS and the method to set up the model for both analysis, modal and harmonic, has been included.

4.1 Finite Element Analysis

FEA is the simulation of any physical phenomenon using the numerical technique that can accurately - but approximately - solve the partial differential equations, known as FEM or Full Order Model. This technique is useful since most of the systems in engineering, including complex mechanical and structural vibration problems, can be expressed as partial differential equations. The FEM can solve problems such as stress analysis, heat transfer, fluid flow and electromagnetic among others. All the problems are solved by simulations in software.

The basic idea of FEM is to divide the body into finite elements, often just called elements, connected by nodes and obtain an approximate solution. These elements are considered to behave as continuous structural members. This process is usually known as finite element mesh and the procedure is called mesh generation.

Since it is very complex to find the exact solutions in the original structure, considering the specified loads, then, an approximation solution is assumed for each finite element. The point is if the solutions have been properly chosen then, they can converge to the exact solution of the total structure as the element size is reduced (Rao, 2011).

First of all, when treating dynamic problems, the principle of virtual work needs to be considered.

The principle says that equilibrium between work done by internal stresses and external loads is required when an admissible deformation configuration is considered. In other words, the compatibility equations and essential Boundary Conditions (BC) have to be fulfilled (Lund and Lindgaard, 2020).

When considering equilibrium, the change in internal work due to virtual displacements - left-hand-side (LHS), corresponds to the change in external work - right-hand-side (RHS), see Equation 4.1.

$$\int_V \delta\epsilon_{ij}\sigma_{ij}\,dV = \int_V \delta u_i F_i\,dV + \int_S \delta u_i \Phi_i\,dS - \int_V \delta u_i \rho \ddot{u}_i\,dV - \int_V \delta u_i \kappa_d \dot{u}_i\,dV \tag{4.1}$$

u_i	Displacements, $i = 1, 2, 3$
δu_i	Virtual displacements
σ_{ij}	Stress tensor
ϵ_{ij}	Strain tensor
$\delta\epsilon_{ij}$	Virtual strain due to δu_i
F_i	Body forces
Φ_i	Surface forces
ρ	Density
κ_d	Viscous damping factor

As the focus is on finite elements, then the above expression can be rewritten in FE form or discrete domain. See Equation 4.2 for a single element. From left to right, the LHS terms are inertial forces, viscous forces and internal stresses; the RHS terms are body forces, surface traction and nodal forces.

$$\int_{V_e} \{\delta u\}^T \rho\{\ddot{u}\}\,dV + \int_{V_e} \{\delta u\}^T \kappa_d\{\dot{u}\}\,dV + \int_{V_e} \{\delta\epsilon\}^T\{\sigma\}\,dV =$$
$$= \int_{V_e} \{\delta u\}^T\{F\}\,dV + \int_{S_e} \{\delta u\}^T\{\Phi\}\,dS + \sum_{i=1}^{n}\{\delta u\}_i^T\{p\}_i \tag{4.2}$$

$\{F\}$	Body force
$\{\Phi\}$	Surface traction
$\{p\}_i$	Concentrated nodal loads
$\{\delta u\}$	Virtual displacement
$\{\delta\epsilon\}$	Virtual strain due to $\{\delta u\}$
ρ	Density
κ_d	Viscous damping factor

Now, the FE discretization and the separation of time and spatial variables are outlined, refer to Equation 4.3.

$$\{u(x,t)\} = [N(x)]\{d(t)\} \quad , \quad \{\dot{u}(x,t)\} = [N(x)]\{\dot{d}(t)\} \quad , \quad \{\ddot{u}(x,t)\} = [N(x)]\{\ddot{d}(t)\} \tag{4.3}$$

Here, $\{\dot{d}\}$ is discrete in space but continuous in time. This is known as semidiscretization and therefore:

$$\{\delta u\} = \delta([N]\{d\}) = [N]\{\delta d\} \quad and \quad \{\delta \epsilon\} = \delta([B]\{d\}) = [B]\{\delta d\} \tag{4.4}$$

By inserting the FE discretization into the equilibrium equation then, Equation 4.5 is obtained. Here, from left to right, the integral terms from the LHS are: mass matrix $[m]$, damping matrix $[c]$ and internal nodal forces $\{r^{int}\}$; and from the RHS, the terms inside the square brackets corresponds to the external nodal forces $\{r^{ext}\}$. Here, the mass and damping matrices are formulated for the same shape function $[N]$ used for interpolation of the displacements.

$$\{\delta d\}^T \left[\int_{V_e} \rho[N]^T[N]\,dV\{\ddot{d}\} + \int_{V_e} \kappa_d[N]^T[N]\,dV\{\dot{d}\} + \int_{V_e} [B]^T\{\sigma\}\,dV \right] =$$
$$= \{\delta d\}^T \left[\int_{V_e} [N]^T\{F\}\,dV + \int_{S_e} [N]^T\{\Phi\}\,dS + \sum_{i=1}^{n}\{p\}_i \right] \tag{4.5}$$

The expression from below is valid for any arbitrary kinematic admissible displacement $\{\delta d\}$ and thus:

$$[m]\{\ddot{d}\} + [c]\{\dot{d}\} + \{r^{int}\} = \{r^{ext}\} \tag{4.6}$$

Considering linear elastic materials, then $\{\sigma\} = [E][B]\{d\}$. Hence, the internal node forces are calculated as shown in Equation 4.7, where $[k]$ is the stiffness matrix.

$$\{r^{int}\} = \int_{V_e} [B]^T\{\sigma\}\,dV = \int_{V_e} [B]^T[E][B]\{d\}\,dV = \int_{V_e} [B]^T[E][B]\,dV\{d\} = [k]\{d\} \tag{4.7}$$

If now the global level is considered then, for linear elastic materials, the dynamic equilibrium equation is as shown in Equation 4.8.

$$[M]\{\ddot{D}\} + [C]\{\dot{D}\} + [K]\{D\} = \{R^{ext}\} \tag{4.8}$$

The global matrices and vectors can be expressed as shown in Equation 4.9.

$$[M] = \sum_{n=1}^{N_e}[m] \;\;,\;\; [C] = \sum_{n=1}^{N_e}[c] \;\;,\;\; [K] = \sum_{n=1}^{N_e}[k] \;\;,\;\; \{R^{ext}\} = \sum_{n=1}^{N_e}\{r^{ext}\} \tag{4.9}$$

Depending on the value of $\{R^{ext}\}$, different problems can be considered:

- $\{R^{ext}\} = \{0\}$ - Eigenfrequency problem.
- $\{R^{ext}\} = \{0\}$ and initial conditions $\{D\}|_{t=0} = \{D_0\}$ and $\{\dot{D}\}|_{t=0} = \{V_0\}$ - Free vibrations with nonzero initial conditions, displacements are found for $t \in [0, T]$.
- $\{R^{ext}\} = \begin{bmatrix} \cos(\omega t + \phi) \\ ... \end{bmatrix} \{R_0^{ext}\}$ - Steady-state harmonic vibrations ($t \to \infty$).

- $\{R^{ext}\}$ given as a function of time and initial conditions $\{D\}|_{t=0} = \{D_0\}$ and $\{\dot{D}\}|_{t=0} = \{V_0\}$ - Time-history analysis, dynamic response of the structure for $t \in [0, T]$.
- $\{R^{ext}\}$ as a random excitation in time - Random vibrations, looking for standard deviation values of displacements, stress...

The problems covered in this report are the eigenvalue problem, subsection 4.2.1 and the steady-state harmonic vibrations, subsection 4.2.2.

4.2 Vibration Analysis

The focus of this project is made on the first and third problems from the above list, meaning the eigenvalue problem and harmonic analysis. The defined theory is the framework of the software, ANSYS, to build the mathematical model and be able to solve the problem. Therefore, the application of this theory will be seen in chapter 5.

4.2.1 Undamped Free Vibrations - Eigenvalue Problem

The eigenvalue problem is the same as saying free vibration analysis. Moreover, the method used for solving these problems is known as modal analysis. Modal analysis is the study of the dynamic properties of systems in the frequency domain. It is an indispensable tool in understanding the structural dynamics of objects and it is the most fundamental linear dynamics analysis (Gjelstrup, 2021). Essentially, it looks for the natural frequencies of a structure, which only depend on the stiffness and the mass of the model. It is also the typical common dynamic simulation for many other dynamic simulations such as harmonic, random vibration, response spectrum and transient dynamic (AnsysInnovationCourses, 2020).

Modal analysis studies are based on the applied forces, how structures and objects vibrate and how resistant they are. It allows machines and structures to be tested, optimised, and validated to identify if any structure is exposed to forces that may introduce damaging or destructive resonant frequencies without damping.

Modal analysis is performed for free vibrations and it retrieves eigenfrequencies and eigenmodes (Rao, 2011). For solving a dynamic response of a structure, the bases are set in the general equation of motion, on a global level, refer to Equation 4.8.

Since natural frequencies, and associated mode shapes, are the structure's property and they are independent of any loading then, the RHS of the equation is zero. Moreover, for general modal analysis, the damping effects are usually not taken into account and therefore, the term can be eliminated. The final equation looks like Equation 4.10 and is for a free undamped vibrations system.

$$[M]\{\ddot{D}\} + [K]\{D\} = \{0\} \tag{4.10}$$

The stiffness matrix, $[K]$, relates the applied forces to the displacement and, for one element, it is the volume integral over the element, see Equation 4.11 (Cook et al., 2002).

$$[K] = \int_{V_e} [B]^T[E][B]\, dV \tag{4.11}$$

$[B]$	Strain-displacement matrix	[Varies]
$[E]$	Constitutive matrix - Young's Modulus	[Pa]

The constitutive matrix, $[E]$, is derived based on the stress-strain relations from the elasticity theory. The constitutive matrix is constant when the material is homogeneous within the element. The strain-displacement matrix relates nodal displacements, $[d]$, to strains, $[\varepsilon]$ in the element. Therefore, the strains can be expresses as $\varepsilon = [B]d = [\partial][N]$.

On the other hand, the mass matrix, $[M]$, is a discrete representation of a continuous mass distribution as shown in Equation 4.12.

$$[M] = \int_{V_e} \rho[N]^T[N]\, dV \tag{4.12}$$

ρ	Density (homogeneous material)	$[kg/m^3]$
$[N]$	Shape functions	[Varies]

This is known as *consistent mass matrix* formulation. Here, consistent means that it comes directly from finite element discretization and uses the same shape functions as the element stiffness matrix.

With the focus on the time domain, when the loads are zero then, it describes a structure without any motion or constant velocity. Therefore, the acceleration is zero, $\{\ddot{u}(t)\} = 0$, and no meaningful results are obtained. However, if the focus is made on the frequency domain, interesting results are found. For treating the problem in the frequency domain then, it has to be assumed that every point of the structure experiences harmonic motion.

Harmonic motion means that all points from a structure are vibrating at the same angular frequency, ω, but with different amplitudes, A, or magnitude of the deformation and phase angle, θ, $x = A\sin(\omega t + \theta)$. This can be interpreted as the relative timing of the vibration.

If the harmonic motion is assumed for every point of the structure, the displacement and acceleration vectors can be expressed as shown in Equation 4.13 and Equation 4.14 respectively.

$$\{D\} = \{\bar{D}\}\sin(\omega_i t + \theta_i) \tag{4.13}$$

$$\{\ddot{D}\} = -\omega_i^2\{\bar{D}\}\sin(\omega_i t + \theta_i) \tag{4.14}$$

$\{\bar{D}\}$	Nodal amplitudes	[m]
ω_i	Angular frequency	[rad/s]
t	Time	[s]
θ_i	Phase angle	[s]

By substitution in Equation 4.10, the eigenvalue problem is obtained, see Equation 4.15.

$$([K] - \lambda[M])\{\bar{D}\} = \{0\} \;\; ; \;\; where \;\; \lambda = \omega^2 \tag{4.15}$$

$$
\begin{array}{c|l}
\lambda = \omega_i^2 & \text{Eigenvalue} \\
\{\bar{D}\} & \text{Eigenvector}
\end{array}
$$

The trivial solution is if $\{\bar{D}\}$ from Equation 4.15 is equal to zero. In order to avoid this solution, the determinant is set inside the brackets as shown in Equation 4.16.

$$det([K] - \lambda[M]) = 0 \;\; ; \;\; where \;\; \lambda = \omega^2 \tag{4.16}$$

As $[M]$ and $[K]$ are known matrix, the determinant can be solve for λ, Equation 4.17.

$$\lambda = \frac{[K]}{[M]} = \omega^2 \tag{4.17}$$

By taking the square root, the eigenvalues or the angular frequencies are found, ω_i. This frequency is related to the natural frequency by Equation 4.18, given in Hertz [Hz] or cycles per second, by dividing it over 2π.

$$f_i = \frac{\omega_i}{2\pi} = \frac{1}{2\pi}\sqrt{\frac{k}{m}} \tag{4.18}$$

The eigenvectors or mode shapes can be found from Equation 4.15, $\{\bar{D}\}$. Mode shape is the deformation pattern at the given natural frequency, f_i, and they represent relative deformations. They are essentially vectors that represent directions in the coordinate system and the value of the components is not absolute. For a realistic modal analysis, mode shapes can be plotted on different scales but still represent the same mode shape. Therefore, the absolute magnitude of the deformation in the modal analysis has no meaning.

Generally, the number of mode shapes is equal to the number of degrees of freedom of the system, meaning the size of the system matrix. The higher the frequency mode, the more limited effect has on the dynamic behaviour of the structure unless the excitation frequency is also high or when it is necessary to capture the rigid body behaviour. Therefore, the necessary modes are directly related to the structure and the loading environment.

4.2.2 Forced Vibrations - Harmonic Analysis

Harmonic analysis determines the steady-state response of a structure that is subjected to loads that vary sinusoidally over time. Also known as forced vibration analysis.

From the previous sections, the general dynamic equilibrium equation for a linear elastic material was found, refer to Equation 4.8. Later on, for free undamped vibrations, the generalised eigenvalue problem equation was derived, refer to Equation 4.15. After solving the eigenvalue

problem equation, the eigenfrequencies and eigenvectors - modes - were obtained. They gave information on the excitation frequencies that could case resonance. However, the solution did not provide any information regarding the actual deformations, $\{D\}$. For this reason, harmonic analyses are performed.

For setting the harmonic analysis, the applied force has to be defined first. Three main types can be considered for a spring-mass system (BrownUniversity):

- External forcing - models the behaviour of a system which has a time varying force acting on it.
- Base excitation - models the behaviour of a vibration isolation system. A prescribed motion is given to the base of the spring so that the mass vibrates.
- Rotor excitation - models the effect of a rotating machine mounted on a flexible floor. The mass vibrated due to the rotation of the crack with the small mass.

The force applied on the analyses from chapter 5 is base excitation which prevents excitation from passing from a vibrating base through its mount into the structure. It is selected since it is the standard excitation for electronic components according to the Nordtest method. The goal is to minimize the vibrations of the mass or structure, knowing the acceleration that the base has which makes the mass move (Rao, 2011). Generally is known as support motion or seismic excitation, see Figure 4.1.
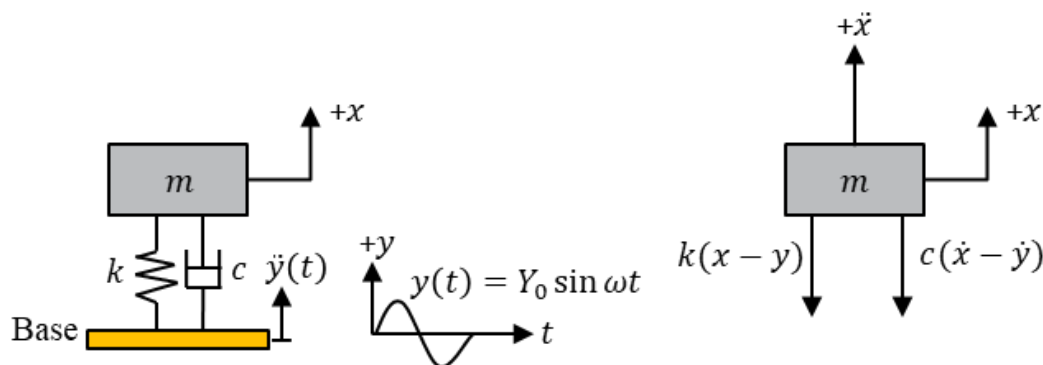

Figure 4.1. *Base excitation force.*

Here $y(t)$ denotes displacement of the base and $x(t)$ the displacement of the mass from its static equilibrium position at time t. Thus, the net elongation of the spring is $x - y$ and the relative velocity between the two ends of the damper is $\dot{x} - \dot{y}$, Equation 4.19.

$$m\ddot{x} + c(\dot{x} - \dot{y}) + k(x - y) = 0 \tag{4.19}$$

Considering that the $y(t) = Y_0 \sin \omega t$, it can be seen that the given excitation to the base is equivalent to the application of a harmonic force of magnitude A to the mass.

$$m\ddot{x} + c\dot{x} + kx = ky + c\dot{y} = kY_0 \sin \omega t + c\omega Y_0 \cos \omega t = A \sin(\omega t - \alpha) \tag{4.20}$$

$$A = Y_0 \sqrt{k^2 + (c\omega)^2} \tag{4.21}$$

$$\alpha = \tan^{-1}\left[-\frac{c\omega}{k}\right] \tag{4.22}$$

Finally, the problem can be solved with one of these methods:

- Full Harmonic Method - all the forces are added to the RHS of the full FEM and the dynamic equation is directly solved by integration.
- Reduced Harmonic Method - use the reduced structure matrices to solve the equation of motion. The equations are reduced to the master's degrees of freedom (DoF).
- Mode Superposition Method - the forces are decomposed into modes. The different modes are considered and then superimpose the results for each of them.

The focus of this project is made on the Mode Superposition and therefore, a greater explanation is made. This method uses a linear combination of mode shapes to determine the displacement vector of the structure. Therefore, it is based on the solution of the free undamped vibration problem. With this method, the solver finds the response of the structure over a range of frequencies. The overall response is the function of the considered modes then, it is desirable to include a wide variety of modes so as not to leave out any important mode (Cook et al., 2002).

The Mode Superposition Method decouples the ordinary system of second-order partial differential equations by a transformation of variables. Meaning that it converts the system n x n simultaneous equations into n uncoupled equations that can be solved independently. This method is based on the properties of the eigenvectors, they have linear independently and orthogonality.

If the stiffness and mass matrices, from the eigenvalue problem, are symmetric then, eigenvectors are orthogonal concerning the matrices, see Equation 4.23.

$$\{\bar{D}\}_i^T [M] \{\bar{D}\}_i = 0 \ , \ \ and \ \ \{\bar{D}\}_i^T [K] \{\bar{D}\}_i = 0 \ , \ \ i \neq j \tag{4.23}$$

The eigenvectors are only a mode shape and therefore they can be scaled. Let's consider the nodal displacements $\{\bar{D}\}_i^T$ and normalised with respect to the mass matrix, Equation 4.24.

$$\{\bar{D}\}_i^T [M] \{\bar{D}\}_i = 1 \ , \ \ then \ \ \{\bar{D}\}_i^T [K] \{\bar{D}\}_i = \omega_i^2 \tag{4.24}$$

The modal matrix, $[\Phi]$, and the diagonal spectral matrix, $\lceil \omega^2 \rfloor$, are then define as in Equation 4.25.

$$[\Phi] = [\bar{D}_1, \bar{D}_2 ... \bar{D}_n] \quad and \quad \lceil \omega^2 \rfloor = \lceil \omega_1^2, \omega_2^2 ... \omega_n^2 \rfloor \tag{4.25}$$

One of the properties of the eigenvectors, obtained from the eigenvalue problem, is that they are a set of linearly independent vectors. Therefore, it is possible to express an arbitrary displacement vector, $[D]$, as a linear combination of the eigenvectors, see Equation 4.26. The columns of the modal matrix are the eigenvector and the modal displacements are contained in $\{Z\}$.

$$\{D\} = [\{\bar{D}\}_1 \{\bar{D}\}_2 \{\bar{D}\}_3 \dots \{\bar{D}\}_{n_{eq}}]\{Z\} = [\Phi]\{Z\} \ , \ \{\dot{D}\} = [\Phi]\{\dot{Z}\} \ , \ \{\ddot{D}\} = [\Phi]\{\ddot{Z}\} \ (4.26)$$

If the eigenvectors are normalized then, the modal matrix has the properties shown in Equation 4.27. Notice that $\lceil \ \rfloor$ represent diagonal matrices.

$$[\Phi]^T[M][\Phi] = \lceil I \rfloor \quad , \quad [\Phi]^T[K][\Phi] = \lceil \omega^2 \rfloor \tag{4.27}$$

Considering the dynamic equation of motion at the global lever, Equation 4.8, substituting Equation 4.26 and multiplying by $[\Phi]^T$ then, Equation 4.28 is obtained.

$$\{\ddot{Z}\} + [C_\Phi]\{\dot{Z}\} + \lceil \omega^2 \rfloor\{Z\} = [\Phi]^T\{R^{ext}\} = \{P\} \tag{4.28}$$

Here, $[C_\Phi]$ is the diagonal matrix that can be calculated as $[C_\Phi] = \alpha\lceil I \rfloor + \beta\lceil \omega^2 \rfloor$ when the damper is proportional. However, it is more common to have a modal dampening and therefore, $[C_\Phi]$ can be defined as the diagonal matrix with the ith diagonal coefficient as $2\zeta_i\omega_i$, where ζ_i is the damping ratio and it is defined for each mode. Hence, an experimental value of ζ_i can be found for each mode. As the damping matrix and $\lceil \omega^2 \rfloor$ are both diagonal then, Equation 4.28 is uncoupled. The generic equation for any mode is defined as in Equation 4.29.

$$\ddot{Z}_i + 2\zeta_i\omega_i\dot{Z}_i + \omega^2 Z_i = P_i \quad where \quad P_i = [\Phi]^T\{R^{ext}\} \tag{4.29}$$

Where $\{\Phi\}_i$ is the $i$the column of $[\Phi]$ and thus, $\{\Phi\}_i$ is the ith eigenvector $\{\bar{D}\}_i$ that has been normalise with respect to the mass matrix. Moreover, the modal load P_i is a known time function. Equation 4.29 has to be integrated in time for every i. Exact integration is possible for some specific loading, however, for general loading, direct integration can be used. For integrating, the initial conditions have to first be obtained. This can be done by inverting Equation 4.26 and considering that $[\Phi]^{-1} = [\Phi]^T\{D\}$. Knowing that values from $\{D\}$ and $\{\dot{D}\}$ for $t = 0$, then $[Z]$ and $[\dot{Z}]$ can be calculated as in Equation 4.30.

$$\{Z\} = [\Phi]^T[M]\{D\} \quad , \quad \{\dot{Z}\} = [\Phi]^T[M]\{\dot{D}\} \tag{4.30}$$

When the structure is partly or completely unconstrained, then up to the six first columns from the modal matrix are rigid-body modes, with no elastic forces in the physical structure. If it is an undamped structure, then $\ddot{Z}_i = P_i$ for rigid-body motion - which is the normal case (Cook et al., 2002).

In harmonic analysis, the frequencies that involve the most kinetic energy are those near the natural frequencies of the structure. There are two methods in ANSYS to retrieve the frequencies:

- Even frequency spacing. The number of intervals is defined and the software divides the frequency range equally according to the number of intervals indicated. Therefore, there is

always the same hertz difference between intervals. In addition, the *user defined frequencies* option can be activated to additional include the natural frequencies obtained from the modal analysis.

- Automatic frequency spacing. The number of clusters is defined and the software provides an approximate method of choosing suitable imposed frequencies.

By using the automatic frequency spacing or *cluster* option then, depending on the established damping, the imposed frequencies will be closer or further from the natural frequencies since the resonance peaks narrow when the damping is reduced (ANSYS, 2009). The imposed frequencies are calculated as:

$$\Omega^i_{-j} = \frac{\omega_i}{a_{ij}} \tag{4.31}$$

$$\Omega^i_{+j} = \omega_i \cdot a_{ij} \tag{4.32}$$

Equation 4.31 gives slightly lower frequencies than the natural frequencies, ω_j, whereas Equation 4.32 slightly higher. The spacing parameter is defined as in Equation 4.33.

$$a_{ij} = 1 + (\zeta_i)^b \tag{4.33}$$

$$b = \frac{2(N-j)}{N-1} \qquad where \quad j = 1, 2, 3, ...N \tag{4.34}$$

a_{ij}	Spacing parameter
ζ_i	Modal damping
b	Coefficient
N	Integer constant between 2 and 20

Moreover, each natural frequency and the midway between are also considered as imposed frequencies when doing automatic frequency spacing. Figure 4.2 shows two typical resonance peaks and the imposed frequencies chosen by this method.
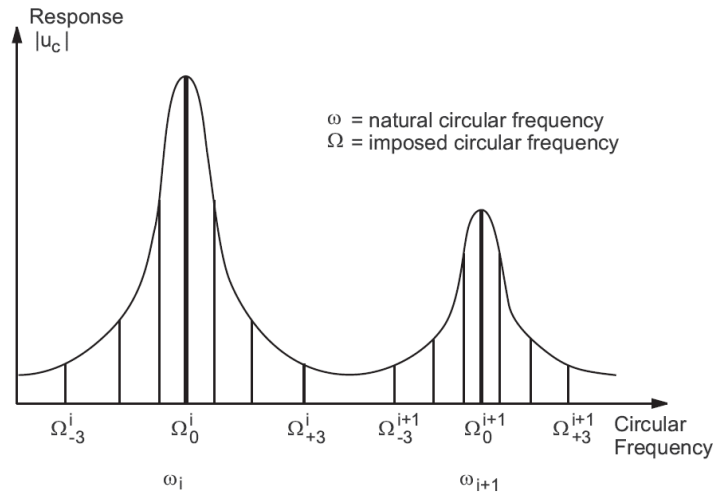
Figure 4.2. *Automatic frequency spacing (ANSYS, 2009).*

From the harmonic analysis, three results are expected:

- Frequency response plot - the value of the quantity over a range of frequencies, deformation vs. frequency range.
- Phase response plot - lag between input and output responses.
- Contour plot - distribution of stresses, strains, etc at a given frequency, usually at the highest frequency found from the frequency response plot.

If the system is excited at a natural frequency then, resonance might be present and it can vibrate tending to infinity amplitude. By introducing a small amount of damping, the number is limited to a finite value and therefore the solution is more realistic. The damping effect introduces lag between responses.

In order to understand and anticipate how vibrations are translated into structure–borne noise, Equivalent Radiated Power (ERP) - frequency response plot - can be used. It is a simple way to characterize structural borne noise and it provides information about maximal possible acoustic radiation of panels for specific frequency domain excitation, no air modelling is needed and no equations systems have to be solved (Huang and Cui, 2016). The no need of including the fluid to decrease the effort, time and cost. ERP is obtained from deriving the complex intensity equation in frequency domain, Equation 4.35 (Luegmair, 2015).

$$\vec{\underline{I}} = \underline{p} \cdot \vec{\underline{v}} \tag{4.35}$$

$$
\begin{array}{c|l}
\underline{I} & \text{Complex intensity} \\
\underline{p} & \text{Complex pressure} \\
\underline{v} & \text{Complex particle velocity}
\end{array}
$$

If the intensity is integrated over the area A with an explicit spatial orientation then, the acoustic power, W, is:

$$W = \Re \left\{ \int_A \vec{\underline{I}} \, d\vec{A} \right\} \tag{4.36}$$

Thus, the pressure and spacial particle velocity have to be known for each point or node, which is only possible if the full fluid-structure is modelled. Hence, the assumption of plane wave radiation is considered. Meaning that from a rigid plane radiating structure surface, only plane waves can be emitted. A plane wave is characterized by having only one dimension and having the sound pressure and particle velocity in phase. The resulting impedance, Z, is calculated as in Equation 4.37 and it is real.

$$Z = \frac{\hat{p}}{\hat{v}} = \rho_F \cdot c_F \tag{4.37}$$

Z	Impedance
$\hat{p}$	Amplitude of sound pressure
$\hat{v}$	Amplitude of particle velocity
ρ_F	Density of air
c_F	Sound velocity in air

Then, by substitution of Equation 4.37 in Equation 4.35, and considering a constant density and sound velocity in homogeneous media, Equation 4.36 can be simplified to:

$$W = \rho_F \cdot c_F \int_A \hat{v}^2 \, dA \tag{4.38}$$

Generally, in linear vibroacoustic, the coupling relationship that exists between structure and fluid is given by the equal of the normal velocity of the structural surface, $v_{S,n}$, and the particle velocity of the fluid, v_F, on the structural face. Meaning $v_{S,n} = v_F$ and thus, the particle velocity from Equation 4.38 can be substituted by normal velocity of the structure surface. Therefore, the frequency dependent ERP formula is as shown in Equation 4.39 and it is possible to estimate the radiated acoustic power, W_{rad}, only from the structural behaviour of the model, in [W].

$$W_{rad} = \rho_F \cdot c_F \int_A |\hat{v}_{S,n}|^2 \, dA \tag{4.39}$$

The above equation evaluates the ERP value in a simulation for every element and frequency and therefore, numerous curves are calculated. Thus, the average ERP of the results is used to minimize the results data. It can be done either with spatial averaging or with frequency averaging. In this project, the first method is used and means that the integration over the surface A is not only done for one element but many elements like a panel. Therefore, it will result in a mean value of all elements that are contained by the panel. It is possible to identify the frequencies where big power is radiated by the surface but it is not possible to detect the exact area inside the panel which is causing the peak.

Generally, it is useful to know the sound power level of a structure as it characterizes the intrinsic acoustic power of an acoustic noise source. This value allows to objectively compare the sound output without knowing the environment where the structure is tested or the distance at which the measures were taken (Brüel and Kjær). There are two methods, the direct method and the comparison method. In this case, the direct method is used and an imaginary surface that covers the device under test is defined. Then, sound pressure measurements are made at several points on the surface. It is spatially averaged and corrected for the influence of the acoustical environment. Later, the sound power level can be calculated by adjusting the ratio of the surface area to the reference surface area of $1 \, \text{m}^2$ since this is where the sound power lever is equivalent to the sound pressure level. The sound power level radiated by the sound source, in [dB], can be calculated as in Equation 4.40. This magnitude, Sound power level, is used in the different harmonic analysis to study which model has greater noise.

$$L_W = 10 \cdot \log_{10} \left(\frac{W_{rad}}{W_{ref}} \right) \tag{4.40}$$

L_W	Sound power level
W_{ref}	Reference sound power (10^{-12} W by default)
W_{rad}	Radiated sound power or ERP

As the results from the ERP plot can be difficult to analyse and decide which model has more noise then, the Root Mean Square (RMS) value can be calculated for each of the models. Generally, the RMS value is useful as it is directly related to the energy content of the vibration profile and thus the destructive capability of the vibration. RMS also takes into account the time history of the waveform (Hanly, 2018). As the RMS value takes into account the changes in the curve over time, it gives us information on how much energy is stored in the vibration which in turn gives information on how powerful the vibration is (ReVibe). Therefore, the lower the value the better. In this case, it is used to have only one number that covers all frequencies for the noise, refer to Equation 4.41 for the general form.

$$RMS = \sqrt{\frac{x_1^2 + x_2^2 + ... + x_N^2}{N}} \tag{4.41}$$

Vibration Analysis 5

As mentioned in section 4.2, two analyses are included, first modal analysis and then, based on the results, the harmonic analysis is performed. Both analyses are based on the theory explained in section 4.2. First, the modal analysis node needs to be set up and then the harmonic response node is attached to the solution so those are the input on the new analysis. Later, the different materials are defined and then the geometry is uploaded to the software as it has been previously created in CATIA. Then, the association with the different parts and materials is done as well as the connections between parts. Once everything is defined, the mesh has to be set up and then the analysis settings have to be defined. In this case, the goal was to represent the real conditions of mounting and therefore, two fixed supports have been defined on the holes where the screws are going to be positioned when mounting it with the stator housing. Depending on the study, different options have been selected for getting the modal analysis results as well as for the harmonic analysis, these will be specified in each section. All the analyses are performed in ANSYS Workbench 2021 R2 as mentioned previously and a more detailed explanation of the simulations set up can be found in Appendix A.

As a rule of thumb, the frequency domain of the modal analysis has to be 1,5 times that of the harmonic form. As it is desired to include from 0 Hz to 3.000 Hz in the harmonic analysis, then the modal analysis has to be set up from 0 Hz to 4.500 Hz. Therefore, the study range is very wide and many modes need to be retrieved. However, it is known that not all the modes have the same effect on the structure as some are known as local modes and others as global modes. Local modes primarily affect a specific component and global modes affect the entire structure. When looking into local modes a finer mesh is needed to capture accurate results on the affected area. The focus of this project is on global modes, since the most important vibrations are those that occur throughout the case and not the small electronic components, as these contribute the most to the sound emission, and not that fine mesh is needed. Refer to Figure 5.1 and Figure 5.2 to see how the vibrations affect the structure, depending on which kind of mode it is. Generally, at higher frequencies, modes become local in nature, rather than global so makes sense to focus on the low frequencies.
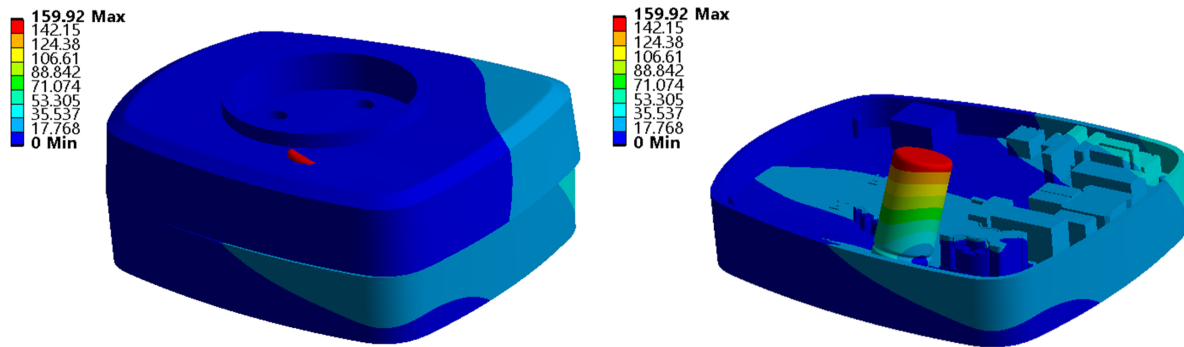
*Figure 5.1. Example of local mode on the structure, mode 7.*
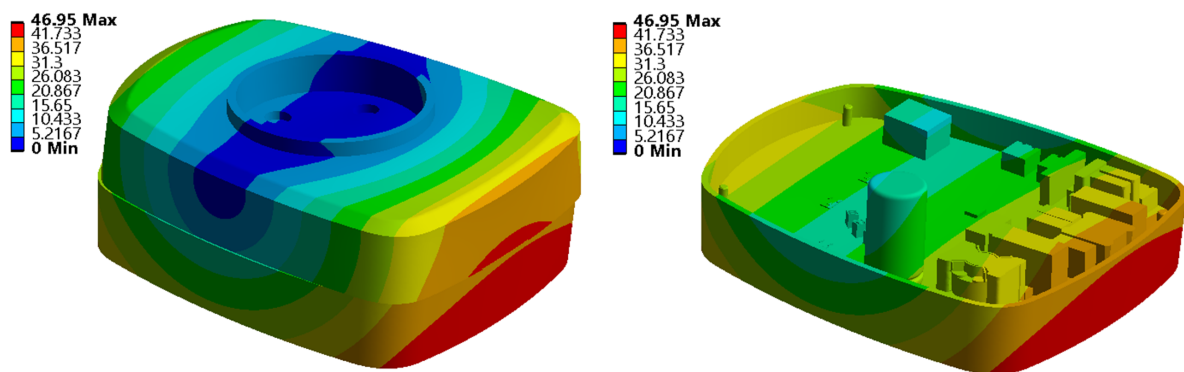
Figure 5.2. Example of global mode on the structure, mode 1.

It is known that the model from DMS3 can withstand the vibrations as it is nowadays being used and no issues have been found. Thus, this model is used as the benchmark and it will be compared to the model from section 2.2. Note that for every analysis, an accurate mesh is needed. However, the more elements are present in the model, the more computing time is needed. Therefore, a study on the mesh is performed to see the influence on the results. Moreover, a study on the influence of the material is included, aluminium against polycarbonate. However, it is necessary to perform a prior directional study on the application of the force that defines the harmonic analysis.

5.1 Benchmark Study

The first section of this chapter covers the benchmark study where the model from last semester, DMS3, is compared to the model from section 2.2 as the first one is considered the standard or point of reference. As explained in the DMS3 project, (Bermejo, 2022), only two parts are present, the bottom part made of aluminium and the cover made of polycarbonate. As the focus of the past project was only on the thermal part, the definition of the contact zones was not overdeveloped. However, when studying vibrations, depending on how the contact regions are established, different results will be achieved. For this reason, it has been decided to include the screws connecting the bottom and the top part to simulate the real conditions as much as possible. Moreover, in practice, there is a gasket between the two parts and therefore, they are not in direct contact and this is how it has been defined in ANSYS. Note that the PCB

has not been included to be able to compare results with the previous project as no PCB was incorporated in that model. Refer to Figure 5.3 for the geometry of DMS3 and to Figure 5.4 for the geometry of DMS4 without the PCB.
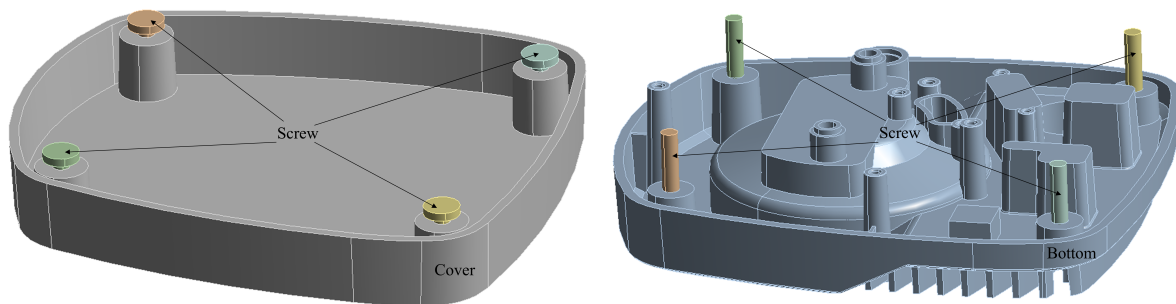
Figure 5.3. *DMS3 geometry.*
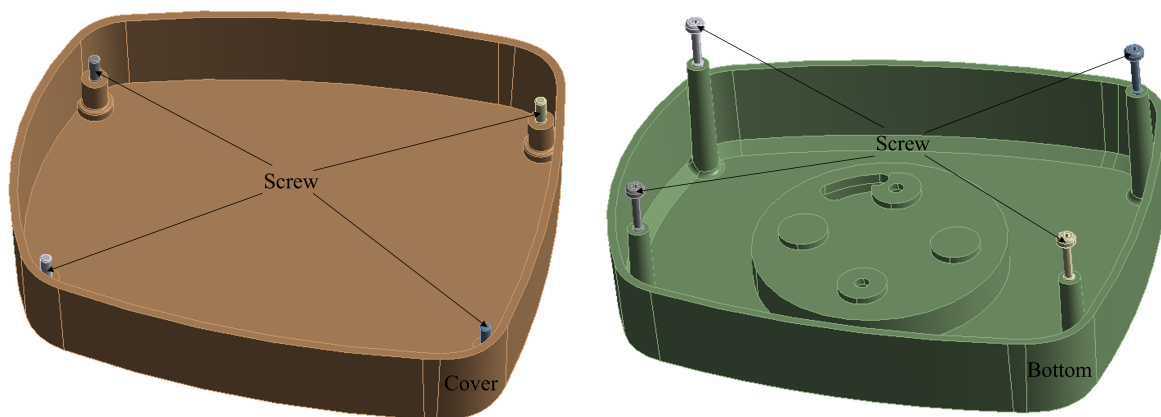
**Figure 5.4.** *DMS4 without the PCB geometry, DMS4_noPCB*

Modal Analysis

In order to perform the modal analysis of both models, a body sizing of 1 mm is defined for all bodies and the fixed supports are set, meaning through the two holes where the stator housing is connected, as shown previously in Figure 2.3. In addition, the same frequency range has been set for both models, 0 Hz to 4.500 Hz. After running the modal analysis for both models, it can be appreciated that DMS4_noPCB has lower frequencies than DMS3 and therefore it is more likely to have vibration issues. This is as expected as the frequencies are directly related to the Young's Modulus of the material, the lower the material property value then the lower the frequencies are. In this case, the aluminium's Young's Modulus is more than 3 times the one from polycarbonate, Table 2.1. Thus, the frequencies of the DMS3 model are expected to be higher as one of the parts of the case is made of aluminium. It is evident that when the model starts with lower frequencies then, it needs to retrieve more modes to achieve the stated 4.500 Hz frequency.

When the PCB is included then, some additional stiffness is introduced and this could mean an increase in frequencies. However, as the mass is increased by a factor of 3 when adding the PCB, then the frequencies would be decreased. As shown in the figure below, the mass increases

more than the stiffness and therefore it results in a decrease in the frequencies when the PCB is included in - DMS4 model. Refer to Figure 5.5 to see the three curves of frequencies concerning the modes for the DMS3 model, the DMS4_noPCB model and the DMS4 model.
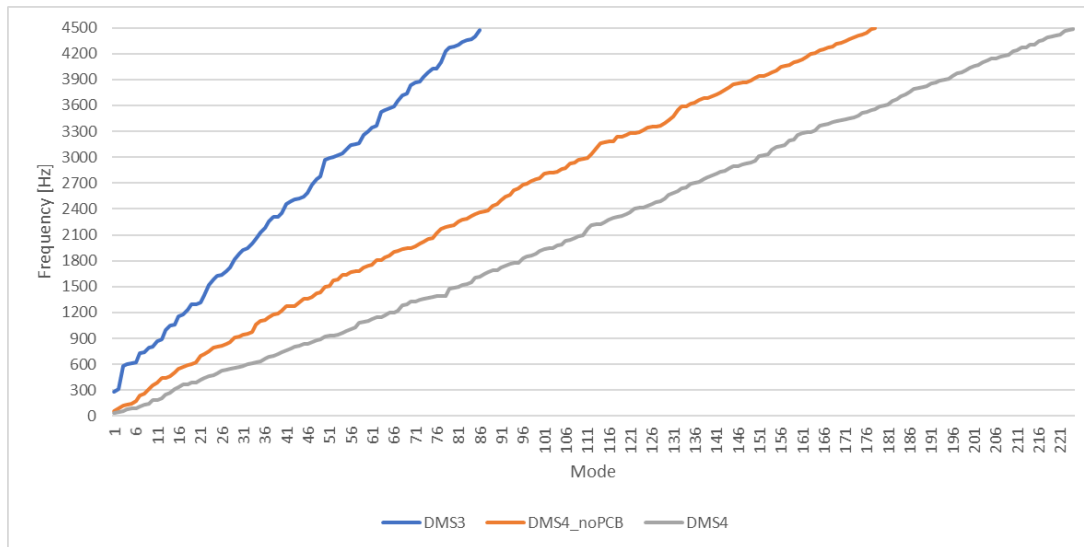
Figure 5.5. *Frequency values for the different modes for the benchmark study when performing modal analysis.*

Harmonic Analysis

Later, the harmonic analysis is performed to evaluate which of the models is better in terms of noise. For setting up this analysis, it is necessary to define first the force that governs this analysis. In this case, it is an acceleration with base excitation, Figure 4.1, through the previously defined boundary conditions or fixed support. The magnitude selected is $1\,\mathrm{mm/s^2}$ in the z-direction. This direction has been selected as it is expected to be the one with the highest excitation, refer to Figure 5.9 for verification. The range of frequencies to search for in this study goes from $0\,\mathrm{Hz}$ to $3.000\,\mathrm{Hz}$.

The method used is Mode Superposition meaning, the modal analysis is first computed to retrieve the natural frequencies and mode shapes. Then, the mode superposition solution is obtained by combining those mode shapes. Even frequency spacing, with *user defined frequencies* option activated, has been used in order to evaluate the harmonic response. As 1.000 solution intervals are defined then, there is an increment of $3\,\mathrm{Hz}$ for each frequency until the $3.000\,\mathrm{Hz}$ is achieved. Moreover, the natural frequencies are included in the results. With this method, some peaks might be missing for not using the *cluster* option.

Moreover, the included viscous damping is of $2\,\%$, recommended by Grundfos. Notice that this damping magnitude is accurate for the aluminium but not totally for the polycarbonate as in reality is higher. Considering the definition of damping as the reduction in the magnitude of oscillations by the dissipation of energy then, the higher the damping ratio the lower the vibrations are. For this reason, even if the number for polycarbonate is not accurate, the real results will be better than in the simulations as no high vibrations will be present. Therefore, it is assumed as a safe choice.

When looking into Figure 5.6 it is possible to appreciate the ERP of the three models, in dB. Note that the closer to the frequency range operation of the pump, the more likely is to have the same excitation on the pump and the case and therefore failure due to resonance. However, it is important to consider the uncertainty of 10% to 20% and thus, it is not sure that the same frequencies will be hit in any of the cases. In case this would happen then, it is possible to slightly modify or shift the frequencies by adding extra material and the problem would be solved. Moreover, as shown previously, when the PCB is incorporated then the frequencies and the modes shapes are also modified.
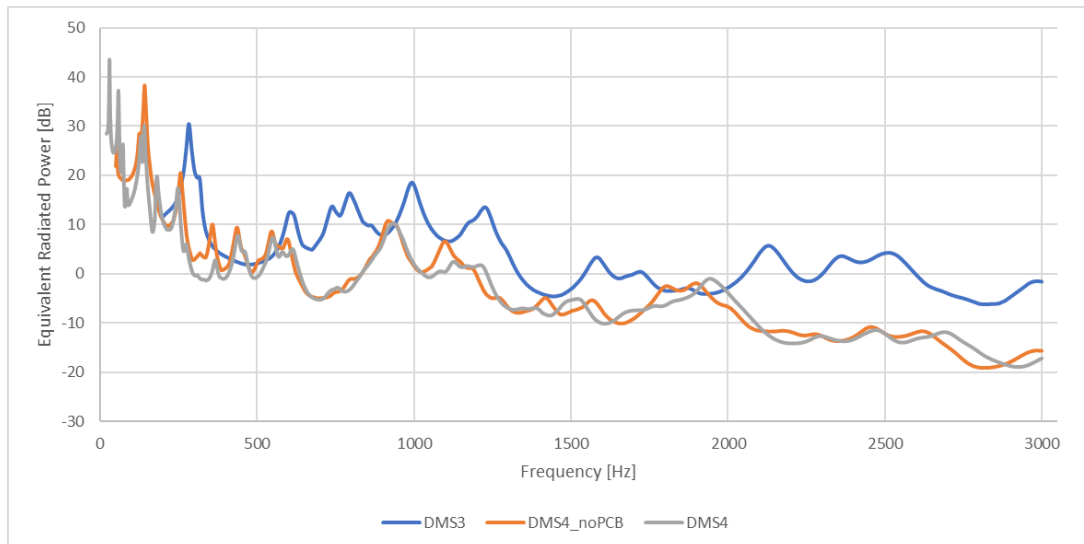
Figure 5.6. *Equivalent Radiated Power in dB for the benchmark study when performing harmonic analysis.*

Note that the results for the DMS3 model and DMS4_noPCB are similar, considering a shift of approximately $150\,\text{Hz}$ in the positive x-direction for the DMS3 model. Therefore, if the curve from the past model is moved this quantity to the left then, one curve is laying on top of the other. With this change, it is expected that the values of the DMS4_noPCB are in general slightly lower. However, it can be appreciated that the maximum peak in the new model is bigger than in the old one and therefore the noise from the DMS4 model is expected higher. Moreover, it is known that by increasing the mass of the model the vibrations can be decreased. As the DMS4_noPCB model is the 44% of the DMS3 model, it is expected that the DMS3 model will have lower noise. In addition, the mass from the DMS4 model is 3 times the DMS4_noPCB and hence, the noise from the DMS4 should be lower. Thus, there is no clear answer for it and for this reason the RMS is calculated. It is important to consider the same range of frequencies and as the DMS4_noPCB model and DMS4 model start earlier than the DMS3 model, then the last modes of these two have to be removed to have the same number of information in all three cases. As shown in Table 5.1, the RMS value of the DMS3 model is the lowest and thus better. For this reason, a parametric study is done later on in chapter 7, to investigate if it is possible to minimize the noise of the new model.

Model	RMS [dB]
DMS3	8,977
DMS4_noPCB	13,776
DMS4	11,284

Table 5.1. *Root Mean Square values for the benchmark study.*

5.2 Mesh Study

As mentioned in section 4.1, the body has to be divided into finite elements and it is done with the mesh generation. Depending on the quality of the mesh, the results will be more precise or less. Sometimes, if not enough elements are created within an area then, the results might not show the appropriate behaviour. Nevertheless, it is important to consider also the computational time as the number of elements is directly related to it and therefore to the price. Ideally, ANSYS recommends having at least two elements in the thickness of every part to be able to capture normal and shear stresses accurately. If this is not the case, shear locking may appear, which in reality does not exist, as the linear elements are not able to capture the kinematic deformation. This will make the element appear stiffer than it really is. However, as the goal is to look into eigenvalues and eigenfrequencies, it is not as important as if the interest is in stresses assuming that the model will not be overly stiff. Moreover, since the focus of this project is on the global modes, not that fine mesh is needed as if the interest will be on the local modes.

An initial study is made to analyse different meshes and reach convergence on the results. The first mesh - Mesh 1 - is a coarse mesh, with the automatic mesh defined by ANSYS. Then, for the second mesh - Mesh 2, body sizing is used for the three biggest components, the PCB, the bottom part and the cover part, with an element size of 2 mm while the rest of the components are kept automatic. The third mesh - Mesh 3 - is defined with a body sizing of 0,5 mm for the small components such as DPAK-Die, DPAK-S, DPAK-G, R4, R5, R6 and SMPC, whereas the rest, medium and big components, are set to 2 mm. The next mesh, Mesh 4, is similar to the previous one, but now the components with medium size are set with a body sizing of 1,75 mm. The following mesh, Mesh 5, is everything set a body sizing of 1 mm and finally, Mesh 6, is everything set to 0,5 mm. In Table 5.2, the difference in body sizing can be seen, for each mesh, as well as the influence of the mesh refinement in the number of elements, nodes and solving time. Note that only 20 modes are extracted for this study.

Name	Mesh 1	Mesh 2	Mesh 3	Mesh 4	Mesh 5	Mesh 6
Body Sizing [mm]		Big C=2	Small C=0,5 Med C=2 Big C=2	Small C=0,5 Med C=1,75 Big C=2	All C=1	All C=0,5
Elements	99.899	406.484	448.843	473.738	3.260.583	24.971.814
Nodes	219.817	788.837	866.682	916.421	5.416.022	38.425.846
Time	1 min	3 min	2 min	2 min	70 min	13 h

Table 5.2. *Mesh study, C = Components.*

Based on the mesh study, the frequencies for different meshes, corresponding to the first 20 modes, are compared and evaluated with respect to Mesh 6 as it is considered the "perfect mesh" and it has been found that there is a convergence in the mesh. Note that the values calculated are percentage error, PE, following Equation 5.1 (Indeed, 2021).

$$PE = \frac{|Approx - Exact|}{Exact} \cdot 100 \tag{5.1}$$

Figure 5.7 show the calculations made following the previous equation to compare Mesh 1 to Mesh 5 with respect to Mesh 6 for the percentage error. Note that it is desired to not have more than 5 % variation between the selected mesh and the perfect mesh to reach convergence.
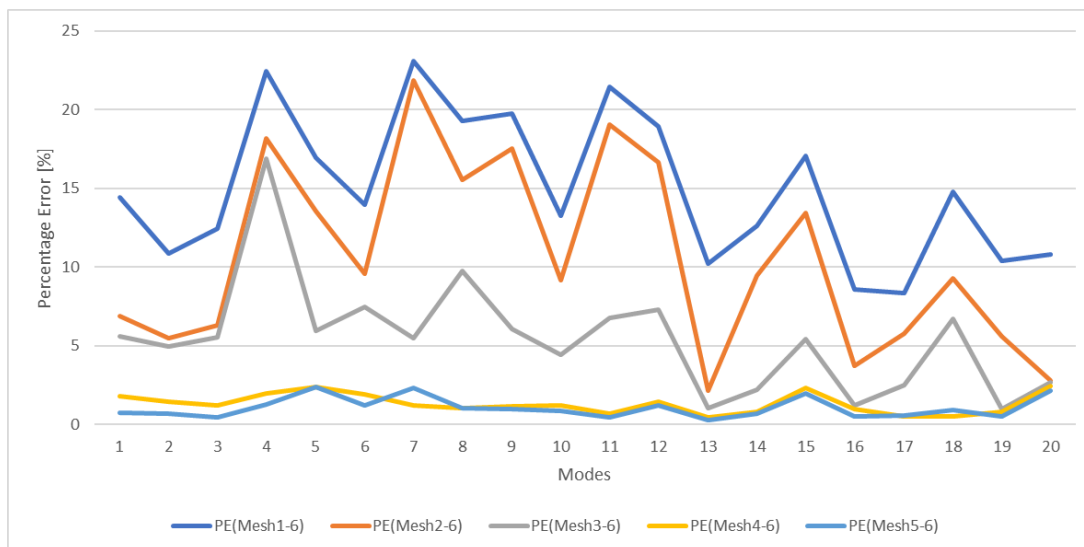

Figure 5.7. *Percentage error of the eigenfrequencies in the mesh study, with respect to the perfect mesh.*

As it can be seen from the previous figure, the percentage error of Mesh 4 and Mesh 5, with respect to the perfect mesh, do not go over 5 %. Thus, as mentioned above, it can be stated that convergence has been found in the mesh and the results of the different analyses will be accurate when one of these meshes is used. Even though Mesh 5 is more proximate to the perfect mesh, the solving time of 70 min makes it impossible to use in a parametric study and therefore, it has been decided that Mesh 4, with 2 min solving time, will give accurate results regarding the time limitations of the project and the following analysis are done with this mesh.

Mesh 4 will be used in all following analyses unless otherwise indicated, refer to Figure 5.8. This mesh uses the element type SOLID186 and SOLID187, 3D structural solids with 20 and 10 nodes respectively. Moreover, CONTA174 and TARGE170 are used where contact is defined, contact and target surfaces, following Table 2.3. They are related by a common real constant for each pair.
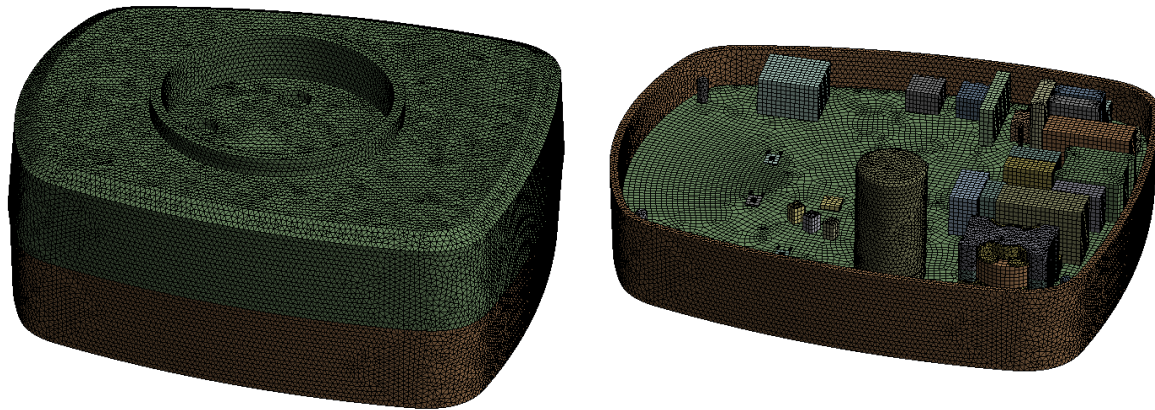
*Figure 5.8.* *Selected mesh for the analysis.*
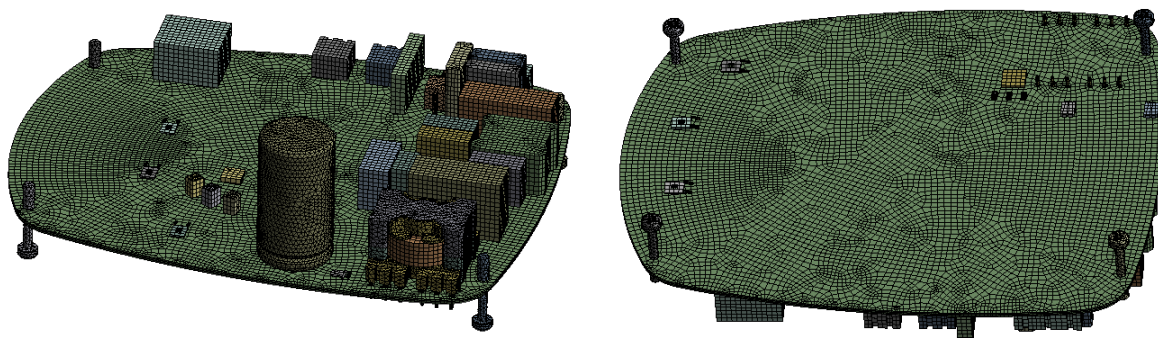
Figure 5.8. *Selected mesh for the analysis.*

5.3 Directivity Study

As mentioned in section 5.1, a basic excitation acceleration of magnitude $1\,\mathrm{mm/s^2}$ is defined through the fixed supports to run the forced vibration or harmonic analysis. This magnitude has to be established in one of the three possible directions, x-, y- or z-direction and therefore, a direction study is needed since the results will be affected by the direction in which the magnitude is applied. The goal of this study is to find the direction which is more critical and thus threatens the structure.

The model used is the one described in section 2.2, with the materials from Table 2.2, known as DMS4. As the interest is made in the harmonic analysis, following the Mode Superposition method then, the modal analysis is run first to find all the modes in the frequency range from $0\,\mathrm{Hz}$ to $4.500\,\mathrm{Hz}$. Then, the forced vibration analysis is set in the same way as in section 5.1, same frequency range, even frequency spacing, activated *user defined frequencies* option with the retrieved frequencies from the modal analysis, same damping effect and same acceleration magnitude. However, the direction of the acceleration is varied from one simulation to another, meaning that three independent simulations were run and each of the directions was studied individually. Figure 5.9 shows the ERP when the acceleration is applied in the three different directions and Table 5.3 the RMS values. The focus is on low frequencies, from about $0\,\mathrm{Hz}$ to $800\,\mathrm{Hz}$, as these can cause the model to go into resonance.
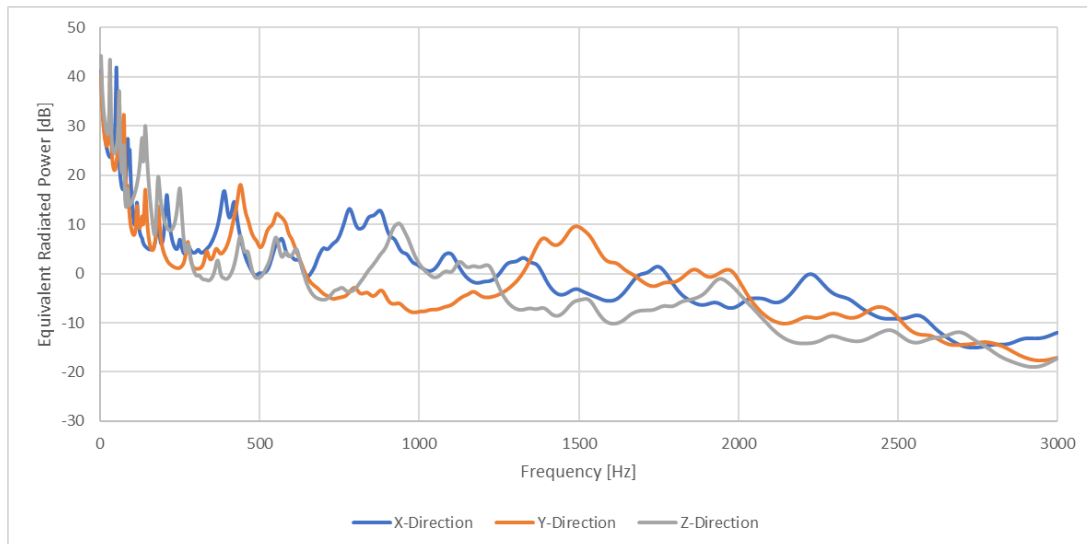
Figure 5.9. *Equivalent Radiated Power in dB for the directivity study when performing harmonic analysis.*

Directivity study	RMS [dB]
x-direction	8,885
y-direction	9,636
z-direction	10,927

Table 5.3. *Root Mean Square values for the directivity study.*

Considering that the three models are the same, with the only difference in the acceleration direction then, it is evident that the natural frequencies for all models are the same. The ERP curves show that some modes are much more excited than others for the different directions. As mentioned, the focus of the project is at low frequencies and here the highest values are obtained when the acceleration is applied in the z-direction. When looking into the RMS values, the highest value is also given for the z-direction even though there is no great difference between directions. This is caused by the fact that a kinematic excitation - base excitation - is introduced instead of a forced excitation. Thus, the amplitude is already limited as the magnitude of the acceleration is the input data.

Therefore, it is evident that the z-direction is critical. This is because the largest available area is in this direction and therefore, it will move - vibrate - the most. As mentioned previously, the higher the RMS the more powerful the noise is and therefore more dangerous for the system. This conclusion corresponds to the expectations from section 5.1. Therefore, the rest of the studies are only going to be done with the acceleration in the z-direction as it is the most critical one and the one that is more interesting to improve in the parametric study from chapter 7 in the low frequency range, from $0\,\text{Hz}$ to $800\,\text{Hz}$.

5.4   Material Study

Now, the materials are evaluated. As mentioned in chapter 1, the idea is to change the material from aluminium to polycarbonate to decrease the cost of the piece. However, the material will influence the results and therefore, it has been decided to include a comparison of results for both materials when the model described in section 2.2 is used. The first model has both parts of the case, bottom and cover, made of polycarbonate as these are the real model. The second model has the bottom made of aluminium and the cover made of polycarbonate, similar to the DMS3 project. For the final model, both parts are defined as aluminium. Notice that the materials from the other components remain the same for both studies, Table 2.2.

Modal Analysis

After performing the modal analysis, Figure 5.10 is obtained. As it can be seen in the figure, the highest frequencies are achieved when the model is made of aluminium only and the lowest when it is fully made of polycarbonate. This is as expected regarding the material's property, Young's Modulus, with respect to the stiffness and therefore to the frequencies - the higher the Young's Modulus, the higher the stiffness and therefore the frequencies, refer to Equation 4.11 and Equation 4.18.
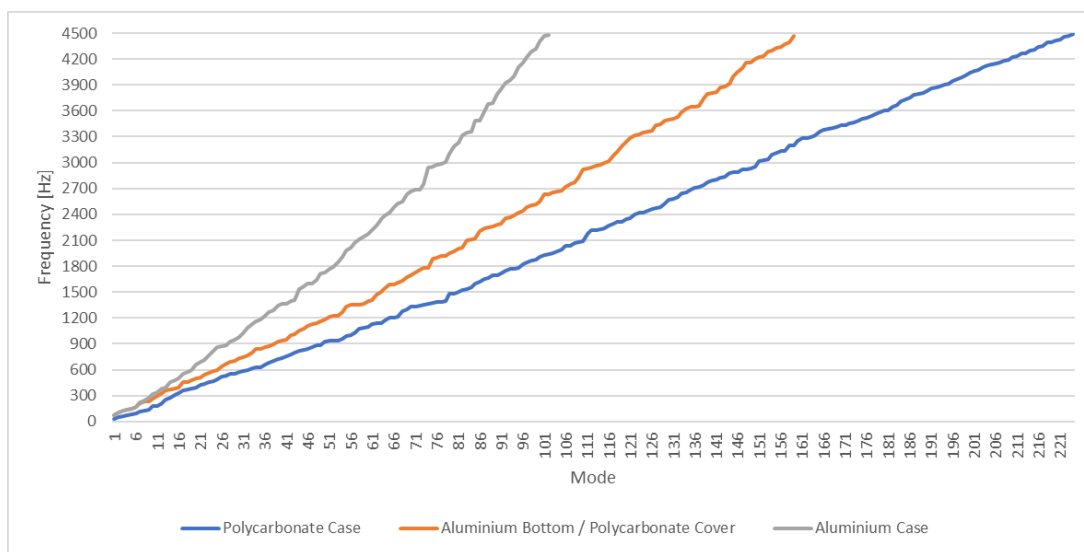

Figure 5.10. *Frequency values for the different modes for the material study when performing modal analysis.*

Harmonic Analysis

Later on, the harmonic analysis is performed to identify the best and the worst in terms of noise, as a function of the material used on the case. The model used is DMS4, section 2.2, the frequency range is from $0\,\mathrm{Hz}$ to $3.000\,\mathrm{Hz}$ and automatic frequency spacing method is used. This option allows solutions to be clustered about the natural frequencies and thus, the results are smoother and more accurate when tracing the response curve. The number of clusters, in this case 10, means that there will be 10 points clustered on either side of the natural frequency of the structure (Kiran, 2008). In addition, the damping ratio of $2\,\%$ has also been defined.

Once everything is set up, the analysis is run to obtain the ERP and compared it to the different models.
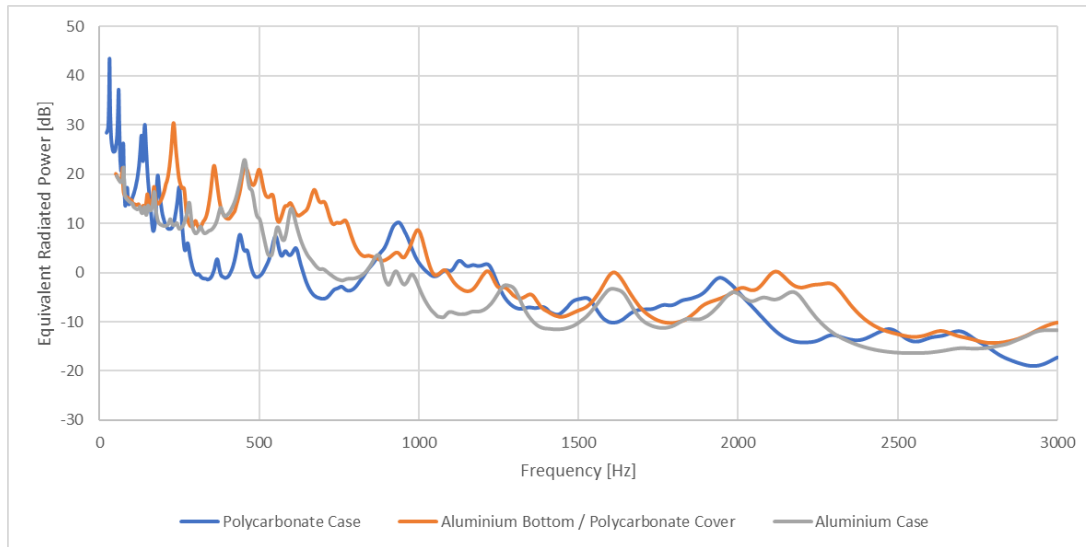
Figure 5.11. *Equivalent Radiated Power in dB for the material study when performing harmonic analysis.*

For high frequencies, the full polycarbonate case seems better, however, with a focus on the low frequencies, the maximum peak is one $10\,\text{dB}$ more than the mix of materials and almost $20\,\text{dB}$ compared to the full aluminium. As there is no clear answer, the RMS values are calculated to verify the previous statement, Table 5.4. Notice how they have been divided into low, middle and high frequencies to study which case is better for each range.

Model	0-500 Hz	500-1.000 Hz	1.000-3.000 Hz
Polycarbonate Case	17,905	5,051	10,165
Mix Aluminium and Polycarbonate Case	17,665	10,999	7,876
Aluminium Case	13,884	5,024	10,241

Table 5.4. *Root Mean Square values for different frequency ranges for the material study, in [dB].*

From the above table, it can be appreciated that, depending on the frequency range, the best and worst studied cases in terms of noise changes. For low frequencies, from $0\,\text{Hz}$ to $500\,\text{Hz}$, the full aluminium has the lower value and thus the lower the noise whereas the full polycarbonate has the highest. In the middle frequencies, $500\,\text{Hz}$ to $1.000\,\text{Hz}$, the best is again the full aluminium but the worst is the mix of aluminium and polycarbonate. Then, for the high frequencies range, $1.000\,\text{Hz}$ to $3.000\,\text{Hz}$, the one with the lowest RMS value is the mix of aluminium and polycarbonate case and the worst is the full aluminium. This agrees with what is shown in Figure 5.11. As the focus of the project is on low frequencies and the real case is only made of polycarbonate, it is desired to decrease the noise of the model in this range and therefore, a parametric study is done in chapter 7.

Thermal Analysis 6

One of the objectives of the DMS3 project was to perform a thermal analysis of the control box, based on the input of some energy sources, to analyse what was the maximum temperature reached by the model. In this project, the same is done but considering the model from section 2.2. There are two solving methods for heat transfer simulations, either using a conduction-based solver such as ANSYS Workbench or a CFD solver, also known as fluid-dynamic solver, such as FloEFD from CATIA V5. When using the second type, the solid and the fluid are considered as well as the solid-fluid interaction. These solvers are more expensive and complex. When using the conduction-based solver then, only solids are considered and the interaction with fluids is set as a boundary condition of convection. For doing so, the film coefficient and the ambient temperature have to be defined by careful experiments for complex models. Therefore, it evaluates the effect of a fluid flow without actually modelling the fluid. It is an inexpensive and easy method and therefore it is the one used in this project. However, the input data was given by Grundfos in the FloEFD solver and therefore it has been used as a reference to find by trial and error the film coefficients and ambient temperatures for the natural convection. Thus, the results from the CFD solver are considered the exact results. Refer to Appendix B for a more detailed explanation of the simulation set up.

As mentioned previously, the power sources need to be again defined as they are modified accordingly to the model. Then, the steady-state condition has been assumed even though in reality the model temperature is a function of time to minimize the computational time. The thermal study has been done for three cases: polycarbonate case, aluminium bottom and polycarbonate cover, and aluminium case.

6.1 CFD or Fluid-Dynamic Solver

The software used to solve the heat transfer simulation by means of a CFD or fluid-dynamic solver is FlOEFD. This solver takes into account not only the solids but also the fluid and the interaction between the two. Normally, this solver is more accurate than the conduction-based solver, since it is not necessary to define the film coefficient or the ambient temperature. Therefore, the results of this software have been used to know when the expected results have been found in the conduction-based solver. Nevertheless, Grundfos provided the model and the thermal set up so only the results were retrieved, refer to Figure 6.1. Note that apart from the heat sources, radiation of the PCB and the case, as well as natural convection, are applied. The ambient temperature is considered to be 55 °C.

From the below figures, it can be seen that the components that have the highest heat are the

DPAK, then the copper layers that are on the PCB and then the transformer, with a temperature of approximately 101 °C to 115 °C. The outer enclosure does not have a uniform distribution and the temperature range is from approximately 57 °C to 93 °C. The hottest areas of the enclosure are those closest to the hot electronic components and the PCB area, while the coolest areas of the enclosure are those closest to the components that do not radiate heat.
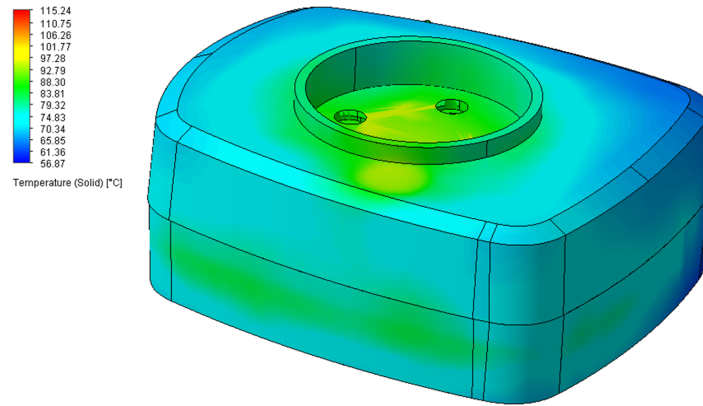
Figure 6.1. Control box results from FloEFD solver.
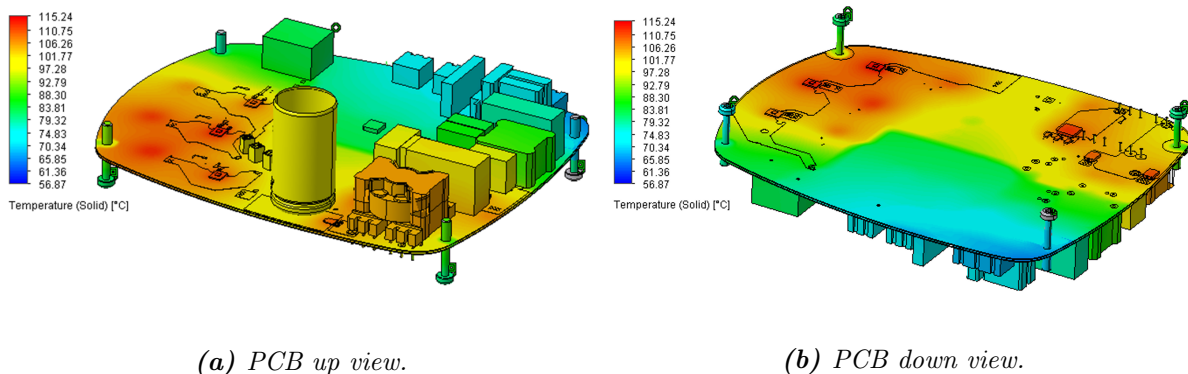
*(a)* PCB up view.   *(b)* PCB down view.

Figure 6.1. Components of the PCB, up and down view, results from FloEFD solver.

6.2   Conduction-Based Solver

The software used to run the simulations, and subsequently for parametric study, is the steady state-thermal node of ANSYS Workbench, a conduction-based solver. It has been decided to use the same mesh as in vibration analyses, Mesh 4 from Table 5.2 and no further investigation has been done as it is considered that the mesh will not influence excessively on the results as only thermal analysis is being done. The different power sources, heat transfer coefficients and temperatures that are present in the model are stated in this section. The three different models considered are the same as previously studied in section 5.4. As in this software, it is not possible to include the volume heat sources in $[W]$ as in FloEFD then, it is necessary to modify the units to be per unit volume $[W/mm^3]$ and thus apply it as internal heat generation.

Figure 6.2 shows the PCB, up and down, with all the components and their names and Table 6.1 the values of the input heat sources. Note that the volume, as well as the power per volume of each component, is also included in the table to be able to apply the heat source inside ANSYS.

(a) *PCB top face view.*

(b) *PCB down face view.*
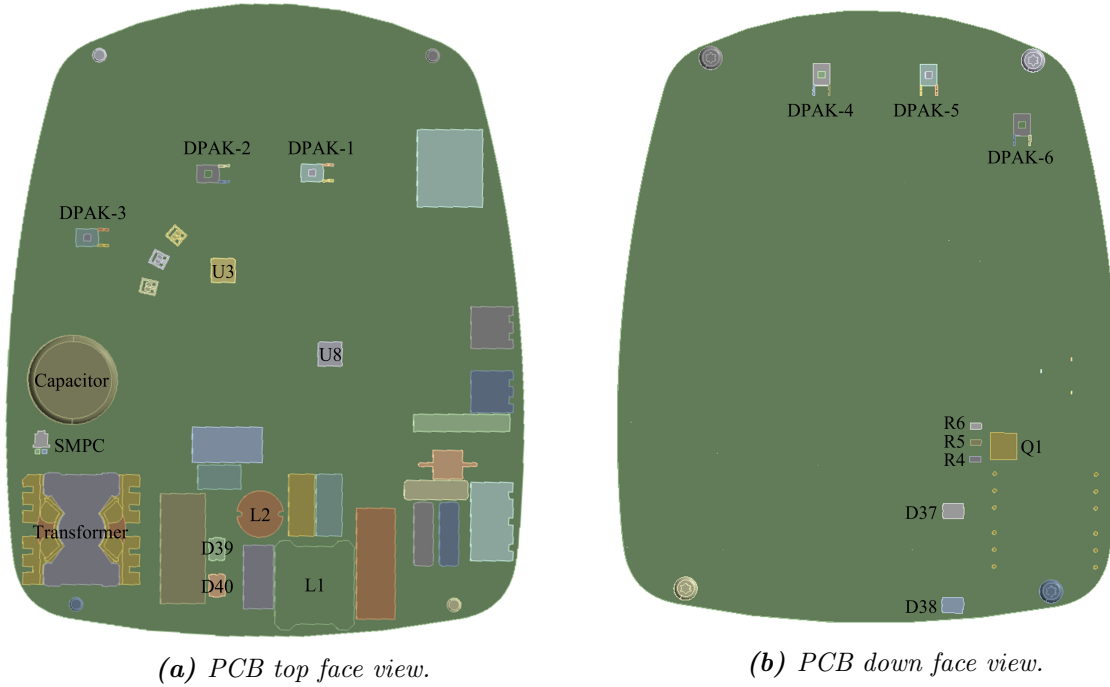
Figure 6.2. *Components of the PCB with a heat source, up and down view.*

Component	Volume $[mm^3]$	Value $[W]$	Value $[W/mm^3]$
Capacitor	24.249	0,3	$1,237 \cdot 10^{-5}$
DPAK-1 - Die DPAK-2 - Die DPAK-3 - Die DPAK-4 - Die DPAK-5 - Die DPAK-6 - Die	1	1,17	1,17
D37 D38 D39 D40	35,684	0,54	$1,513 \cdot 10^{-2}$
L1	8.527,4	0,3	$3,518 \cdot 10^{-5}$
L2	1.011,8	0,2	$1,977 \cdot 10^{-4}$
Q1	70,4	0,95	$1,349 \cdot 10^{-2}$
R4 R5 R6	4,198	0,1	$2,382 \cdot 10^{-2}$
SMPC	6,927	0,83	$1,198 \cdot 10^{-1}$
Transformer - Core (2)	4.371,4	0,315	$7,206 \cdot 10^{-5}$
Transformer - Winding	2.882	0,3	$1,041 \cdot 10^{-4}$
U3 U8	83,087	0,05	$6,018 \cdot 10^{-4}$

Table 6.1. *Input volume heat sources for the steady-state thermal analysis.*

Moreover, a surface heat flow of 1,3 W is defined on the top face of the PCB. In addition, radiation is defined with an emissivity coefficient of 0,9, considering the FR4 material, from both faces of the PCB with an ambient temperature of 95 °C. Then, the heat is absorbed by the inside of the case and conducted through the case to the outer surface of it. Later, radiation is again defined from the outer faces of the case with an emissivity coefficient of 0,9 for the polycarbonate material and 0,02 for the aluminium and an ambient temperature of 55 °C. In addition, the boundary condition of 95 °C where the stator house is located has also been included. Finally, natural convection should be defined around the case. However, in steady-state thermal analysis in ANSYS, it is only possible to include forced convection by defining the film coefficient and the ambient temperature, as a conduction-based solver is used.

As mentioned previously, those two values have to be found by careful experiments or empirical relations. Note that the experiments have been carried out to have similar results to the ones from FloEFD and therefore, the material used for the control box is polycarbonate. It will be assumed that these values are correct even if the material of the case is modified. Several numerical calculations have been done in order to get a first approximation. For doing so, first, the sum of the power dissipated and the dissipation area for each of the sections of the model have been obtained. Then, the heat flux has been calculated as in Equation 6.1.

$$q_c = \frac{Q}{A} = h \cdot (T_S - T_B) = h \cdot \Delta T \tag{6.1}$$

q_c	Heat flux	$[W/mm^2]$
Q	Heat rate	$[W]$
A	Cross-sectional area	mm^2
h	Film coefficient	$[W/(mm^2 \cdot °C)]$
T_S	Surface temperature	$[°C]$
T_B	Bulk or ambient temperature	$[°C]$
ΔT	Different of temperatures	$[°C]$

Therefore, the film coefficient is a function of the heat flux and the difference in temperature. As the temperatures are unknown, it has been assumed as a 10 °C variation between the surface temperature and the ambient temperature as they are in a small close space. As the ambient temperature is also needed, an assumption has been made based on the results from the previous section. Refer to Table 6.2 for the values of the heat source, the surface of heat dissipation, the film coefficient and the ambient temperature values. Four different values are calculated:

- PCB_TopFace - heat dissipated and dissipation surface area of the electronic components and PCB from the top face.
- InnerSurface_TopFace - heat absorbed and absorption surface area of the inner surface of the bottom part, part in contact with the air of the top face of the PCB.
- PCB_DownFace - heat dissipated and dissipation surface area of the electronic components from the bottom face.
- InnerSurface_DownFace - heat absorbed and absorption surface area of the inner surface of the cover part, part in contact with the air of the down face of the PCB.

Mention that a fifth convection boundary condition has been included to simulate the heat going from the outer surface of the case and then to the external air. Note that usually the film coefficient of the air at $22\,°C$ is usually $5 \times 10^{-6}\,[\text{W}/(\text{mm}^2\,°C)]$ for the simplified case but as it increases with the temperature then, it has been adjusted to the actual ambient temperature for the outer surface. Nevertheless, no further investigation has been done.

Components	Heat rate [W]	Surface [mm^2]	Heat flux [W/mm^2]	Film coefficienta [$W/(mm^2 \cdot °C)$]	T_B [$°C$]
PCB_TopFace	8,55	35.335,357	$2,42 \cdot 10^{-4}$	$2,420 \cdot 10^{-5}$	95
InnerSur_TopFace		51.774	$1,651 \cdot 10^{-4}$	$1,651 \cdot 10^{-5}$	
PCB_DownFace	5,84	271,57	$2,15 \cdot 10^{-2}$	$2,150 \cdot 10^{-3}$	75
InnerSur_DownFace		44.628	$1,309 \cdot 10^{-4}$	$1,309 \cdot 10^{-5}$	
OuterSurface	-	-	-	$1 \cdot 10^{-5}$	55

***Table 6.2.*** *Convection as boundary conditions.*

As mentioned in section 2.2, the PCB has been modified to only one solid made of FR4 material, glass-reinforced epoxy laminate material, and no layers of coppers. Therefore, it is evident that the conduction of the heat is better when copper is present due to the isotropic thermal conductivity properties, $394{,}7\,\text{W/m}\,°C$, rather than the FR4 value of $0{,}38\,\text{W/m}\,°C$. Thus, by adjusting this parameter from the FR4, it is possible to improve the conductivity and extract more heat from the electronic components into the PCB and hence decrease the temperature of the overall model. After performing different analyses, it was concluded that when increasing the value to $20\,\text{W/m}\,°C$ then, enough accurate results were obtained compared to the results from the CFD solver, see below for results.

6.3 Material Study

A materials study has been done to see the influence on the results as a function of the material of the case. Three different study cases are considered: full polycarbonate case, mix of polycarbonate and aluminium case and full aluminium case.

Polycarbonate Case

The results from the previous calculations of the film coefficient and ambient temperature, among the different heat sources and radiation properties, lead to Figure 6.3.
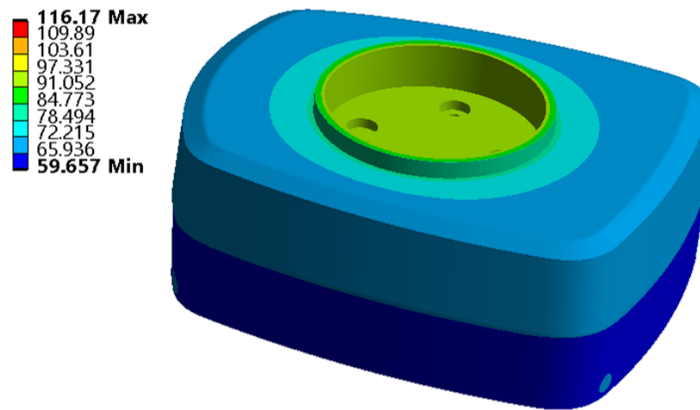
Figure 6.3. *Control box results from ANSYS solver, for polycarbonate case.*
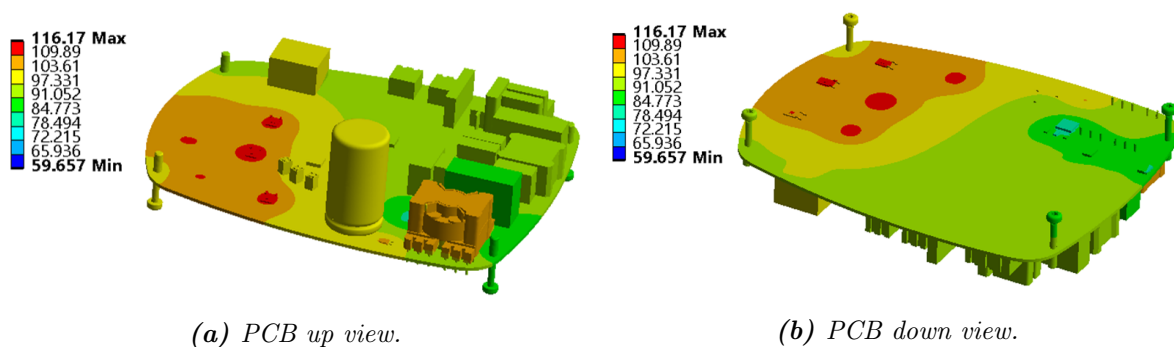

(a) PCB up view.   *(b) PCB down view.*

Figure 6.3. *Components of the PCB, up and down view, results from ANSYS solver, for polycarbonate case.*

The obtained values from the simulations from the electronic components and the PCB are almost the same as the ones with the FloEFD, with approximately 5 % difference. However, notice that it seems that the electronic components that do not dissipate heat are now in general a bit warmer than previously in FloEFD. This might be due to the adjustment of the isotropic thermal properties of the PCB as in reality no explicit net of copper might be present there and thus no heat will be conducted in that area. On the other hand, it can also be due to not extracting properly the heat from the inside of the case to the outside as almost no difference is found in the case in the areas close to colder or warmer components. Regardless, as only relative studies are done, this is a sufficient valid approximation. In addition, the focus of this analysis is on the PCB and not the case, since the highest temperature is expected on the board, and the results are fairly close there. Therefore, these values will be used for the rest of the simulations.

As mentioned in section 2.1, the properties of the materials are a function of the temperature but also of the exposition time. In this case, the maximum temperature does not go over the critical one, $135\,°C$, and therefore it should be safe to operate even after long periods as the analyses are done once the equilibrium is reached and the temperature will remain constant over time.

Aluminium Bottom and Polycarbonate Cover

For this part, the material of the bottom part of the case has been changed to aluminium in order to simulate the conditions from the DMS3 project. It can be appreciated from Figure 6.4 that the heat distribution on the PCB and the electronic components is slightly modified. The maximum temperature has decreased about 1 °C and the area close to the screws has now a lower temperature compared to the previous case. This difference can be explained by the fact that heat is extracted faster from the inside and therefore the temperature near the screws is lower. However, notice that it can also be due to the errors in how the simulations are set up. The temperature that the bottom part achieves goes from 85 °C to 97 °C approximately when before it was from 66 °C to 75 °C roughly. This means that now, as the aluminium thermal properties reveal better heat conduction than polycarbonate, refer to Table 2.1 then, more heat is transferred to the outside and therefore higher temperatures are found on the outer surface of the case. Notice that now the cover part of the case has also 2 °C more. Even though the temperature of the bottom part has been elevated, the model can withstand the temperatures with no issues and it will not affect the mechanical properties of the material.
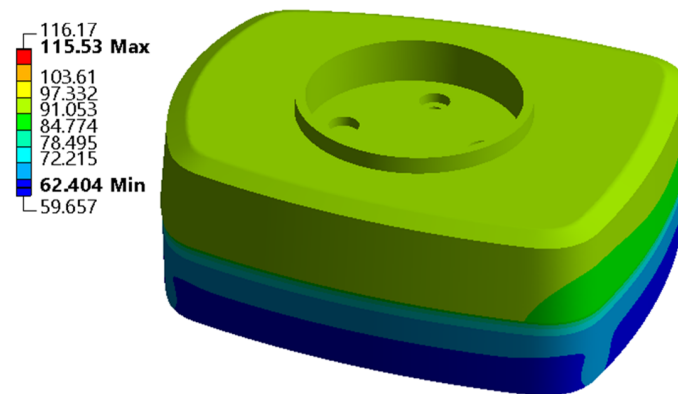
Figure 6.4. *Control box results from ANSYS solver, for aluminium bottom and polycarbonate cover. Modified contour legend.*

*(a)* *PCB up view.*   *(b)* *PCB down view.*
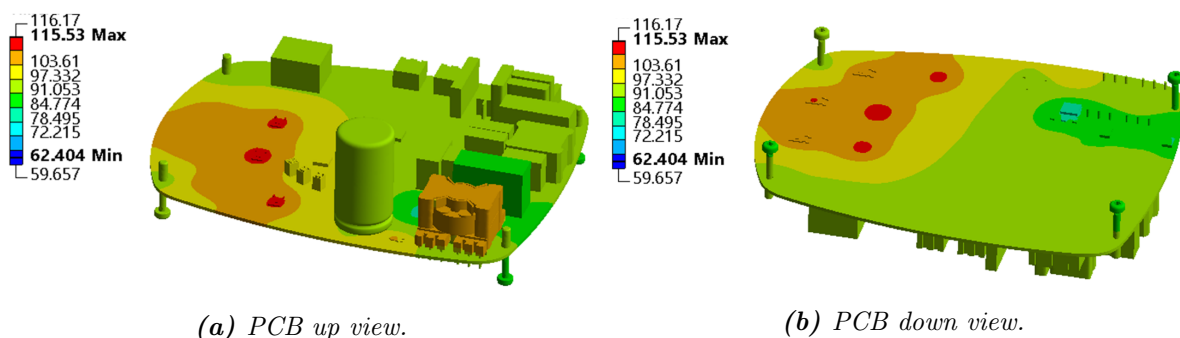
Figure 6.4. *Components of the PCB, up and down view, results from ANSYS solver, for aluminium bottom and polycarbonate cover. Modified contour legend.*

Aluminium Case

Now, both parts of the control box are set to aluminium. Figure 6.5 shows that some more variations of temperature are found. Not only on the cover part that has increased its overall

temperature by $20\,^\circ\mathrm{C}$ and keep the same as in the previous section for the bottom part made of aluminium. Moreover, the inside of the PCB looks similar to the previous case but with lower temperatures on the screw areas. The model can withstand the temperatures with no issues, as explained in the other two cases. Notice that the maximum temperature has decreased about $2\,^\circ\mathrm{C}$ with respect to the full polycarbonate case.
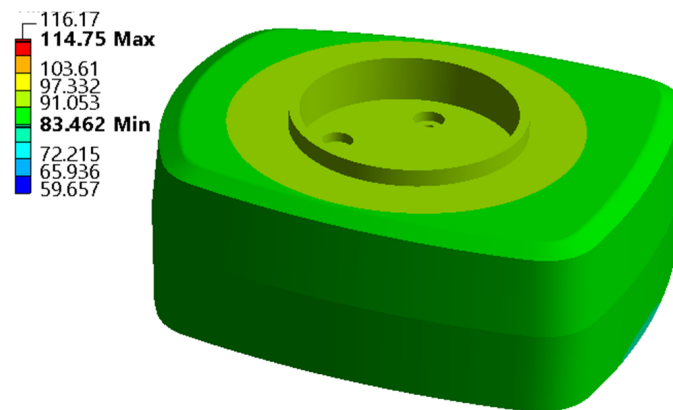
Figure 6.5. *Control box results from ANSYS solver, for aluminium case. Modified contour legend.*

(a) *PCB up view.*   **(b)** *PCB down view.*
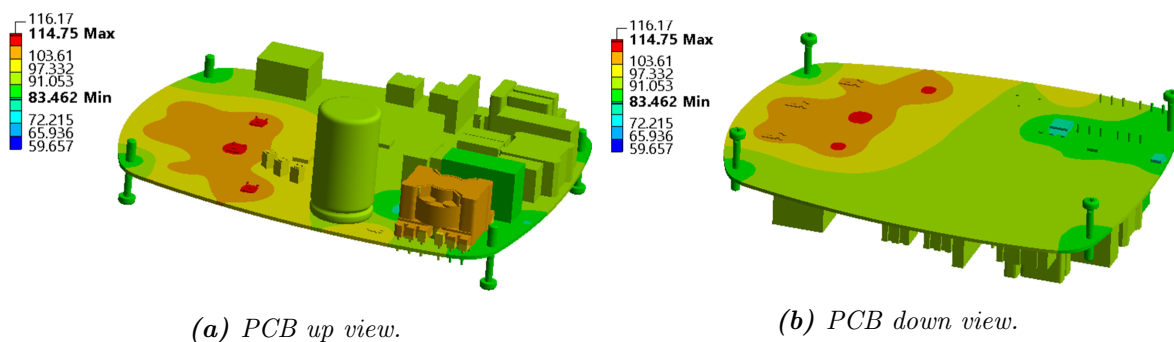
Figure 6.5. *Components of the PCB, up and down view, results from ANSYS solver, for aluminium case. Modified contour legend.*

Therefore, there is also an influence of the material of the case with respect to the temperature gradient. The better the conduction properties of the material, the higher will be the temperature of the control box as more heat will be dissipated. Thus, the maximum temperature of the model will decrease with the presence of aluminium.

Parametric Study 7

This chapter is based on the results of the previous chapters of the vibration analysis, chapter 5, and the thermal analysis, chapter 6. In the vibration chapter, it is concluded that some changes are necessary to decrease the noise to the values of the DMS3 model and in the thermal analysis that the model can withstand the temperature without problems. However, the lower the maximum temperature of the model, the better it will be to extend the lifetime of the components.

It is believed that by modifying the position of the screws that connect the three main parts and varying the thickness of the case it is possible to modify the results of noise and temperature. Therefore, it is desired to find the best combination of parameters that minimize the noise and temperature of the model. Therefore, a parametric study was performed to see the influence of the parameters on the results. Note that for speeding up the simulations, the model for the vibrations has been simplified.

7.1 Parameters Definition

It is believed that by modifying the position of the screws that connect the three main parts and varying the thickness of the case it is possible to modify the results of noise and temperature. Thus, eight parameters have been defined to control the position of the four screws with respect to the origin of the model. The designation of the parameters is given by the letter "S" followed by the number of the screw, from 1 to 4, and the letter "x" or "y" according to the axis on which the dimension is considered. Thus, the created parameters are $S1x, S1y, S2x, S2y, S3x, S3y, S4x, S4y$. Moreover, these parameters have been used to modify the position of the holes on the PCB as well as the screw towers from the bottom and cover parts since their location has to correspond to the location of the screws. As it is a desire to control the position, the parameters to define the location with respect to the three-axis have been defined for the four screws. Note that all screws and holes have the same starting and finishing point, meaning that the location on the z-direction is the same for all four, respectively, and it is not intended to be changed. This is due to the fact that if they are modified then, the other parts, cover and bottom, will not fit with the PCB and screws.

In addition, one more parameter has been defined to modify the thickness of the case, named T. This parameter has been chosen since it is known that the vibrations can be minimised if the mass of the structure is increased. Notice that even if the thickness of the case is modified, the stator housing connection should remain the same so that it always fits. Therefore, the geometry of the bottom part of the case has been modified so this is possible. Moreover, the geometry has been modified too in order to have the screw towers always with the same shape and have

always contact between the PCB and the inner walls of the cover. Refer to Figure 7.1 for the identification of the parameters.
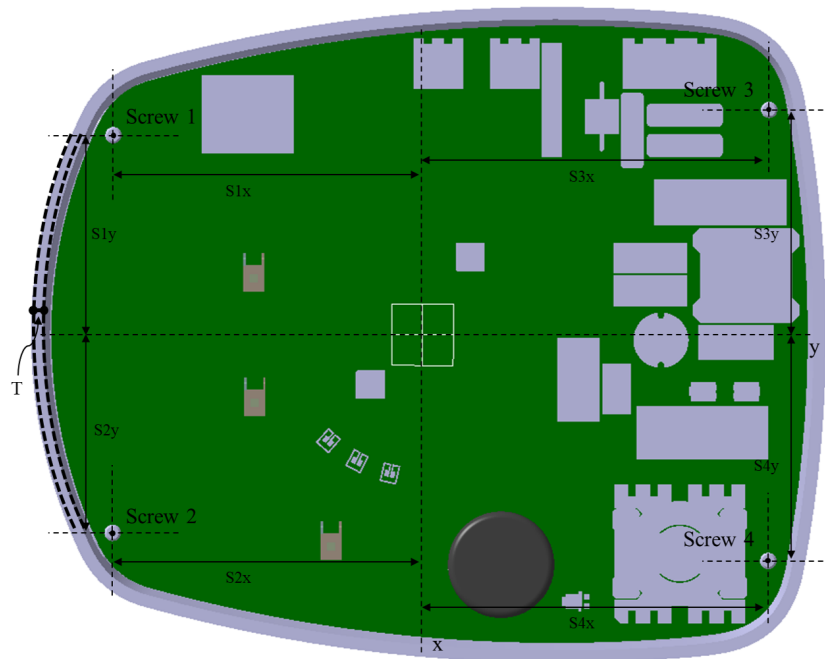
Figure 7.1. *Location of parameters for the sensitivity study.*

The parametric study is based on Taguchi Method, developed by Dr. Genichi Taguchi. It uses a robust design of experiments to decrease the variations in a process. The main goal is to produce a high-quality product with a low manufacturing cost. Several experiments are defined to investigate the effect of different parameters that define the process performance. It is based on the use of orthogonal arrays to organize the parameters and the levels in which they have to be varied.

Using this method, pairs of combinations are tested instead of all possible combinations. With few experiments, the parameters with more impact on the product quality can be identified and therefore, the time and cost will be minimized (Fraley et al., 2021). It has been decided to use the nine created parameters and five levels of study, refer to Table 7.1. Notice that the first level corresponds to the initial values of the parameters. Following the Taguchi Array Selector then, an L50 array is needed (YorkUniversity, 2004). This means that 50 different combinations are defined to analyse the influence of the parameters in the results.

Level/Parameter	S1x	S1y	S2x	S2y	S3x	S3y	S4x	S4y	T
1	48,5	75,5	48,5	75,5	55,0	84,5	55,0	84,5	3,0
2	43,5	70,5	43,5	70,5	50,0	79,5	50,0	79,5	1,0
3	38,5	65,5	38,5	65,5	45,0	74,5	45,0	74,5	9,0
4	33,5	60,5	33,5	60,5	40,0	69,5	40,0	69,5	5,0
5	28,5	55,5	28,5	55,5	35,0	64,5	35,0	64,5	7,0

***Table 7.1.*** *Values for each parameter and level, in mm.*

7.2 Model Simplification Study

Considering that Taguchi Method propose 50 combinations of parameters, based on 9 parameters and 5 levels, then, 50 simulations need to done and each of them must be agile. Therefore, it has been decided to eliminate the smallest electronic components from the PCB to decrease the computational time, when doing vibration analysis. Figure 7.2 shows the PCB with the full model with a red cross on top of all the components that have been eliminated for defining the simplified model.

**(a)** *Top face.*   **(b)** *Down face.*

Figure 7.2. *Components of the simplified model.*

When the simplified model is used, the solving time of the modal analysis decrease 30 min approximately and enough accurate results are obtained, refer to Figure 7.3.
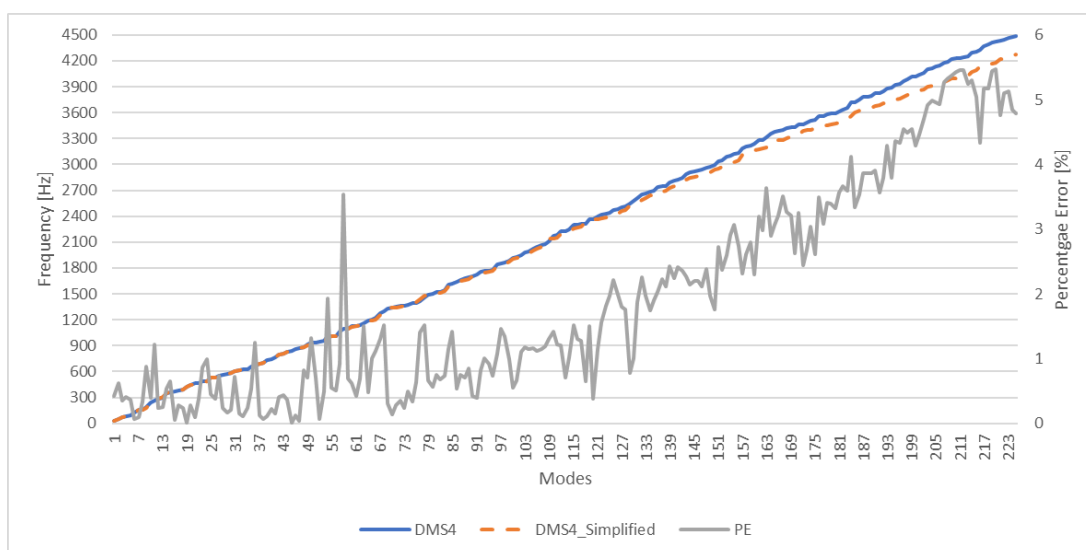
Figure 7.3. *Model simplification study.*

As it can be seen from the picture above, the eigenfrequencies from both models are almost the same as the percentage error, Equation 5.1, do not go over 5 % for most of the cases. Notice that this is not true for frequencies over 3.600 Hz. However, as the study is focused on low frequencies, up to 800 Hz then, the results from the simplified model - DMS4_Simplified - are accurate enough. After performing the harmonic analysis for this simplified model and comparing it with the full DMS4 model, it can be concluded that the results are very similar, Figure 7.4.
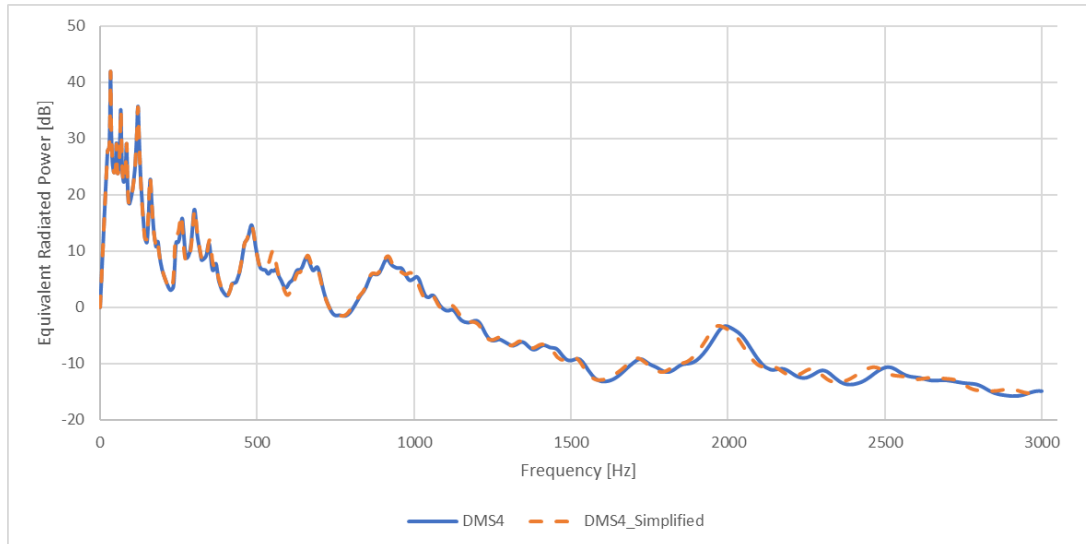
Figure 7.4. *Model simplification study.*

Therefore, this simplified model will be used for the parametric study simulations when doing vibrations in order to decrease the computational solving time. Nevertheless, for the thermal analysis, all the electronic components are considered as they influence significantly the results.

7.3 Parameters Influence

Once the model is adapted to be able to control the position of the screws as well as the thickness of the case and the different experiments are defined then, the maximum value of the ERP in [W] of each of them can be retrieved and converted into [dB] with Equation 4.40. Note that the objective function is discontinuous, which means that the ERP value obtained is not for the same frequency in the different experiments. However, it gives a good approximation for deciding which combination is better for the noise. Mention that only the harmonic analysis has been included in the report since the modal analysis showed only a small change in the resonances. On the other hand, the modal shapes that influence the noise, which is reflected in the harmonic analysis, are more affected. In addition, the maximum temperature of the model has also been extracted to compare the results of the different designs. The proposed combination of parameters and values as well as the maximum ERP value and temperature, for each of the 50 experiments, are shown in Table 7.2.

Exp	S1x	S1y	S2x	S2y	S3x	S3y	S4x	S4y	T	ERP$_{max}$	Temp$_{max}$
1	48,5	75,5	48,5	75,5	55,0	84,5	55,0	84,5	3,0	41,754	116,3
2	48,5	70,5	43,5	70,5	50,0	79,5	50,0	79,5	1,0	49,865	116,2
3	48,5	65,5	38,5	65,5	45,0	74,5	45,0	74,5	9,0	39,210	115,8
4	48,5	60,5	33,5	60,5	40,0	69,5	40,0	69,5	5,0	39,738	117,4
5	48,5	55,5	28,5	55,5	35,0	64,5	35,0	64,5	7,0	39,250	115,9
6	43,5	75,5	43,5	65,5	40,0	64,5	55,0	79,5	9,0	39,033	116,1
7	43,5	70,5	38,5	60,5	35,0	84,5	50,0	74,5	5,0	40,128	115,8
8	43,5	65,5	33,5	55,5	55,0	79,5	45,0	69,5	7,0	39,724	115,8
9	43,5	60,5	28,5	75,5	50,0	74,5	40,0	64,5	3,0	40,394	116,0
10	43,5	55,5	48,5	70,5	45,0	69,5	35,0	84,5	1,0	49,484	116,4
11	38,5	75,5	38,5	55,5	50,0	69,5	40,0	84,5	9,0	39,175	116,0
12	38,5	70,5	33,5	75,5	45,0	64,5	35,0	79,5	5,0	39,599	115,9
13	38,5	65,5	28,5	70,5	40,0	84,5	55,0	74,5	7,0	39,691	115,9
14	38,5	60,5	48,5	65,5	35,0	79,5	50,0	69,5	3,0	40,710	116,2
15	38,5	55,5	43,5	60,5	55,0	74,5	45,0	64,5	1,0	50,010	116,2
16	33,5	75,5	33,5	70,5	35,0	74,5	35,0	74,5	3,0	39,816	116,0
17	33,5	70,5	28,5	65,5	55,0	69,5	55,0	69,5	1,0	49,945	116,1
18	33,5	65,5	48,5	60,5	50,0	64,5	50,0	64,5	9,0	39,019	116,2
19	33,5	60,5	43,5	55,5	45,0	84,5	45,0	84,5	5,0	40,361	116,0
20	33,5	55,5	38,5	75,5	40,0	79,5	40,0	79,5	7,0	39,582	115,9
21	28,5	75,5	28,5	60,5	45,0	79,5	40,0	74,5	1,0	50,128	117,2
22	28,5	70,5	48,5	55,5	40,0	74,5	35,0	69,5	9,0	38,951	115,9
23	28,5	65,5	43,5	75,5	35,0	69,5	55,0	64,5	5,0	39,315	116,2
24	28,5	60,5	38,5	70,5	55,0	64,5	50,0	84,5	7,0	39,575	116,1
25	28,5	55,5	33,5	65,5	50,0	84,5	45,0	79,5	3,0	41,392	116,0
26	48,5	75,5	48,5	60,5	35,0	69,5	45,0	79,5	7,0	39,324	116,2
27	48,5	70,5	43,5	55,5	55,0	64,5	40,0	74,5	3,0	40,633	117,3
28	48,5	65,5	38,5	75,5	50,0	84,5	35,0	69,5	1,0	49,763	116,1
29	48,5	60,5	33,5	70,5	45,0	79,5	55,0	64,5	9,0	39,297	116,1
30	48,5	55,5	28,5	65,5	40,0	74,5	50,0	84,5	5,0	40,188	115,7
31	43,5	75,5	43,5	75,5	45,0	74,5	50,0	69,5	7,0	39,428	116,3
32	43,5	70,5	38,5	70,5	40,0	69,5	45,0	64,5	3,0	39,884	116,0
33	43,5	65,5	33,5	65,5	35,0	64,5	40,0	84,5	1,0	47,888	116,1
34	43,5	60,5	28,5	60,5	55,0	84,5	35,0	79,5	9,0	39,508	115,8
35	43,5	55,5	48,5	55,5	50,0	79,5	55,0	74,5	5,0	40,338	116,1
36	38,5	75,5	38,5	65,5	55,0	79,5	35,0	64,5	5,0	39,895	116,0
37	38,5	70,5	33,5	60,5	50,0	74,5	55,0	84,5	7,0	39,678	115,8
38	38,5	65,5	28,5	55,5	45,0	69,5	50,0	79,5	3,0	40,582	115,8
39	38,5	60,5	48,5	75,5	40,0	64,5	45,0	74,5	1,0	48,670	116,3
40	38,5	55,5	43,5	70,5	35,0	84,5	40,0	69,5	9,0	39,226	117,5
41	33,5	75,5	33,5	55,5	40,0	84,5	50,0	64,5	1,0	50,207	116,0
42	33,5	70,5	28,5	75,5	35,0	79,5	45,0	84,5	9,0	39,186	115,8
43	33,5	65,5	48,5	70,5	55,0	74,5	40,0	79,5	5,0	40,108	116,1
44	33,5	60,5	43,5	65,5	50,0	69,5	35,0	74,5	7,0	39,384	115,9
45	33,5	55,5	38,5	60,5	45,0	64,5	55,0	69,5	3,0	40,438	116,1

Table 7.2. *Influence of the screw positions and case thickness in vibrations and temperature, following Taguchi Method. Parameters in [mm], ERP in [dB] and Temp in [°C].*

Exp	S1x	S1y	S2x	S2y	S3x	S3y	S4x	S4y	T	ERP$_{max}$	Temp$_{max}$
46	28,5	75,5	28,5	70,5	50,0	64,5	45,0	69,5	5,0	39,503	115,9
47	28,5	70,5	48,5	65,5	45,0	84,5	40,0	64,5	7,0	39,461	117,4
48	28,5	65,5	43,5	60,5	40,0	79,5	35,0	84,5	3,0	40,765	116,1
49	28,5	60,5	38,5	55,5	35,0	74,5	55,0	79,5	1,0	49,737	116,0
50	28,5	55,5	33,5	75,5	55,0	69,5	50,0	74,5	9,0	39,237	116,0

Table 7.2. *Influence of the screw positions and case thickness in noise and temperature, following Taguchi Method. Parameters in [mm], ERP in [dB] and Temp in [°C].*

From the results, a correlation matrix can be obtained. It is a simple table that displays the correlation coefficients for different variables. It depicts the correlation between all the possible pairs of values in the table with the use of the Pearson Product-Moment Correlation (PPMC) coefficient or Pearson correlation coefficient, Equation 7.1.

$$r = \frac{\sum_{i=1}^{n}(x_i - \bar{x})(y_i - \bar{y})}{\sqrt{\sum_{i=1}^{n}(x_i - \bar{x})^2}\sqrt{\sum_{i=1}^{n}(y_i - \bar{y})^2}} \tag{7.1}$$

r	Pearson correlation coefficient
x_i	Individual sample for the first variable
$\bar{x}$	Sample mean for the first variable
y_i	Individual sample for the second variable
$\bar{y}$	Sample mean for the second variable
n	Sample size

This coefficient is a measure of the linear association between two variables that goes from -1 to +1. If the values are negative then there is a negative correlation between variables and positive if the value is positive. If the coefficient is a 0 then, there is no correlation between the variables. The greater the distance from 0, the stronger the relationship between the variables (LaerdStatistics, 2020). Notice that the cells have been coloured for an easier understanding of the correlation coefficients where green means positive correlation, red means negative correlation and white means no correlation, refer to Figure 7.5.

	S1x	S1y	S2x	S2y	S3x	S3y	S4x	S4y	T	Max ERP
Max ERP	-0,001	-0,006	0,001	-0,023	0,048	0,069	0,029	0,014	-0,782	1
Max Temp	0,004	0,029	0,294	-0,041	-0,034	0,038	-0,178	-0,214	-0,094	0,108

Figure 7.5. *Correlation matrix.*

From the figure above it is evident that the greatest influence on the maximum radiated power is due to the thickness of the case. As it is a negative value then, the correlation is negative. Meaning that when the thickness of the case increase, the maximum radiated power decrease and therefore, the greater the thickness the lower the noise. Nevertheless, the position of the screws does not seem to affect this response.

On the other hand, the temperature does have a correlation with the position of the screws. It is a medium positive correlation with the x-position of screw 2, $S2x$, meaning that the further

the screw to the x-axis of the model, the higher the temperature. Besides, there is a small-medium negative correlation with the position of screw 4, for both of the positions, $S4x$ and $S4y$. Therefore, the closer the screw to the centre of the model, the higher the temperature.

Moreover, it can be noticed in Figure 7.5 a small positive correlation between both results, equivalent radiated power and temperature. Nevertheless, it is not possible to know which is the dependent variable and which is the independent one. Therefore, it is unknown if it is the higher temperature the one that makes higher the noise or the other way round.

The Pearson correlation coefficient does not reveal if the correlation is statistically significant or not and therefore, the p-value is used to determine whether the null hypothesis should be rejected or not (Minitab). The null hypothesis is a typical statistical theory which suggests that no statistical relationship and significance exists in a set of given single observed variable, between two sets of observed data and measured phenomena (Haldar, 2013). A small p-value is an indicator that the null hypothesis is false and therefore it can be concluded that the Pearson correlation coefficient is different from zero and that a linear relation exists. Generally, the null hypothesis is rejected if the p-value is smaller than 0,05 - meaning that there is at least a 95 % chance that there is a true relationship between variables. The p-value uses the t-distribution, t, from Equation 7.2 with $n - 2$ degrees of freedom.

$$t = \frac{r\sqrt{n-2}}{\sqrt{1-r^2}} \tag{7.2}$$

Figure 7.6 shows the p-values for both responses. maximum radiated power and maximum temperature. Notice how the cells with a value lower than 0,05 have been coloured in green indicating that there is a linear correlation between the variables.

|	S1x	S1y	S2x	S2y	S3x	S3y	S4x	S4y	T
Max ERP	0,991	0,947	0,990	0,817	0,625	0,485	0,764	0,885	7,02E-10
Max Temp	0,978	0,840	0,047	0,778	0,812	0,791	0,221	0,143	0,516

Figure 7.6. *P-values.*

Therefore, it is true that there is a strong linear negative correlation between the thickness of the case and the equivalent radiated power. Moreover, it is true that $S2x$ has a medium linear positive correlation with the temperature. However, the p-value shows that the null hypothesis is true and no real correlation is present with the position of screw 4.

The negative correlation between the thickness and the equivalent radiated power agrees with the expectations as by increasing the mass then, the natural frequency decrease, Equation 4.18. The frequency ration can be calculated as $\frac{\omega}{\omega_n}$, where ω is the system's operating frequency and ω_n is the natural frequency. Hence, it increases when the natural frequencies decrease and it is equal to 1 at the resonance frequency. As it can be appreciated in Figure 7.7, the further from the resonance frequency, the lower the amplitude and therefore the lower the noise. Therefore, by increasing the mass of the system, the natural frequencies are moved away from the resonance frequency and thus the vibrations are decreased.
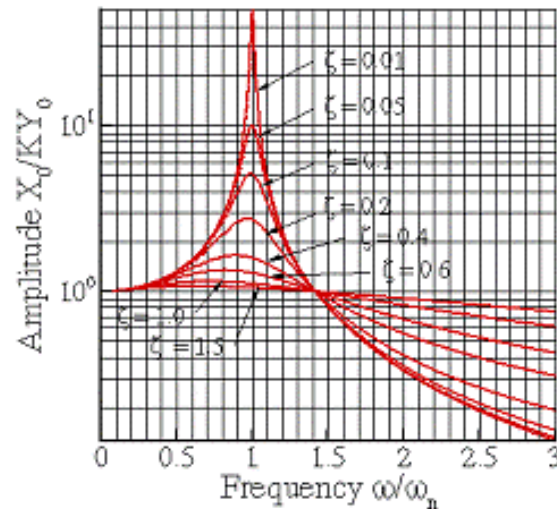
Figure 7.7. *Amplitude of a steady-state vibration of a base excited spring-mass system for different damping ratios (BrownUniversity).*

On the other hand, it is believed that the influence of $S2x$ is given by the fact that when the screw is closer to the x-axis then, it is closer to the DPAK electronic components. Therefore, the temperature of the screw increases and more heat is extracted, refer to Figure 7.8. This is possible since steel, the screw material, is considered a good conductor.
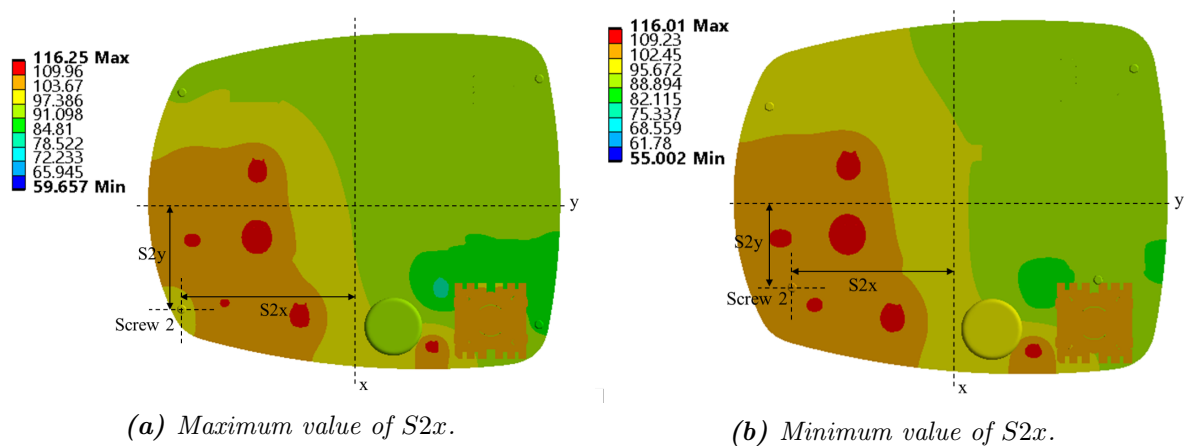
(a) *Maximum value of S2x.*

(b) *Minimum value of S2x.*

Figure 7.8. *Influence of the parameter S2x on the maximum temperature.*

Thus, it is possible to decrease the noise by increasing the thickness of the case and to decrease the temperature by modifying the position of screw 2. The sensitivity study is done from a structural point of view, meaning searching for what is best for the noise. Then, it should be verified by an electronic expert that is possible and that everything functions properly.

Discussion 8

The goal of this project is to study the influence of the material change in the case of the control box, in terms of noise and temperature. Thus, considering the results from the previous chapters, it is evident that material has a great influence on the results. Three different study cases were considered: full polycarbonate case, mix aluminium and polycarbonate case, and full aluminium case.

For the vibration analysis, the modal results were obtained first. It is known that the frequencies are a function of the stiffness matrix, $f_i = \frac{1}{2\pi}\sqrt{\frac{k}{m}}$, and that this matrix is a function of the Young's Modulus material property, $[K] = \int_{V_e}[B]^T[E][B]\,dV$. The higher the material property, the higher stiffness and therefore, the higher frequencies. Considering that the polycarbonate has a Young's Modulus of 2,303 GPa and the aluminium of 69,040 GPa then, the stiffness is higher for the aluminium and therefore the frequencies. This statement is verified with the obtained results as it can be appreciated that the more aluminium is present in the model then, the higher the natural frequencies.

If there are excessive vibrations then, structural and functional issues can be found, such as resonance. This will happen if the natural frequencies match the system's resonant frequencies, in this case, the attached motor to the control box. From the structural point of view, the higher the natural frequencies the better as the low ones are more likely to damage the system. Therefore, it is important to ensure that the natural frequencies are far greater than any possible excitation frequency that the system might have. Considering the results from the modal analysis, it is better for the vibrations point of view when the case is made of aluminium as the natural frequencies are probably greater than the system's operating frequencies. From the noise point of view, the lower the natural frequencies the better, based on the normal hearing range of a human. The human ear perceives frequencies from 20 Hz to 20.000 Hz and the human ear as a dynamic range from 0 dB to 130 dB. However, all sounds over 90 dB are considered damaging (Pujol, 2018). Therefore, based on the modal analysis results and from the noise point of view, the polycarbonate case is considered better than the aluminium one.

Then, the harmonic analysis was done, based on the previous modal analysis results. It revealed that for low frequencies, the less aluminium in the case, the higher the sound power level and therefore the more noise in the model. This can be based on the fact that the natural frequencies of the polycarbonate are closer to the system's operating frequencies and thus the amplitudes of the vibrations are greater. Nevertheless, it is important to consider that it was assumed a damping ratio of 2 % for both materials, polycarbonate and aluminium, based on the recommendations from Grundfos. In reality, this value is higher for the polycarbonate and

therefore, the results from the harmonic analysis seem worst than they are. It is based on the fact that the amplitude of the system decreases as the damping ratio increase, following Figure 7.7. Hence, it is not possible to determine which material case has lower vibrations. To know the exact value of the damping, different tests should have been done. Two extra simulations, with a damping ratio of $3\,\%$ and $4\,\%$ respectively, have been done to compare it with the $2\,\%$ one. Figure 8.1 shows the results and it can be seen how the higher the damping ratio, the lower the sound power level. Thus, the $2\,\%$ value gives conservative results.
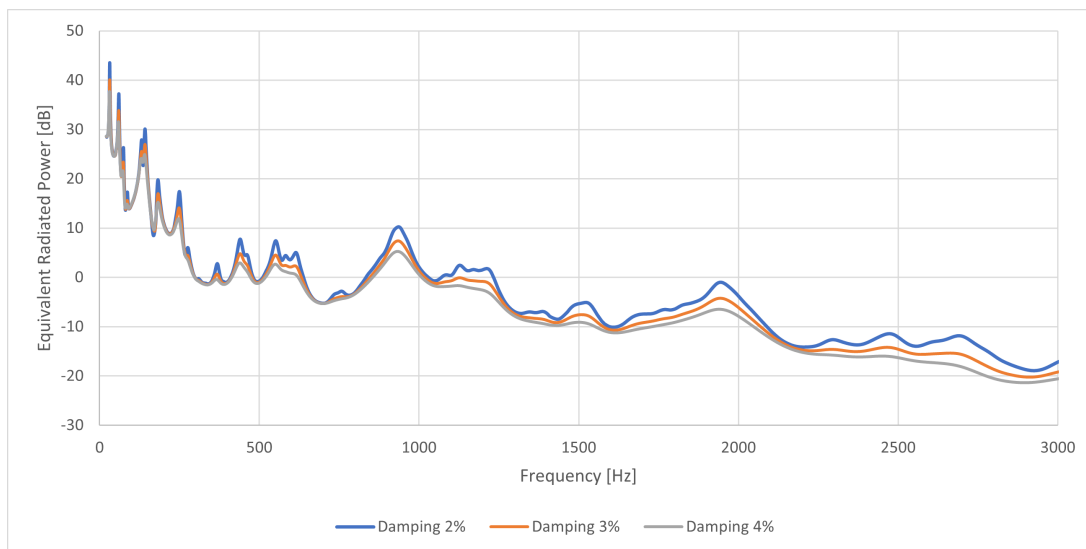
Figure 8.1. *Damping ratio influence when performing harmonic analysis, for the polycarbonate case.*

Moreover, a thermal analysis was done to study how the temperature of the model changes when modifying the material of the case. For this study, it is important to consider the thermal properties of materials as these refer to the response of materials to changes in their temperature and to the application of heat. As a solid absorbs energy in the form of heat, its temperature rises. However, each of the materials reacts differently to the application of heat. Thus, it is evident that the temperature is dependent on the thermal properties of the materials. Some of the thermal properties that have been considered in this project are emissivity and thermal conductivity. The emissivity of the surface of a material is its effectiveness in emitting energy as thermal radiation and thermal conductivity is a measure of a substance's ability to transfer heat through a material by conduction.

In the case of the emissivity property, ϵ, it is the ratio of the thermal radiation from a surface to the radiation from an ideal black surface. The ratio varies from 0 to 1. The surface of a perfect black body has an emissivity of 1 and therefore, the higher the ratio, the more heat is radiated as it is more effective. Considering that the emissivity of the polycarbonate is 0,9 and the one from the aluminium is 0,02 then when the case is made of polycarbonate more heat is transferred to the outside with radiation. If the radiation from the outer surface is calculated for each of the studies, using $q_{rad} = \epsilon \cdot A \cdot \sigma \cdot (T_S^4 - T_B^4)$ and considering that the total heat dissipated, the sum of conduction, convection and radiation, is $14{,}39\,\mathrm{W}$ then, the percentage of the heat transferred by radiation can be obtained. For the full polycarbonate case is a $0{,}2\,\%$, for the mix aluminium and polycarbonate case is $0{,}16\,\%$ and for the full aluminium case is $0{,}03\,\%$. Hence, the results

are not really influenced by this property.

Considering that the thermal conductivity, K, is calculated as $K = \frac{Q \cdot d}{A \cdot \Delta T}$, where Q means the amount of heat transferred then, more heat is transferred when the thermal conductivity is high. Thus, taking into account that the thermal conductivity of the polycarbonate is 0,199 W/m °C and for the aluminium is 155,3 W/m °C, it is clear that whit the presence of the aluminium on the case, more heat will be transferred to the exterior. This will lead to a higher temperature in the case of the control box when it is made of aluminium and this can be observed in the obtained results from the simulations.

The parametric study is defined by the parameters that control the position of the four screws that connect the bottom part, the cover part and the PCB as well as the parameter that controls the thickness of the case. The study revealed that the noise can be minimized by increasing the thickness of the case. This is based on the fact that when the mass of the model increases then, the natural frequencies, ω_n, decrease following $\omega_n = \sqrt{\frac{k}{m}}$. Moreover, it is known that the amplitude of the vibration is a function of the frequency ratio, $\frac{\omega}{\omega_n}$, where ω is the system's operating frequency. When both frequencies are the same then, the resonance frequency is achieved. By decreasing the natural frequencies it is possible to decrease the amplitude of the vibration as the frequencies will not match the system's ones. Moreover, the study showed that by moving the screw 2 closer to the x-axis, situated in the centre of the PCB, then, it is closer to one of the electronic components that dissipate more heat and thus the temperature of the screw increases and more heat is dissipated to the outside. This is possible as the material of the screw is steel and it is a good heat conductor.

Limitations

The idea was to set the simulations as close as possible to the real conditions. However, since the frequency at which the motor operates is unknown, it was decided to include a constant value over time as the input frequency. For this reason, the reality is not fully reflected. However, by establishing this case, the simulations will give worse results than in reality and therefore, it is considered a fair assumption from the point of view of Grundfos experts. Hence, it is not possible to know whether the model will actually withstand the vibrations.

In addition, the geometry of the PCB was modified in order to simplify the case and decrease the computational time. Thus, the value of the isotropic thermal conductivity of the FR4-material was modified by trial and error to try to simulate the behaviour of the different copper and FR4 layers present in the real model.

Finally, the uncertainties should be considered. Not only according to the simplifications that were made but also the ones from setting the simulation. For instance, there might be some mesh deficiencies which could cause a great influence on the accuracy of the results. Therefore, between a 10 % to a 20 % variation should be considered. Additionally, as it is known that the accuracy of the results decreases as the frequency increases then, the results should not be relied upon for high frequencies.

Future Work

It would be beneficial to perform a structural analysis to investigate if the model can withstand the vibrations when it is under working conditions. This will decide if the modal will fail or not even if the operating frequency of the system is unknown.

The equivalent radiated plot was used to understand the vibrations of the model, under forced vibration conditions. Therefore, the assumption of plane wave radiation and the coupling relationship between the structure and the fluid was done. This leads to equal the normal velocity of the structure surface and the particle velocity of the fluid. Thus, the use of this response plot has some limitations on validity based on the assumptions but it leads to a very conservative overestimation. Therefore, it could be investigated with software in which the air is modelled if this implies some limitations when studying the noise of the the model.

In addition, some research could be done regarding the damping ratio of the polycarbonate to have more accurate results and be able to decide which model is worse in terms of vibrations. The logarithmic decrement approach could be used to estimate it only for the fundamental mode. In the case of multiple modes, steady or random vibration tests can be impulsed to capture both force and response signal - accelerations - to build frequency response function. Then, the damping ratio can be estimated by using the half power point method.

Besides, a conduction-based solver was used and therefore, no fluid was defined. Thus, the real conditions of natural convection are represented by forced convection as boundary conditions. Some calculations and several simulations were done but only for the polycarbonate case. Therefore, it should be investigated if the same values can be used when the material of the case is modified to mix aluminium and polycarbonate or full aluminium.

Furthermore, it could be interesting to verify that the results are not influenced by the simplification done on the PCB. Therefore, a comparison between the model used and the actual one, where all the different layers and explicit nets are present, could be done.

Finally, a parametric study was done to evaluate the influence of the defined parameters in the responses. A greater range for the screw positions could be considered to see if it is possible to modify more than $3\,°C$ the temperature. Moreover, the parameters considered are from a structural point of view to minimize noise and temperature and therefore, it should be discussed with the electronic experts to verify if it is possible to make these modifications.

Conclusion 9

The problem formulation on which this report is bases, is the following:

> *"What influence does the material change of the case of a control box have on the noise level and temperature? Can both responses be minimized when the case is made of polycarbonate?"*

In order to answer this question, the motivation or background to develop this project was established in the introduction. It is based on the project *Parametric stability and thermal optimisation analysis of an aluminium part* (Bermejo, 2022) with the goal of analysing how a change in the material of the case will affect the noise and temperature of the model. However, with the change of material from aluminium to polycarbonate, the model had to be adapted to be able to introduce the heat sources and therefore the new model was introduced in the problem analysis. In addition, as the temperature affects the mechanical properties of the material then, a study of the influence was included in the problem analysis.

Subsequently, the numerical scheme in the software used was explained. It includes the theory to set up FEM or numerical model as well as the theory behind the performance of the software to find the results of the vibrations, free and forced vibrations. In order to study the free vibrations, a modal analysis was defined to obtain the natural frequencies of the model. Then, the case of the forced vibrations was defined with the harmonic analysis. This analysis uses the modal analysis results as a base to calculate the displacements or deformations. The equivalent radiated power was used to evaluate the results and study how powerful the noise is in the model. With the use of the magnitude, no medium had to be defined and therefore the computational time decreased.

Later on, the theory was applied to the specific case and different studies were made. First, a benchmark study to compare the vibrations of the new model with the old model. It was concluded that the noise of the new model should be decreased to achieve the same values as in the old model. Secondly, a mesh study was done to verify that the results will give enough accurate results. A mesh with a percentage error of less than 5 % was found, with respect to what was considered a perfect mesh. Thirdly, the material study was done to see how the case material influenced the results in terms of noise. Three cases were studied: polycarbonate case, aluminium bottom and polycarbonate cover, and aluminium case. The study showed that if the case is made of polycarbonate then the natural frequencies are lower than when the case has aluminium. Moreover, it was concluded that when aluminium is not present in the case, the amplitude of the noise is greater at low frequencies and therefore, the model has more noise.

However, due to the not accurate damping ratio for the polycarbonate material, it is not possible to know if this is the real case. Regardless of this, it is desired to find a manner to reduce them in the range of 0 Hz to 800 Hz approximately as is where more noise issues are found when the case is made of polycarbonate.

In addition, a thermal analysis was done in the new model with a conduction-based solver. This analysis consisted in investigating the maximum temperature that the structure achieves when is under working conditions. Moreover, a material study of the case was included. It revealed that the temperature of the PCB and electronic components slightly vary. The changes are mainly in the area where the screws are located by decreasing their temperature with the presence of aluminium. Moreover, the temperature on the case increase with the presence of aluminium. Thus, the overall maximum temperature of the model decrease when the parts are made of aluminium. Regardless of this, all the models can withstand the temperatures with no issues.

Finally, a parametric study was elaborated to study the influence of parameters in the vibrations and thermal analyses when the case is made of polycarbonate. The defined parameters control the position of the screws that connect the cover, the bottom and the PCB as well as the thickness of the case. The goal was to find if any of these parameters can minimize both results, the radiated power and temperature. With this study, it was discovered that if the thickness of the case increases then, the noise decreases as there is a significant negative correlation between the input and the output variable. Moreover, one of the screws has a positive correlation with the temperature and thus, the closer the screw to the centre of the model, the lower the temperature. Therefore, it is possible to minimize the noise and temperature by adjusting the parameters.

Bibliography

ANSYS. Theory reference for the mechanical apdl and mechanical applications, 2009.

AnsysGranta. Ansys granta: Materials information management, 2022. URL
   `https://www.ansys.com/products/materials`.

AnsysInnovationCourses. Modal analysis, 2020. URL
   `https://courses.ansys.com/index.php/courses/modal-analysis/`.

Marta Bermejo. Parametric stability and thermal optimization analysis of an aluminium part,
   2022. URL `www.mp.aau.dk`.

Cole Boucher. What is coefficient of thermal expansion? how to measure it?, 2019. URL
   `https://thermtest.com/`
   `what-is-coefficient-of-thermal-expansion-how-to-measure-it`.

BrownUniversity. Dynamics and vibrations. forced vibrations. URL
   `https://www.brown.edu/Departments/Engineering/Courses/En4/Notes/`
   `vibrations_forced/vibrations_forced.htm`.

Brüel and Kjær. Sound power and sound pressure. URL `https:`
   `//www.bksv.com/en/knowledge/blog/sound/sound-power-sound-pressure`.

Robert D. Cook, David S. Malkus, Michael E. Plesha, and Robert J. Witt Witt. *Concept and
   Applications of Finite Element Analysis*. Wiley, 2002. ISBN 978-0-471-35605-9.

Esther Fleming. What is the maximum temperature for polycarbonate?, 2020. URL
   `https://www.sidmartinbio.org/`
   `what-is-the-maximum-temperature-for-polycarbonate/`.

Stephanie Fraley, Mike Oom, Ben Terrien, John Zalewski, Ross Bredeweg, Jessica Morga, Ryan
   Sekol, and Ryan Wong. Design of experiments via taguchi methods-orthogonal arrays, 2021.
   URL `https://eng.libretexts.org/@go/page/22674`.

Soren Linnet Gjelstrup. What is modal analysis: The ultimate guide, 3 2021. URL
   `https://dewesoft.com/daq/what-is-modal-analysis`.

S.K. Haldar. Statistical and geostatistical applications in geology, 2013.

Steve Hanly. Vibration measurements: Vibration analysis basics, 2018. URL `https:`
   `//blog.endaq.com/vibration-measurements-vibration-analysis-basics`.

Anne Marie Helmenstine. What is young's modulus? definition and equation, 2019. URL
   `https://www.thoughtco.com/youngs-modulus-4176297`.

Yun Huang and Zhe Cui. Evaluation of equivalent radiated power with ls-dyna, 2016.

Editorial Indeed. Percentage difference vs. percentage change: Here's the difference | indeed.com australia, 2021. URL https://au.indeed.com/career-advice/career-development/percentage-difference-calculator.

J G Kaufman. Fire resistance of aluminum and aluminum alloys and measuring the effects of fire exposure on the properties of aluminum alloys, 2016.

Sai Kiran. Harmonic response analysis in ansys, 2008.

LaerdStatistics. Pearson product-moment correlation, 2020. URL https://statistics.laerd.com/statistical-guides/pearson-correlation-coefficient-statistical-guide.php.

Hanbing Liu, Xianqiang Wang, and Yubo Jiao. Effect of temperature variation on modal frequency of reinforced concrete slab and beam in cold regions. *Shock and Vibration*, 2016, 2016. ISSN 10709622. doi: 10.1155/2016/4792786.

Marinus Luegmair. Advanced equivalent radiated power (erp) calculation for early vibro-acoustic product optimization, 2015. URL https://www.researchgate.net/publication/315799640.

Erik Lund and Esben Lindgaard. Notes for course on finite element methods, 2020.

Minitab. Methods and formulas for correlation. URL https://support.minitab.com/en-us/minitab-express/1/help-and-how-to/modeling-statistics/regression/how-to/correlation/methods-and-formulas/.

Rémy Pujol. Human auditory range, 2018. URL http://www.cochlea.org/en/hear/human-auditory-range.

Singiresu S. Rao. *Mechanical vibrations*. Prentice Hall, 2011. ISBN 9780132128193.

ReVibe. Understanding your vibrations. URL https://revibeenergy.com/how-to-analyse-vibrations/.

YorkUniversity. Orthogonal arrays, 2004. URL https://www.york.ac.uk/depts/maths/tables/orthogonal.htm.

ÇAPAR. Contact types and behaviours in structural analysis – yasin Çapar, 2020. URL https://yasincapar.com/contact-types-and-behaviours-in-structural-analysis/.

Vibration Simulations Set Up A

This appendix includes a detailed explanation of how the simulations for vibration analysis are set up inside the ANSYS Workbench software. The version used is 2021R2. The vibration simulation set up is divided into two parts, first the modal analysis and then the harmonic analysis set up. Notice that they are based on the theory from section 4.2.

A.1 Modal Analysis

For doing the modal analysis, the Modal node from ANSYS is selected, Figure A.1. Thus, first, the engineering data has to be defined and then the geometry is uploaded from CATIA V5. Later, the assignation between material and component as well as the contacts between bodies are made. Next, the mesh is defined and finally, the specific properties for the analysis are set.

	A	
1	Modal	
2	Engineering Data	✓
3	Geometry	✓
4	Model	✓
5	Setup	✓
6	Solution	✓
7	Results	✓
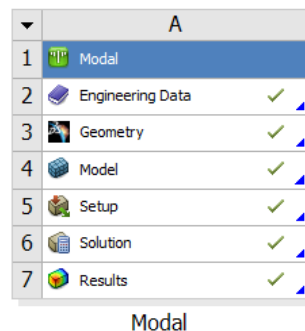
Modal

Figure A.1. *ANSYS Workbench node set up for modal analysis.*

Engineering Data

The materials that each of the components were given by Grundfos and the values of the different properties used are from Granta Design team at ANSYS (AnsysGranta, 2022). The materials considered as well as each property are shown in Figure A.2.

	A	B	
1	Property	Value	
2	Material Field Variables	Table	
3	Density	2713	kg m^-3
4	Isotropic Secant Coefficient of Thermal Expansion		
5	Coefficient of Thermal Expansion	2.278E-05	C^-1
6	Isotropic Elasticity		
7	Derive from	Young's Modulus and Poisson's Ratio	
8	Young's Modulus	6.904E+10	Pa
9	Poisson's Ratio	0.33	
10	Bulk Modulus	6.7686E+10	Pa
11	Shear Modulus	2.5955E+10	Pa

	A	B	
1	Property	Value	
2	Material Field Variables	Table	
3	Density	8942	kg m^-3
4	Isotropic Secant Coefficient of Thermal Expansion		
5	Coefficient of Thermal Expansion	1.674E-05	C^-1
6	Isotropic Elasticity		
7	Derive from	Young's Modulus and Poisson's Ratio	
8	Young's Modulus	1.26E+11	Pa
9	Poisson's Ratio	0.345	
10	Bulk Modulus	1.3548E+11	Pa
11	Shear Modulus	4.684E+10	Pa

(a) *Aluminium alloy, wrought, 6061, T6.* ***(b)*** *Copper, C10100, hard.*

Figure A.2. *Engineering data.*

	A	B	
1	Property	Value	
2	Material Field Variables	Table	
3	Density	4600	kg m^-3
4	Isotropic Elasticity		
5	Derive from	Young's Modulus and Poisson's Ratio	
6	Young's Modulus	2.4E+11	Pa
7	Poisson's Ratio	0.2	
8	Bulk Modulus	1.3333E+11	Pa
9	Shear Modulus	1E+11	Pa

(c) Ferrite.

	A	B	
1	Property	Value	
2	Material Field Variables	Table	
3	Density	1900	kg m^-3
4	Isotropic Secant Coefficient of Thermal Expansion		
5	Coefficient of Thermal Expansion	1.55E-05	C^-1
6	Isotropic Elasticity		
7	Derive from	Young's Modulus and Poisson's Ratio	
8	Young's Modulus	2.46E+10	Pa
9	Poisson's Ratio	0.136	
10	Bulk Modulus	1.1264E+10	Pa
11	Shear Modulus	1.0827E+10	Pa

(d) PCB laminate, Epoxy/Glass fiber, FR-4.

	A	B	
1	Property	Value	
2	Material Field Variables	Table	
3	Density	1160	kg m^-3
4	Isotropic Secant Coefficient of Thermal Expansion		
5	Coefficient of Thermal Expansion	9.786E-05	C^-1
6	Isotropic Elasticity		
7	Derive from	Young's Modulus and Poisson's Ratio	
8	Young's Modulus	2.303E+09	Pa
9	Poisson's Ratio	0.4002	
10	Bulk Modulus	3.846E+09	Pa
11	Shear Modulus	8.2238E+08	Pa

(e) Plastic, PC (copolimer, heat resistant).

	A	B	
1	Property	Value	
2	Material Field Variables	Table	
3	Density	2329	kg m^-3
4	Isotropic Secant Coefficient of Thermal Expansion		
5	Coefficient of Thermal Expansion	2.578E-06	C^-1
6	Isotropic Elasticity		
7	Derive from	Young's Modulus and Poisson's Ratio	
8	Young's Modulus	1.627E+11	Pa
9	Poisson's Ratio	0.27	
10	Bulk Modulus	1.179E+11	Pa
11	Shear Modulus	6.4055E+10	Pa

(f) Silicon, pure.

	A	B	
1	Property	Value	
2	Material Field Variables	Table	
3	Density	7850	kg m^-3
4	Isotropic Secant Coefficient of Thermal Expansion		
5	Coefficient of Thermal Expansion	1.2E-05	C^-1
6	Isotropic Elasticity		
7	Derive from	Young's Modulus and Poisson's Ratio	
8	Young's Modulus	2E+11	Pa
9	Poisson's Ratio	0.3	
10	Bulk Modulus	1.6667E+11	Pa
11	Shear Modulus	7.6923E+10	Pa

(g) Structural steel.

Figure A.2. *Engineering data.*

Geometry

The model was provided by Grundfos in CATIA V5. It consisted of three main parts - bottom, cover and PCB, four screws and 69 electronic components or parts of them. The provided geometry is exactly as in reality and therefore is quite complex in terms of the different PCB layers for better heat conduction. The more complex the geometry, the more solving time is needed. As this project is subjected to time limitations, a simplification of the PCB is done. Initially, the PCB was composed of 7 layers plus 18 explicit nets, refer to Figure A.3.
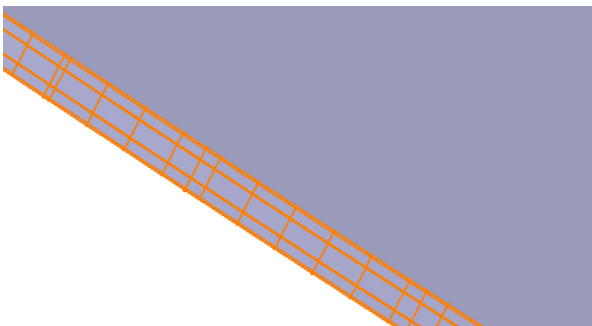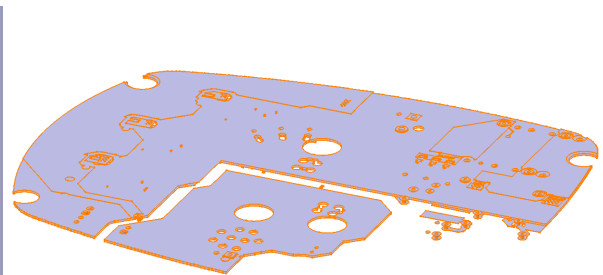

(b) PCB 18 explicit nets.

(a) PCB 7 layers.

Figure A.3. *PCB real appearance.*

All of the layers are on top of each other and they had a total thickness of 1,5 mm. Therefore, it is

decided to create one solid body with the same shape as the PCB body but with the thickness of the sum of the different layers to decrease the computational time, Figure A.4. It is considered that this modification does not have an effect on the vibration analysis but it does have on the thermal analysis. Therefore, some adjustments had to be done as mentioned in section B. Moreover, the provided geometry is modified to be able to set the parametric study of chapter 7 as explained in section 7.1.
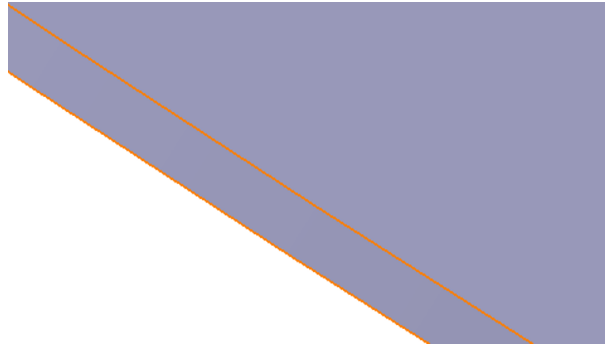
Figure A.4. PCB modified.

Once all the modifications are done, the geometry is imported into ANSYS. The different parts are shown in Figure 2.2 and the assignation of the material to each of the bodies is done following Table 2.2 and the material properties of Figure A.2. Notice how a mix of FR4 and copper is defined for the PCB part but, due to the simplification made, only FR4 material is used for the analysis as it represents the 90 %.

Connections

The contacts between the different bodies and faces have to be defined. The contact behaviour used is surface to surface, where both contact and target are surfaces and they have to be determined which surface is a contact body and which is a target. It is important to identify which is the target body and which is the contact body. Generally, a convex surface is chosen as contact and concave as the target. Besides, a large surface is chosen as a target when the size of one body in contact is very small compared to another one (ÇAPAR, 2020).

Two different types of contacts are considered for contact behaviour, bonded and frictional. The first type is defined when the components are welded to each other such that sliding or separation between faces or edges is not allowed. On the other hand, frictional contact is set for those that can slide and separate as no welding is present. It is set for those who might get in contact under working conditions.

In this case, the defined contacts are shown in Table 2.3. Nevertheless, refer to Figure A.5 for the selected faces for each of the contacts. Notice that "CB" refers to Contact Body and "TB" refers to Target Body.
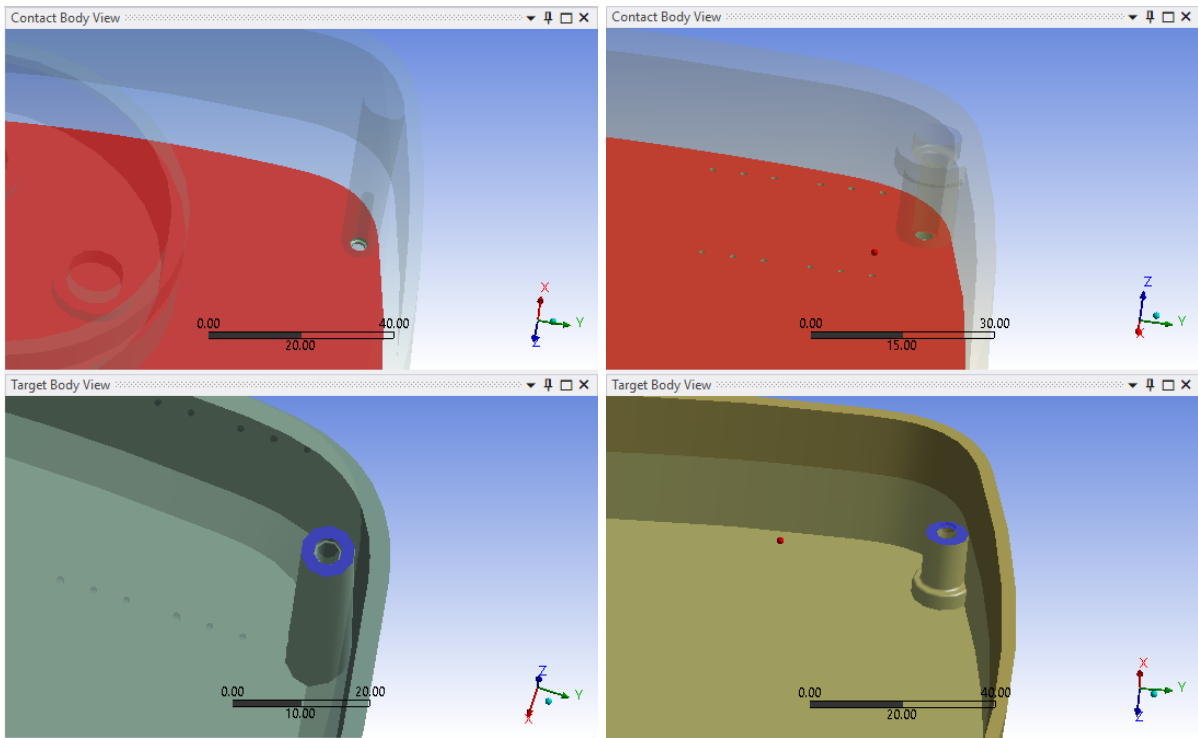
(a) Frictional contact between the PCB, CB, and the bottom part, TB.

(b) Frictional contact between the PCB, CB, and the cover part, TB.

Figure A.5. Contact regions.
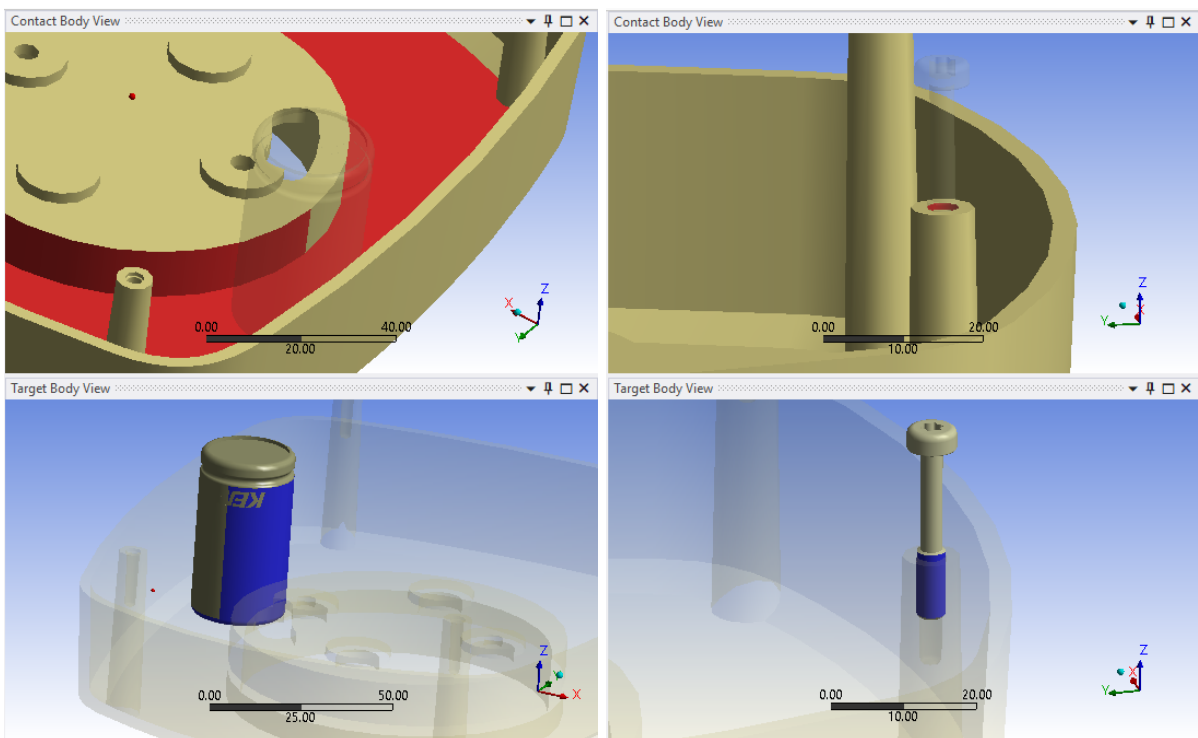
(c) Frictional contact between the bottom part, CB, and the capacitor, TB.

(d) Bonded contact between the bottom part, CB, and the screws, TB.

Figure A.5. Contact regions.
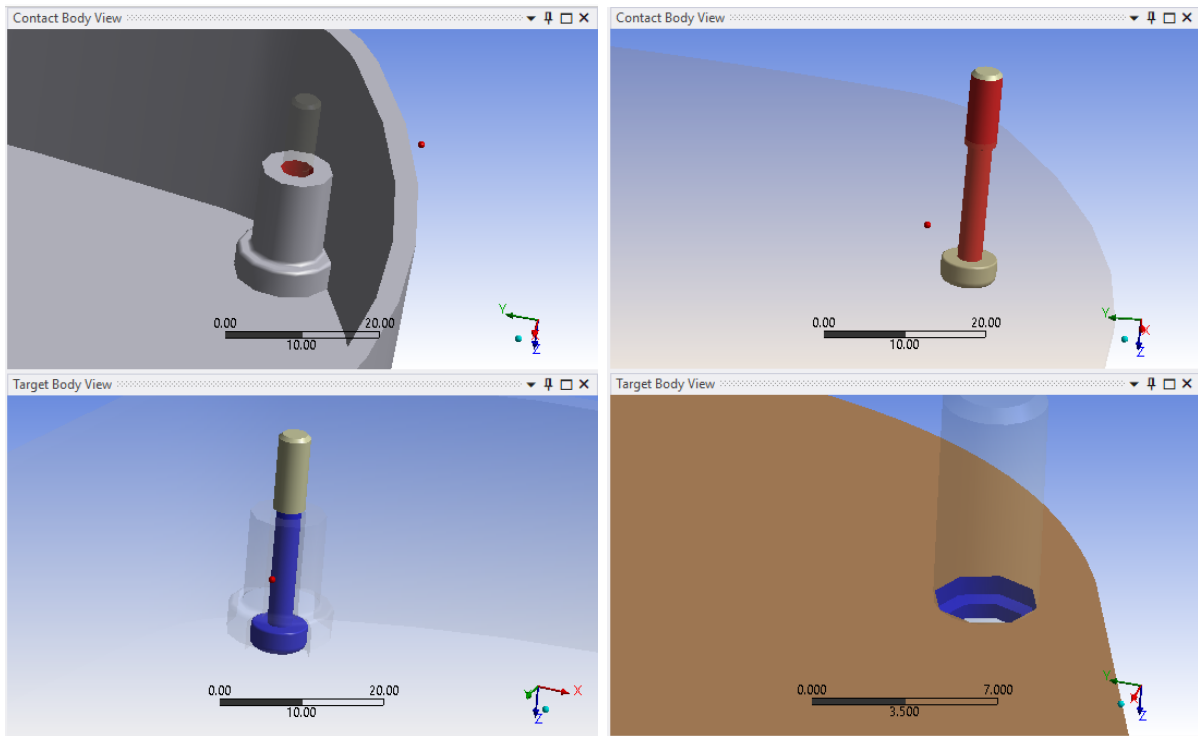
(e) *Bonded contact between the cover part, CB, and the screws, TB.*

(f) *Frictional contact between the screws, CB, and the holes in the PCB, TB.*

Figure A.5. *Contact regions.*
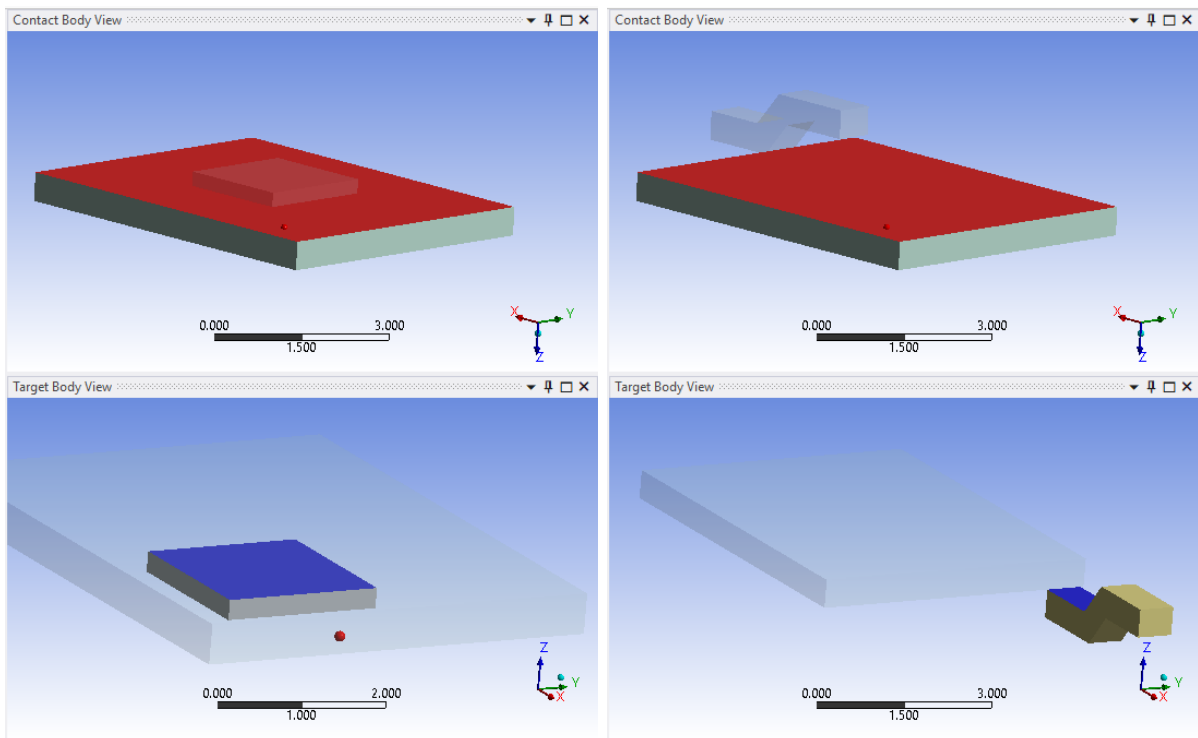
(g) *Bonded contact between the DPAK-D, CB, and the DPAK-Die, TB.*

(h) *Bonded contact between the DPAK-S or DPAK-G, CB, and the DPAK-D, TB.*

Figure A.5. *Contact regions.*
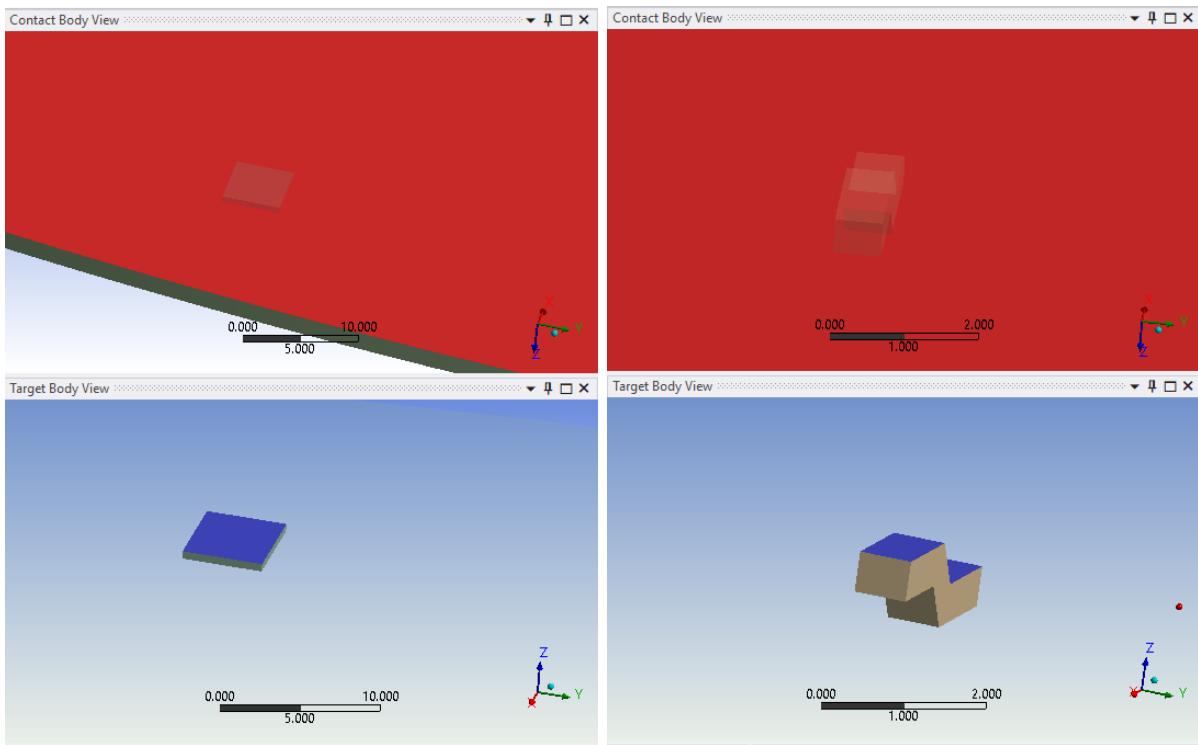
(i) *Bonded contact between the PCB, CB, and the DPAK-D, TB.*

(j) *Bonded contact between the PCB, CB, an ´d the DPAK-S or DPAK-G, TB.*

Figure A.5. *Contact regions.*
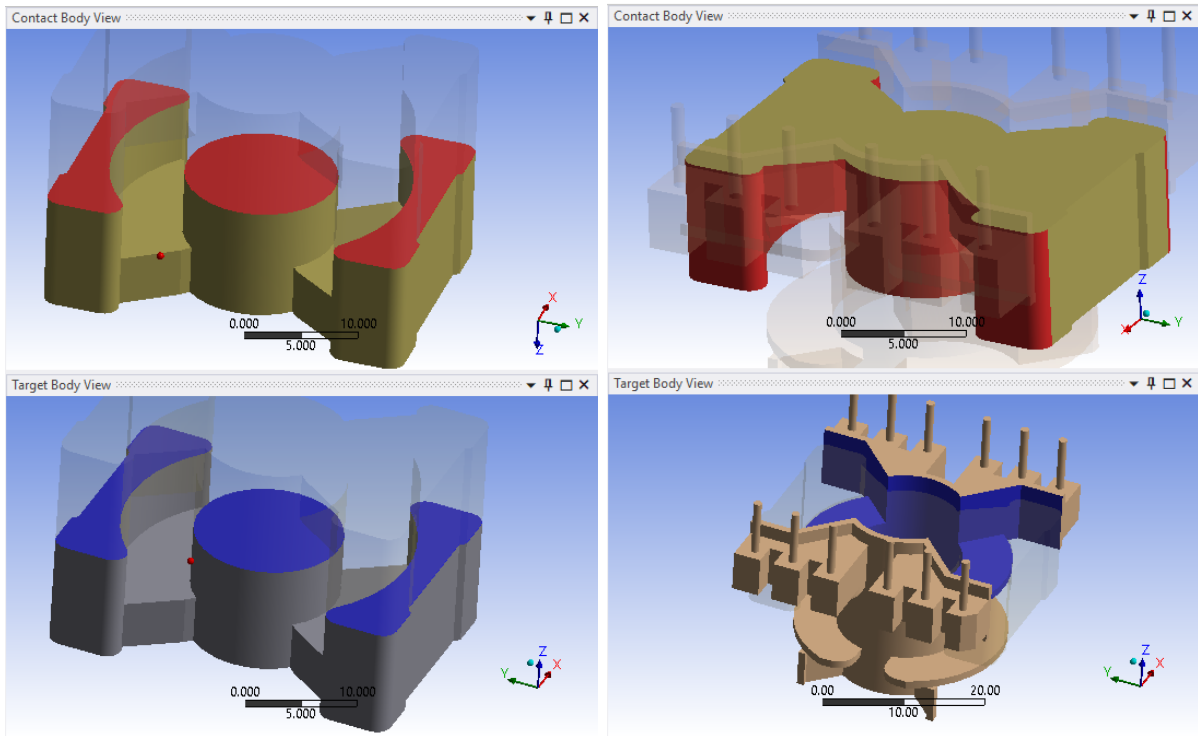
(k) *Bonded contact between the transformer core, CB, and the transformer core, TB.*

(l) *Bonded contact between the transformer core, CB, and the transformer former, TB.*

Figure A.5. *Contact regions.*
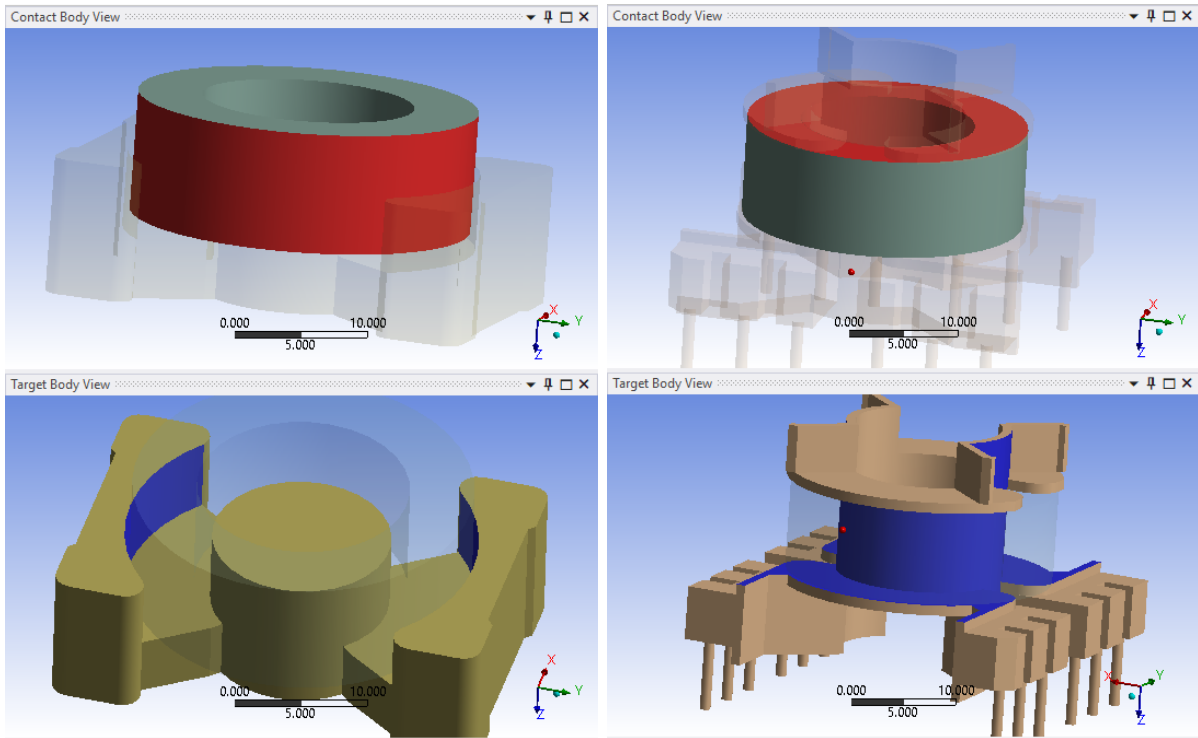
(m) Bonded contact between the transformer winding, CB, and the transformer core, TB.

(n) Bonded contact between the transformer winding, CB, and the transformer former, TB.

Figure A.5. *Contact regions.*
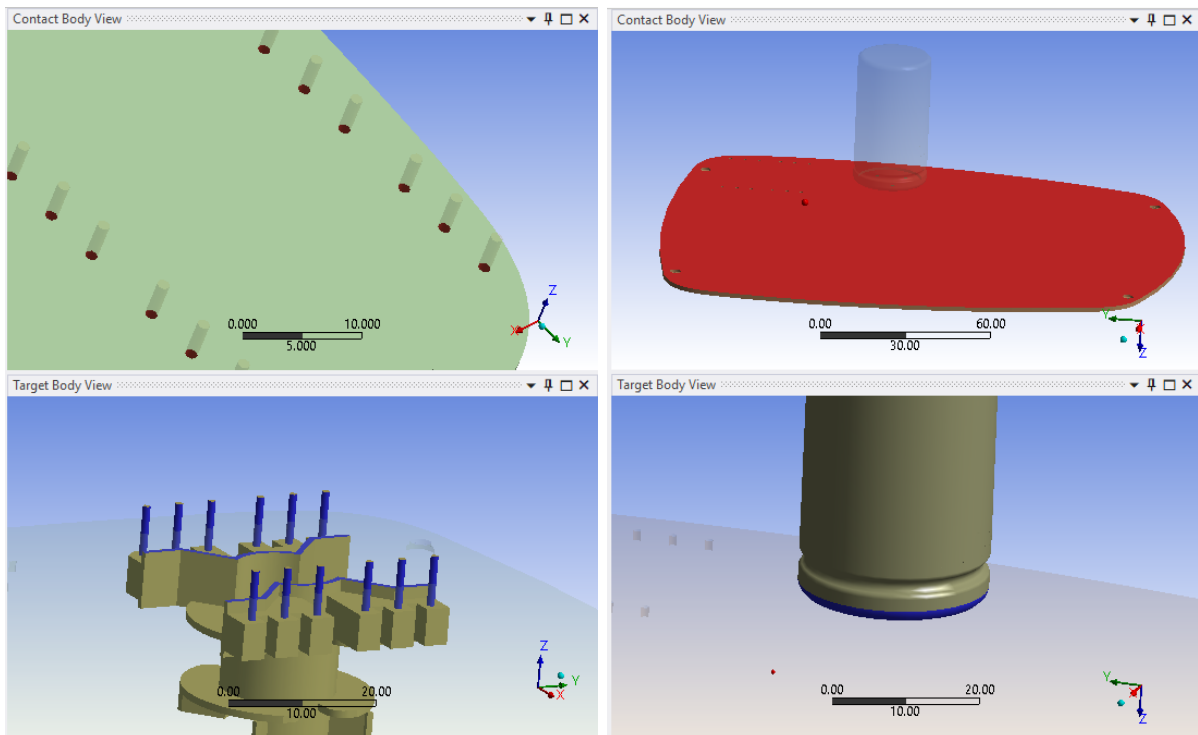
(o) Bonded contact between the PCB, CB, and the transformer former, TB.

(p) Frictional contact between the PCB, CB, and the capacitor, TB.

Figure A.5. *Contact regions.*
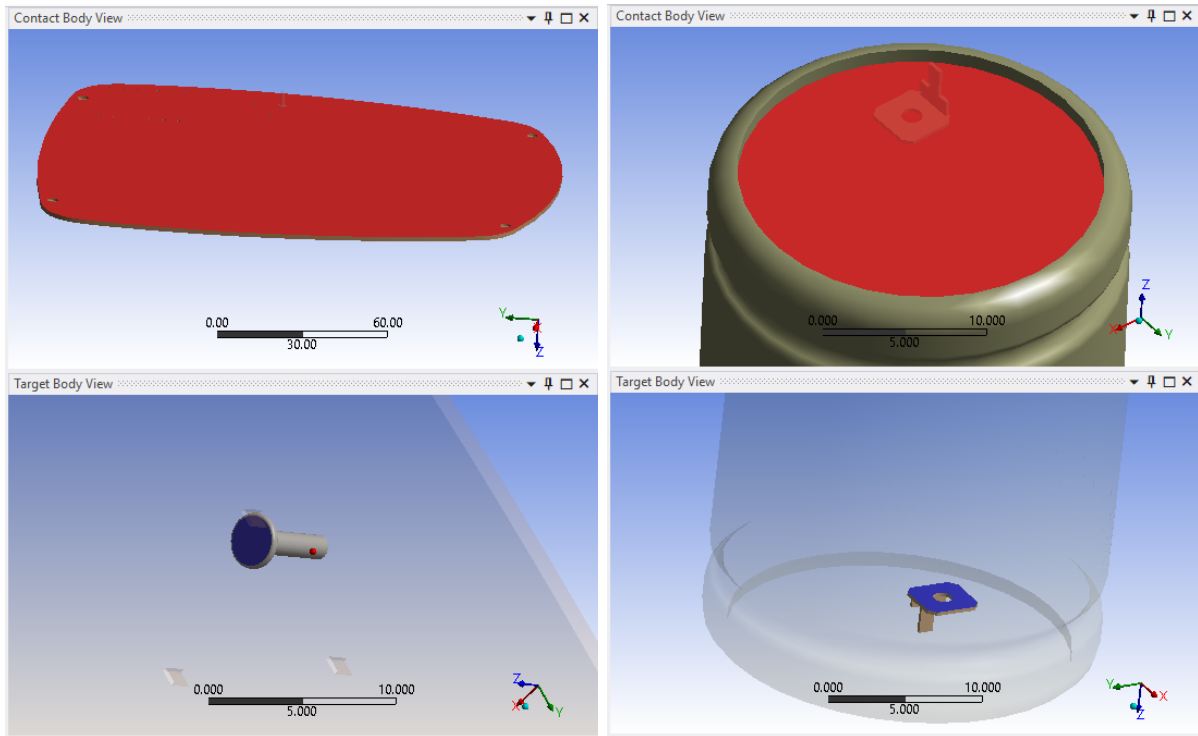
(q) *Bonded contact between the PCB, CB, and the capacitor screws, TB.*

(r) *Bonded contact between the capacitor, CB, and the capacitor pins, TB.*

Figure A.5. *Contact regions.*
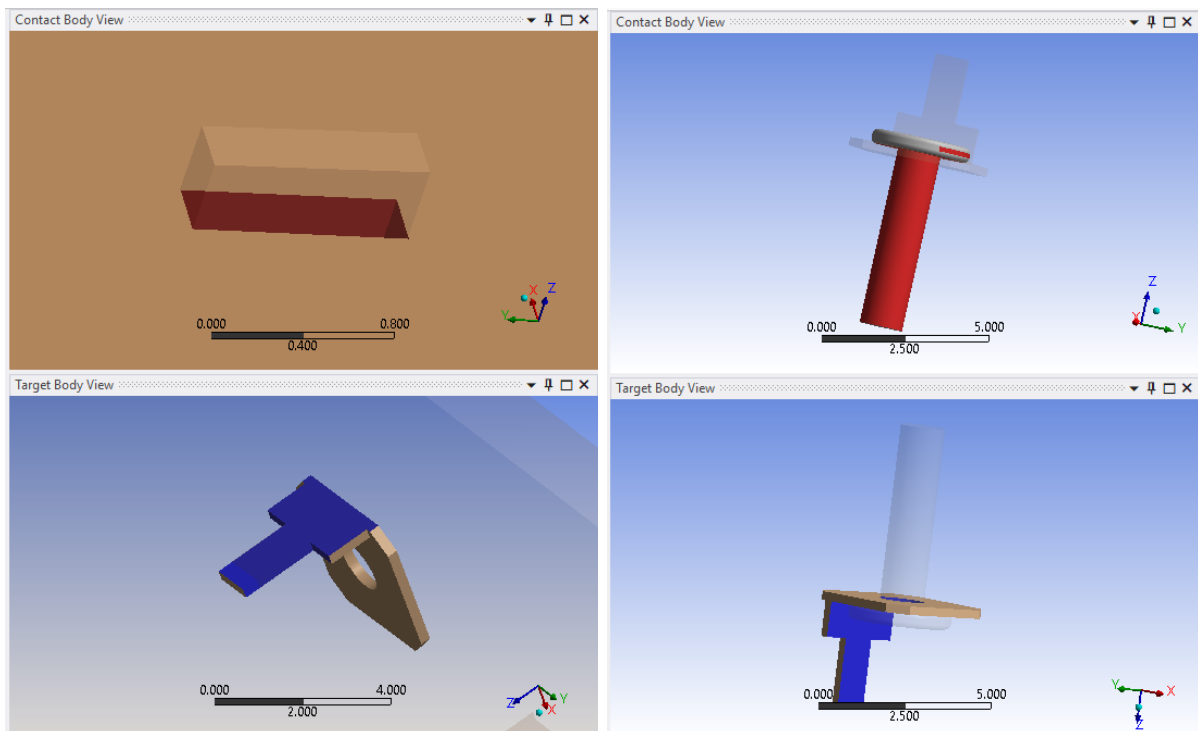
(s) *Bonded contact between the capacitor pins, CB, and the holes in the PCB, TB.*

(t) *Bonded contact between the capacitor screws, CB, and the capacitor pins, TB.*

Figure A.5. *Contact regions.*
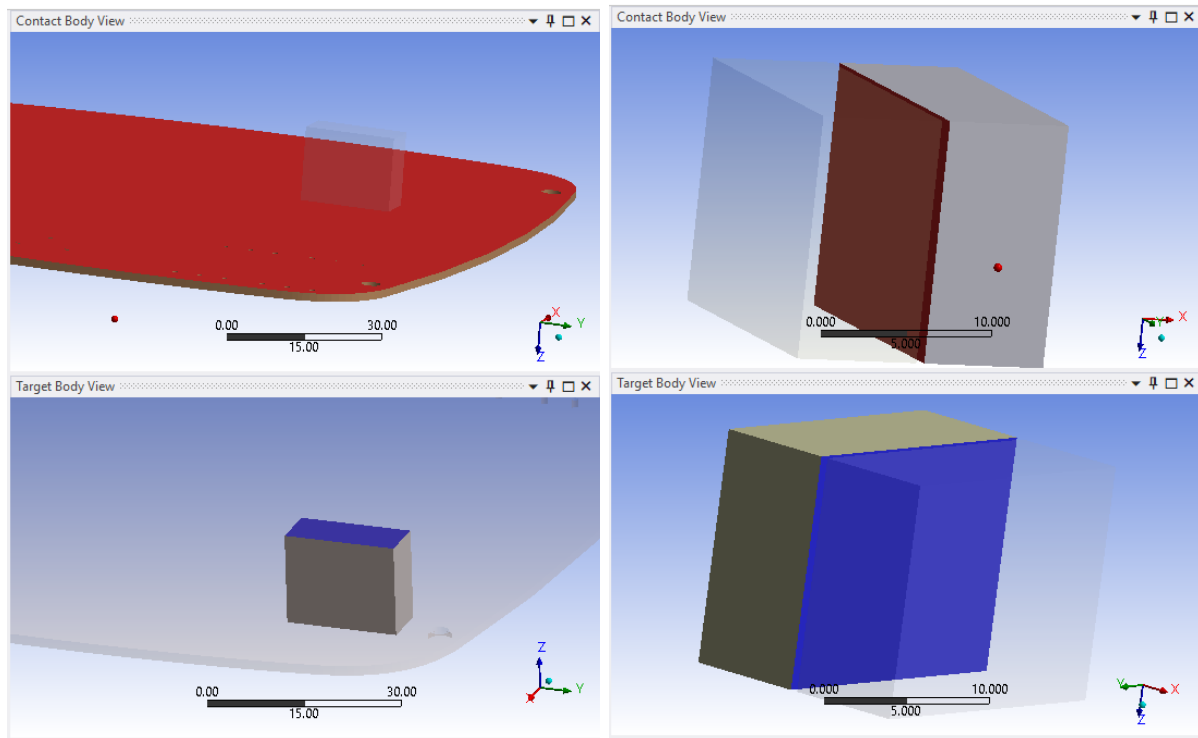
(u) *Bonded contact between the PCB, CB, and the electronic components, TB.*

(v) *Frictional contact between the electronic components, CB, and the electronic components, TB.*

Figure A.5. *Contact regions.*

Mesh

For defining the mesh, a convergence study is done as explained in section 5.2. The goal is to find first the perfect mesh. This mesh has the maximum level of detail and maximum level of refinement, and the results obtained reflect reality. However, as for a perfect mesh, a really fine mesh is needed and then the solving time is extremely high. Thus, it is desired to find another mesh, with a lower solving time, that gives enough accurate results compared to the perfect mesh. Therefore, a convergence study is needed to see how the different meshes affect the results. It is believed that convergence has been reached when the percentage error between the exact or perfect mesh and the approximate mesh is lower than 5 %, refer to Equation 5.1.

In this case, the perfect mesh is assumed to be when all the parts of the model have an element size of 0,5 mm. No further investigation is done as the solving time for the modal analysis, when retrieving 20 modes, is approximately 13 h and hence no finer mesh is tried out. Refer to Figure A.6 to visualize it.
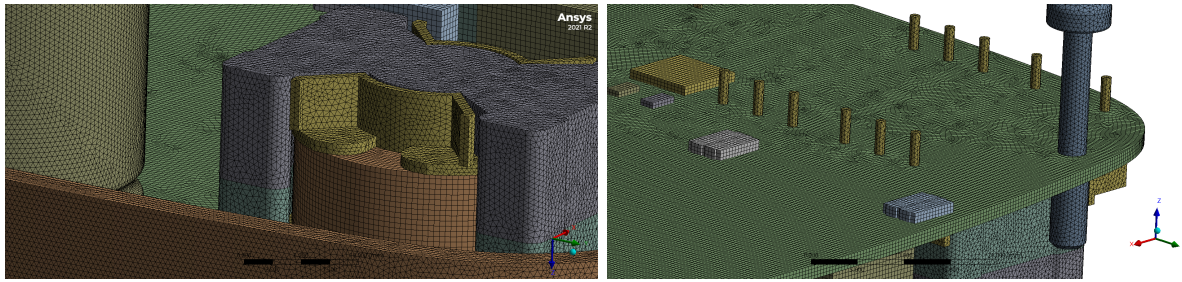
Figure A.6. *Perfect mesh view.*

It is decided that the study would only cover the first 20 modes of the modal analysis as these are the more important ones in terms of noise for the structure. When subtracting these modes, it is possible to evaluate the natural frequencies up to 450 Hz. As the noise that the structure has is more dangerous at low frequencies, only the results in the low range will be evaluated later on. Thus, it is considered that by only extracting 20 modes it is possible to find a good mesh for the important frequencies.

The idea is to set the highest element size possible for the biggest components to decrease the number of elements and therefore the computational time. Moreover, the bigger the component, the less fine mesh is usually needed. In this case, the bottom, the cover and the PCB are considered big components. Since the electronic components have a smaller size, a finer mesh is needed to capture good results. Nevertheless, as there are also different sizes on these components, a differentiation between medium size and small size is done. Refer to Figure A.7 where the components considered as small are marked with a red circle. All the others are considered medium size.
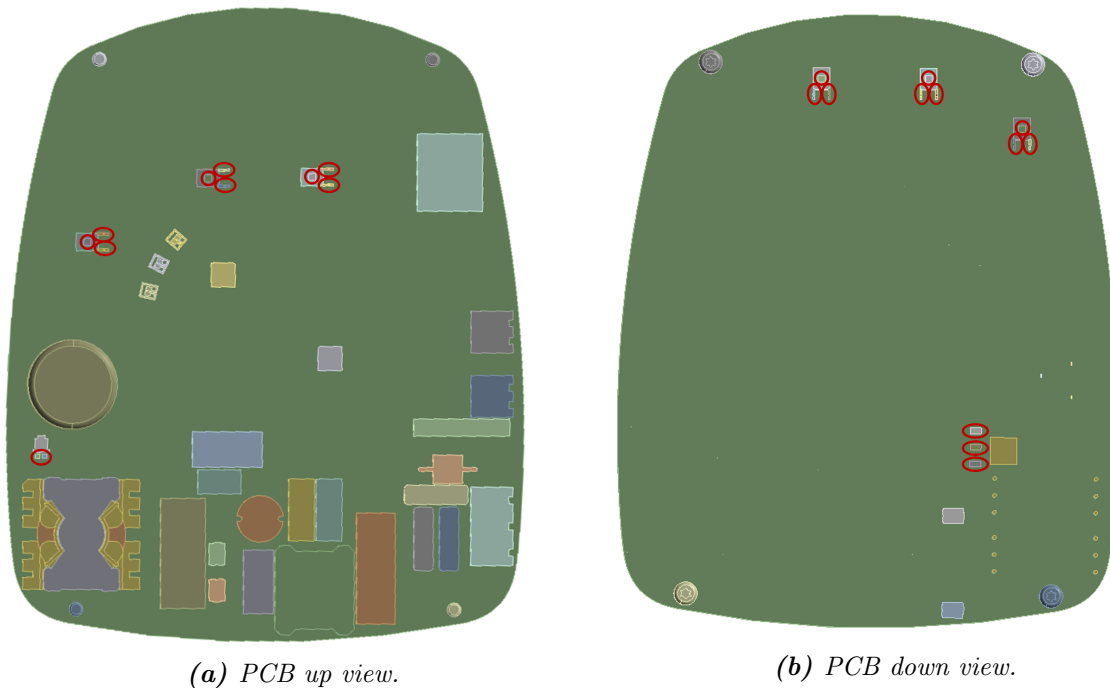
(a) *PCB up view.*   *(b)* *PCB down view.*

Figure A.7. *Small components considered for the mesh study.*

The element size is what is modified depending on the case studied and Table 5.2 shows the

different studied cases. The mesh used in all of the analysis, if not stated otherwise, can be found in Figure 5.8.

Boundary Condition

The last step to fully defining the modal analysis is to set the boundary conditions present in the model. In this case, there is only one given by the mounting conditions. It is known that the control box is attached to the stator house by two screws as shown in Figure 2.3a. Thus, two fixed supports are defined where those screws are located, Figure 2.3b, to constrain the member in all translations and rotations.

Modal Analysis Settings

Inside the setting for the modal analysis, it is possible to define the frequency range of the desired results. There is a rule of thumb that says that the modal analysis frequency range should be 1,5 times the harmonic one. It is known that Grundfos is interested to cover up to 3.000 Hz in the harmonic analysis, even if the focus is on low frequencies up to 800 Hz, to have a big picture of the analyses. Thus, the modal analysis simulations are set up up to 4.500 Hz, if not stated otherwise. However, it has been set that the solver should stop finding more frequencies once 250 modes have been retrieved. This option is generally used to limit the number of solutions when it is unknown how many modes are needed to get all the frequency range. In this case, even though not that many nodes are never necessary, it is used to stop the software in case of error when setting up the simulations, refer to Figure A.8. Mention that no pre-stresses have been set up for the simulations.

Options	
Max Modes to Find	250
Limit Search to Range	Yes
Range Minimum	0. Hz
Range Maximum	4500. Hz

**Figure A.8.** *Modal analysis settings.*

Modal Analysis Results

Once everything is set up then, the modal node looks as in Figure A.9. After running the simulation, the results of the eigenfrequencies and eigenmodes can be found in the window "Tabular Data". Moreover, Total Deformation contour plots can be generated to identify which modes are local and which ones are global, as shown in Figure 5.1 and Figure 5.2.
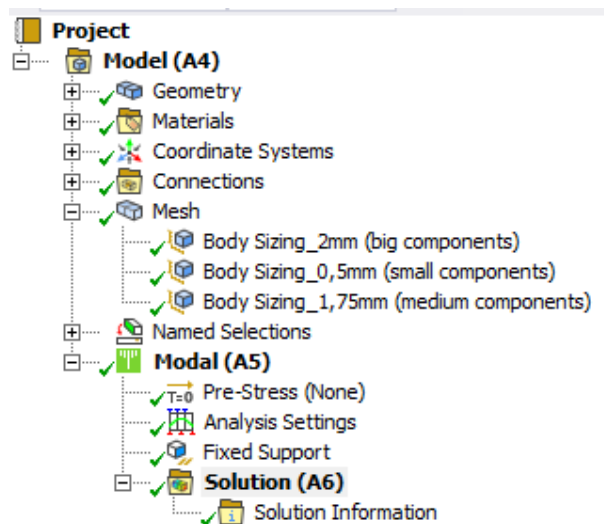
Figure A.9. *Modal analysis simulation.*

A.2 Harmonic Analysis

As explained in subsection 4.2.2, the method used to calculate the forced vibrations is Mode Superposition and therefore, the modal node and harmonic response node have to be connected such that the results from the first one are transferred to the second one as inputs as shown in Figure A.10. Thus, the engineering data, geometry and model set up are shared for both nodes and therefore the set up is the same as in section A.1.
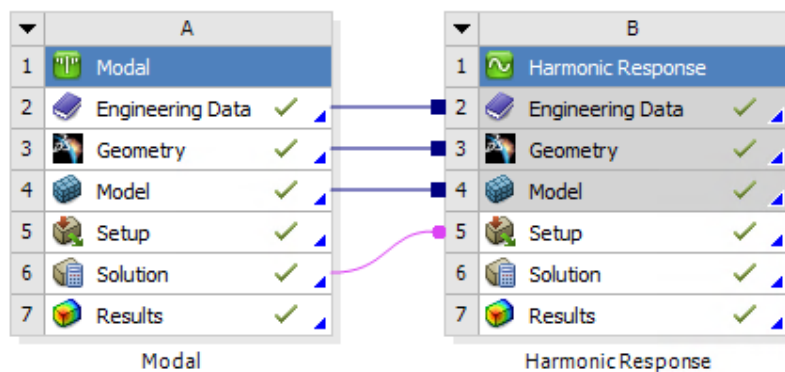
Figure A.10. *ANSYS Workbench nodes set up for modal and harmonic analysis.*

.

Harmonic Analysis Settings

Same as for the modal analysis, the frequency range can be defined and as mentioned in section A.1, and the desired range is from 0 Hz up to 3.000 Hz. As can be appreciated in the figure, the selected solution method is Mode Superposition and cannot be modified due to the set up of the nodes. Moreover, notice the damping ratio defined of 2 %. As explained in subsection 4.2.2, there are two options for retrieving the frequencies on the harmonic analysis,

even frequency spacing and automatic frequency spacing, refer to Figure A.11a and Figure A.11b respectively.

Options	
Frequency Spacing	Linear
☐ Range Minimum	0. Hz
☐ Range Maximum	3000. Hz
☐ Solution Intervals	1000
User Defined Frequencies	On
Solution Method	Mode Superposition
Include Residual Vector	No
Cluster Results	No
Skip Expansion	No
Store Results At All Frequencies	Yes
Rotordynamics Controls	
Output Controls	
Damping Controls	
Eqv. Damping Ratio From Modal	No
Damping Define By	Damping Ratio
☐ Damping Ratio	2.e-002
Stiffness Coefficient Define By	Direct Input
☐ Stiffness Coefficient	0.
☐ Mass Coefficient	0.

Options	
Frequency Spacing	Linear
☐ Range Minimum	0. Hz
☐ Range Maximum	3000. Hz
Cluster Number	10
User Defined Frequencies	Off
Solution Method	Mode Superposition
Include Residual Vector	No
Cluster Results	Yes
Skip Expansion	No
Store Results At All Frequencies	Yes
Rotordynamics Controls	
Output Controls	
Damping Controls	
Eqv. Damping Ratio From Modal	No
Damping Define By	Damping Ratio
☐ Damping Ratio	2.e-002
Stiffness Coefficient Define By	Direct Input
☐ Stiffness Coefficient	0.
☐ Mass Coefficient	0.

(a) *Even frequency spacing.*   (b) *Automatic frequency spacing.*

Figure A.11. *Harmonic analysis settings.*

The even frequency spacing is used in the first two studies in the vibration analysis, benchmark study and mesh study. When defining this method, the number of intervals has to be defined, 1.000 in this case. This means that, for the frequency interval from 0 Hz to 3.000 Hz, the results are calculated for frequencies each 3 Hz. In addition, the user define frequencies option is set as "On" and the natural frequencies from the modal analysis are set as the defined ones. Thus, not only the results for the frequencies with the 3 Hz difference are calculated but also for the natural frequencies.

The second method, the automatic frequency spacing, is used for the material study of both analyses, the vibration and the thermal analyses. Thus, the cluster results option is set as "On" and the cluster number to 10. This means that the software searches for the most relevant frequencies and searches around them for a maximum of 10 frequencies on both sides of the peak.

Harmonic Analysis Results

Once everything is set up then, the Equivalent Radiated Power results can be inserted and the set up looks as in Figure A.12. In this case, the interest is on the outer surface of the case as the goal is to know the noise to which the case is subjected.
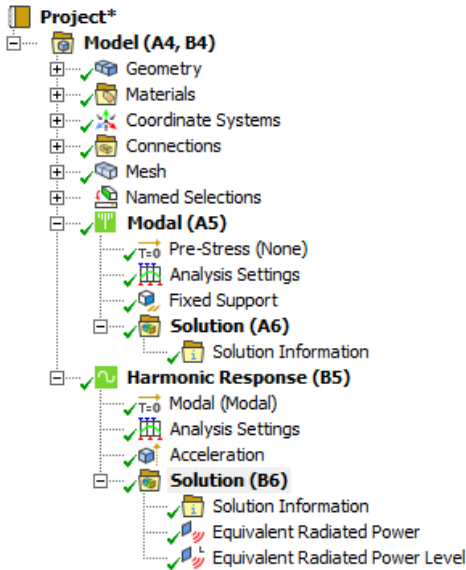
Figure A.12. *Harmonic analysis simulation.*

Thermal Simulations Set Up B

This appendix includes a detailed explanation of how the simulations for thermal analysis are set up inside the ANSYS Workbench software. The version used is 2021R2. A steady-state thermal node from ANSYS Workbench has been used, refer to Figure B.1.
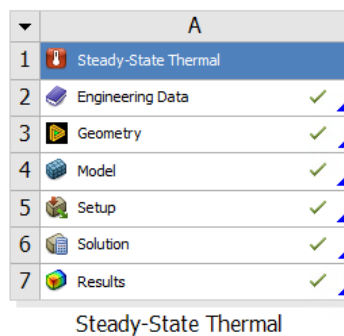
Figure B.1. *ANSYS Workbench node set up for thermal analysis.*

The material, geometry, material assignation, connections or contacts between bodies and mesh is the same as explained previously in section A.1. However, the isotropic thermal conductivity material property value is now considered for the analysis, refer to Table B.1.

Material	Isotropic Thermal Conductivity [W/m.°C]
Aluminium alloy, wrought, 6061, T6	155,3
Copper, C10100, hard	396,7
Ferrite	4
PCB laminate, Epoxy/Glass fiber, FR-4	0,38
Plastic, PC (copolimer, heat resistant)	0,1998
Silicon, pure	154,3
Structural steel	60,5

Table B.1. *Isotropic thermal conductivity data for each of the materials.*

A convergence study of the mesh has not been done for the thermal analysis as it is known that the results will not be influenced excessively by the accuracy of the mesh. Thus, it has been considered that the mesh used for the vibration analysis is good enough for this study and has been used without further investigation. Now, the loads and boundary conditions present in the model have to be defined. These values are provided by Grundfos inside the FloEFD software and therefore, they have to be adjusted to ANSYS.

Power Sources

The different power sources are given in FloEFD as volume heat sources in $[W]$. In the case of ANSYS, an internal heat generation load has to be defined to apply a uniform generation rate inside a body. However, the values have to be in $[W/mm^3]$ and thus conversion of units is needed.

For doing so first, the volume of each body with a heat contribution is extracted. Then, the value used in FloEFD for each of the components had to be divided by the volume of that components. Hence, the magnitude of each load is introduced in ANSYS as a function of the volume. Refer to Figure 6.2 for the location of the components with a heat load and to Table 6.1 for the respective values. In addition, a surface heat of 1,3 W is defined on the top face of the PCB. Figure B.2 shows the loads applied to the bodies and the PCB surface inside ANSYS.

(a) *Internal Heat Generation loads, PCB top face view.*

(b) *Internal Heat Generation loads, PCB down face view.*
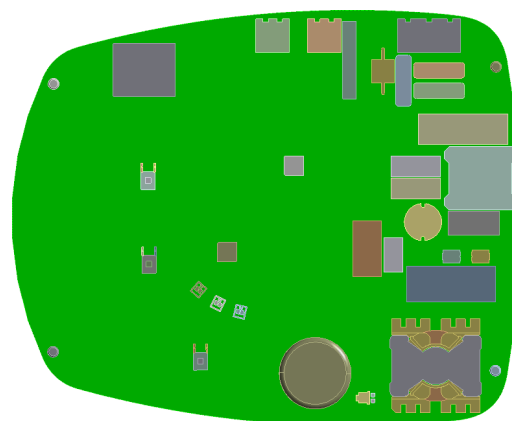
(c) *Heat flow from PCB surface.*

Figure B.2. *Power sources for the steady-state thermal analysis.*

Convection Boundary Conditions

As a conduction-based solver has been used, ANSYS Workbench, then, no fluid is included in the simulations. When a CFD solver is being used then, the fluid is being modelled and the interaction between solid and fluid is being considered automatically. However, with the

conduction-based solver, it is necessary to define manually the interaction between the solid and the fluid with the convection boundary conditions. In order to define the convection, the film coefficient and the ambient temperature are necessary. For complex problems, the way to find these values is by careful experiments - the trial and error method - until the desired results are obtained. However, a numerical method is used first to get a rough approximation and then different adjustments are done until the results from FloEFD - CFD solver - are obtained. The exact results are known as the simulation was already set up in this solver by Grundfos. Thus, the experiments carried out had the objective to find the best fit to have the results that FloEFD shows, Figure 6.1 and Figure 6.1.

Hence, it is necessary to take into account the convection of the electronic components towards the inside of the box, the convection that the inside of the box gets from the electronic components and the convection from the outside of the box towards the outside. As the enclosure is divided by the PCB, shown in green in Figure B.3, there are two different enclosure parts and no air is flowing from one part to the other. Thus, each film coefficient and ambient temperature are different for the upper part and the lower part. They will be referred to as Part 1 and Part 2 respectively.
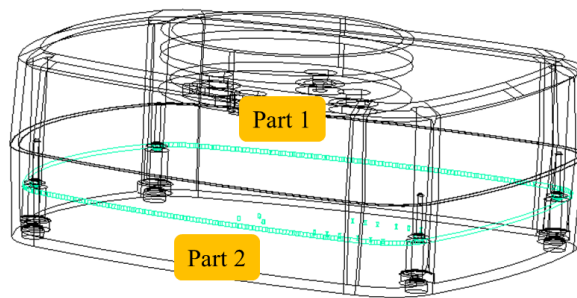

Figure B.3. *Two different enclosure parts inside the control box.*

Thus, five convection boundary conditions are defined, two for Part 1, two for Part 2 and one for the outer shape of the case. Refer to Table 6.2 for the summary of the results.

For the two first convection, the power dissipated by the components from the upper part of the PCB is summed. As shown in Figure B.2a, 14 components dissipate heat to the upper part of the case plus the PCB itself, Figure B.2c. The sum of all these power is 8,55 W and thus is the value that is distributed, considering the surfaces that dissipate and the ones that get the heat. The surfaces that dissipate the heat are those from the components that are in contact with the air, so only the ones show and not the ones defined on the contacts. The sum of all these surfaces give a value of $35.335,357\,\text{mm}^2$ and therefore, the heat flux is $2,42 \times 10^{-4}\,\text{W/mm}^2$ by following Equation 6.1. On the other hand, the surfaces that absorbed the heat from the components in Part 1 are all of the ones from the bottom part in contact with the air. Thus, the surfaces shown in yellow in Figure B.4 are selected and have a surface of $51.774\,\text{mm}^2$. Therefore, the heat flux for the inner surface of Part 1 is $1,651 \times 10^{-4}\,\text{W/mm}^2$.

Convection_Inner_Top: 95. °C, 1.65e-005 W/mm²·°C
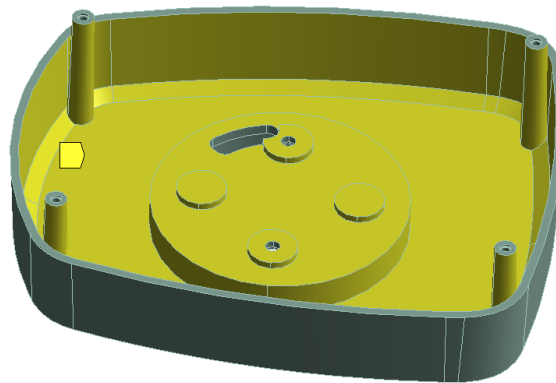
Figure B.4. *Surface for the convection boundary condition of Part 1 that absorbs heat.*

Moreover, Equation 6.1 shows that the film coefficient is a function of the heat flux and the difference in temperature between the surface temperature and the ambient temperature. The ambient temperature intends to characterize the temperature of a fluid at some distance from the solid surface rather than the temperature directly on the surface boundary. As the temperatures are unknown then, estimation is done considering that the upper part inside the case is a small close region. Thus, it is believed that the temperature at a distance from the surface boundary will not be that different to the temperature of the surface itself since the overall temperature of the cavity will be high as not that much heat will be dissipated to the outside. For this reason, a variation of $10\,°\mathrm{C}$ has been considered to calculate the film coefficient and this gives a value of $2{,}420 \times 10^{-5}\,\mathrm{W/mm^2\,°C}$ and $1{,}651 \times 10^{-5}\,\mathrm{W/mm^2\,°C}$ respectively. In addition, the ambient temperature has to be defined. However, this temperature is not the initial one from the outside of the control box, instead is the one that Part 1 has once the steady-state is achieved. Thus, knowing that the temperature range of the PCB goes from $75\,°\mathrm{C}$ to $115\,°\mathrm{C}$, the average of both values is considered as the ambient temperature for Part 1, $95\,°\mathrm{C}$.

The process to calculate the two convection boundary conditions of Part 2 is the same as for Part 1 but considers the new values. In this case, 9 components dissipate heat, Figure B.2b, and the sum of all the power is $5{,}84\,\mathrm{W}$. The area of the seen surfaces of the components is $271{,}57\,\mathrm{mm^2}$ and the heat flux is $2{,}15 \times 10^{-2}\,\mathrm{W/mm^2}$. On the other hand, the surfaces that absorbed the heat from the components in Part 2 all of the ones from the cover part in contact with the air. Thus, the surfaces shown in yellow in Figure B.5 are selected and have a surface of $44.628\,\mathrm{mm^2}$. Therefore, the heat flux for the inner surface of Part 2 is $1{,}309 \times 10^{-4}\,\mathrm{W/mm^2}$.

☐ Convection_Inner_Down: 75. °C, 1.31e-005 W/mm²·°C
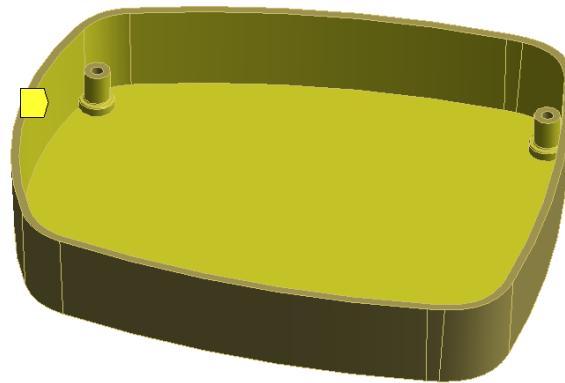
Figure B.5. *Surface for the convection boundary condition of Part 2 that absorbs heat.*

The same temperature difference as for Part 1 is used now for Part 2. Therefore, the film coefficient for the convection boundary condition that dissipates heat on Part 2 is $2{,}150 \times 10^{-3}\,\mathrm{W/mm^2\,°C}$ and the film coefficient for the absorbed heat on Part 2 is $1{,}309 \times 10^{-5}\,\mathrm{W/mm^2\,°C}$. In addition, a guess is made to find the ambient temperature inside Part 2. As less heat is generated in this part, compared to Part 1, it is believed that the temperature in the air will be lower and therefore the cover part will be colder than the bottom part. Thus, different simulations were done until similar values were obtained for the case. It is decided to use $75\,°\mathrm{C}$ as the inner ambient temperature of Part 2 as no better values were found.

Finally, the last convection boundary condition is defined for the outer surface of the case. Hence, all the surfaces of the control box that are in contact with the open air are selected, refer to Figure B.6. Thus, the film coefficient that should be used is the one to represent natural convection. Generally, $5 \times 10^{-6}\,\mathrm{W/mm^2\,°C}$ is considered when the ambient temperature is $22\,°\mathrm{C}$. However, in this case, the temperature of the surroundings of the box is $55\,°\mathrm{C}$ and therefore an adjustment is needed. It is known that the value increase as the temperature increase, thus the trial and error method was used until enough good results were obtained. The different simulations showed that $1 \times 10^{-5}\,\mathrm{W/mm^2\,°C}$ should be used.

☐ Convection_OuterSurface: 55. °C, 1.e-005 W/mm²·°C   ☐ Convection_OuterSurface: 55. °C, 1.e-005 W/mm²·°C
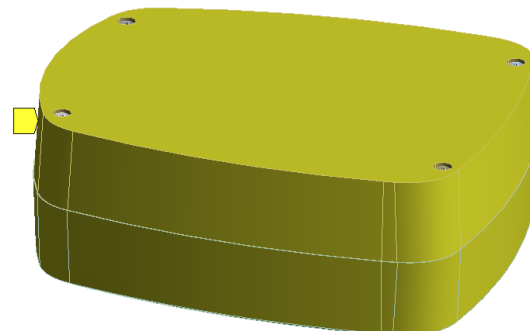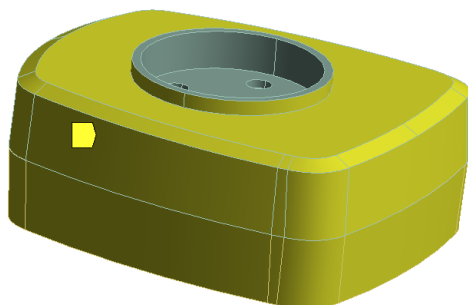
Figure B.6. *Surface for the convection boundary condition of the outer surface of the case.*

Temperature Boundary Condition

In addition, the boundary condition of the temperature of the stator house is considered as in reality this part will have a temperature of 95 ° and it will be transferred by conduction to the control box. Thus, the area where the stator is located is selected, Figure B.7, to apply this boundary condition.
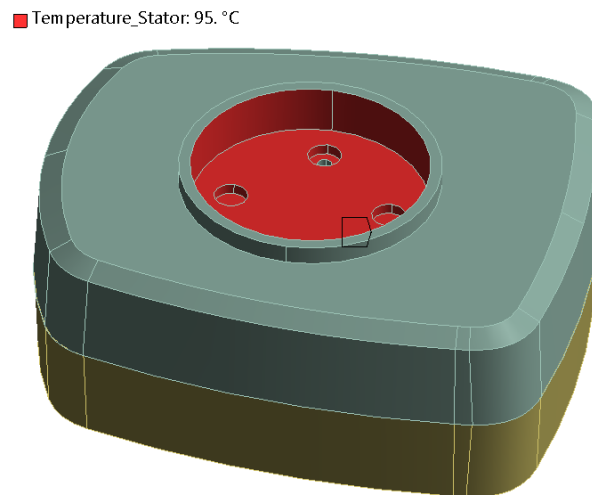
Figure B.7. *Temperature boundary condition on the stator area.*

Radiation Boundary Conditions

Then, radiation is considered. In this case from the outer surface of the case and from the PCB. To define radiation is necessary to define the emissivity coefficient of the material from the surface and the ambient temperature. The value of the temperature has to be defined at some distance from the box and not exactly on the radiation surface.

Therefore, for the radiation of the outer surface of the case, the emissivity coefficient varies depending on the studied case. Table B.2 shows the values used for the different study cases and Figure B.8 the selected faces. The value defined for the temperature is 55 °C for all cases since it is the ambient temperature in the surroundings of the control box, at some distance from the box and not exactly on the surface of the case.

Study Case	Emissivity Bottom	Emissivity Cover
Polycarbonate Case	0,9	0,9
Aluminium Bottom / Polycarbonate Cover	0,02	0,9
Aluminium Case	0,02	0,02

Table B.2. *Emissivity coefficient for the radiation of the outer surface depending on the material of the case.*
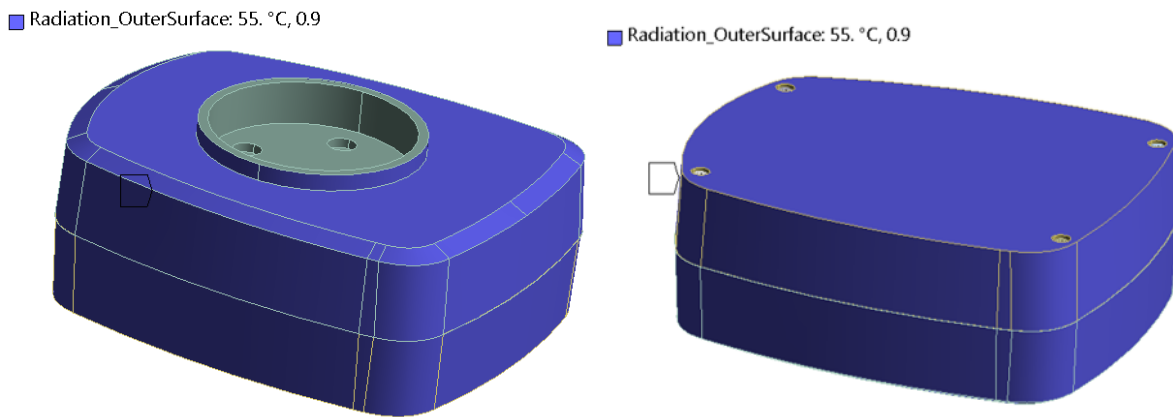
Figure B.8. *Faces selected for the radiation of the outer surface, polycarbonate case.*

Moreover, the radiation from both faces of the PCB is defined, refer to Figure B.9 to see the faces selected. Therefore, the emissivity of the material from PCB is considered. In this case, the material is FR4 and has an emissivity coefficient of 0,9. The ambient temperature considered is the same as for the convection boundary conditions. Therefore, for the upper part is 95 °C and for the down part is 75 °C.
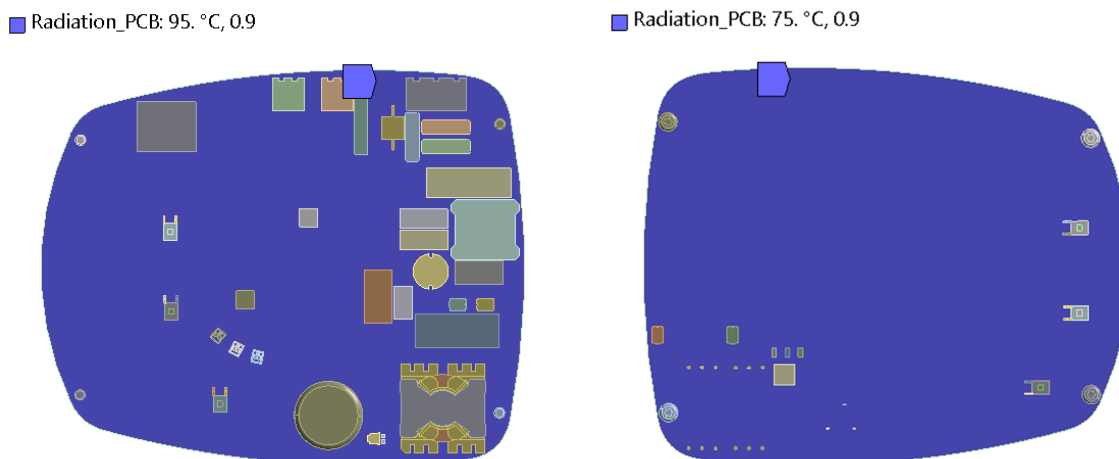

Figure B.9. *Faces selected for the radiation of the PCB.*

Conduction Boundary Conditions

As it is a conduction-based solver then, conduction is already being considered when defining the contact regions between components as well as the values of the isotropic thermal conductivity property of the different materials. As mentioned in section 2.2, the PCB part was modified and only FR4 material is used and no copper layers are present. Thus, the conduction properties of the PCB are modified considering that copper is a good conductor with an isotropic thermal conductivity of 394,7 W/m °C and the FR4 is not, with a value of 0,38 W/m °C as stated in Table B.1. Hence, a manual modification of the property of the FR4 material is done to simulate the real condition of the conduction happening on the PCB. After running several simulations, it was found that by setting the isotropic thermal conductivity of the material of the PCB to 20 W/m °C then, the same heat dissipation along the PCB was obtained as in the CFD solver.

Thermal Analysis Results

Once everything is set up then, all the loads and boundary conditions are under the steady-state thermal node as shown in Figure B.10. Then, the Temperature results for all bodies can be inserted and the results from Figure 6.3 and Figure 6.3 are obtained.
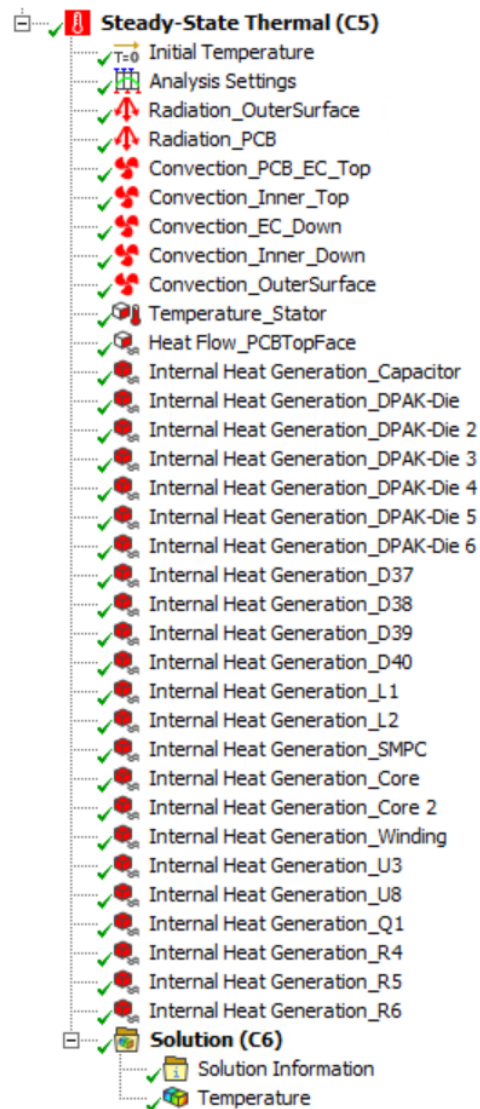
Figure B.10. *Steady-state thermal simulation.*